**Contract No:**

This document was prepared in conjunction with work accomplished under Contract No. DE-AC09-08SR22470 with the U.S. Department of Energy (DOE) Office of Environmental Management (EM).

Disclaimer:

This work was prepared under an agreement with and funded by the U.S. Government. Neither the U. S. Government or its employees, nor any of its contractors, subcontractors or their employees, makes any express or implied:

1) warranty or assumes any legal liability for the accuracy, completeness, or for the use or results of such use of any information, product, or process disclosed; or
2) representation that such use or results of such use would not infringe privately owned rights; or
3) endorsement or recommendation of any specifically identified commercial product, process, or service.

Any views and opinions of authors expressed in this work do not necessarily state or reflect those of the United States Government, or its contractors, or subcontractors.

Analyses of Integrated Waste Treatment Unit (IWTU) TPR-8023 (1&2) Samples Including Simulant, Bed Products, and Wall Scale Formed during Fluidized Bed Steam Reforming of Sodium Bearing Waste into a Carbonate Form

C. M. Jantzen
D. M. Missimer
C. L. Crawford
H. M. Ajo
F. F. Fondeur
M. L. Crowder
P. R. Burket

SRNL.DOE.GOV

DISCLAIMER

Analyses of Integrated Waste Treatment Unit (IWTU) TPR-8023 (1&2) Samples Including Simulant, Bed Products, and Wall Scale Formed during Fluidized Bed Steam Reforming of Sodium Bearing Waste into a Carbonate Form

C. M. Jantzen
D. M. Missimer
C. L. Crawford
H. M. Ajo
F. F. Fondeur
M. L. Crowder
P. R. Burket

August 2016

Savannah River National Laboratory ™

OPERATED BY SAVANNAH RIVER NUCLEAR SOLUTIONS

REVIEWS AND APPROVALS

AUTHORS:

_____   8/31/16
C. M. Jantzen, Engineering Process Development   Date

TECHNICAL REVIEW:

_____   8/31/16
C.L. Trivelpiece, Engineering Process Development, Reviewed per E7 2.60   Date

APPROVAL:

_____   9-1-16
C. C. Herman, Director, Hanford Mission Programs   Date

_____   9/1/2016
J. R. Shultz, Manager   Date
Operations Support Team, Department of Energy, Environmental Management

ACKNOWLEDGEMENTS

EXECUTIVE SUMMARY

This report documents Savannah River National Laboratory (SRNL) analyses of the products from the various vessels in the Integrated Waste Treatment Unit (IWTU) at the Idaho Nuclear Technology and Engineering Center (INTEC) during non-radioactive simulant processing of campaign TPR-8023 (1&2) in November/December 2015. The analyses focus on the identification of unwanted materials deposited in the IWTU during that campaign.

The IWTU is designed to stabilize the acidic low-activity waste known as Sodium Bearing Waste (SBW) through a Fluidized Bed Steam Reformer (FBSR) system. The THOR® FBSR mineralizing technology uses dual reformers to pyrolyze organics in the presence of a fluidization media of steam. Organics not pyrolyzed in the Denitration Mineralization Reformer (DMR) and excess hydrogen are oxidized in the second reformer known as the Carbon Reduction Reformer (CRR). The major vessels of the IWTU FBSR are identified in the illustration below:

Reformer Vessels:
Denitration
Mineralization
Reformer (DMR)
Carbon Reduction
Reformer (CRR)
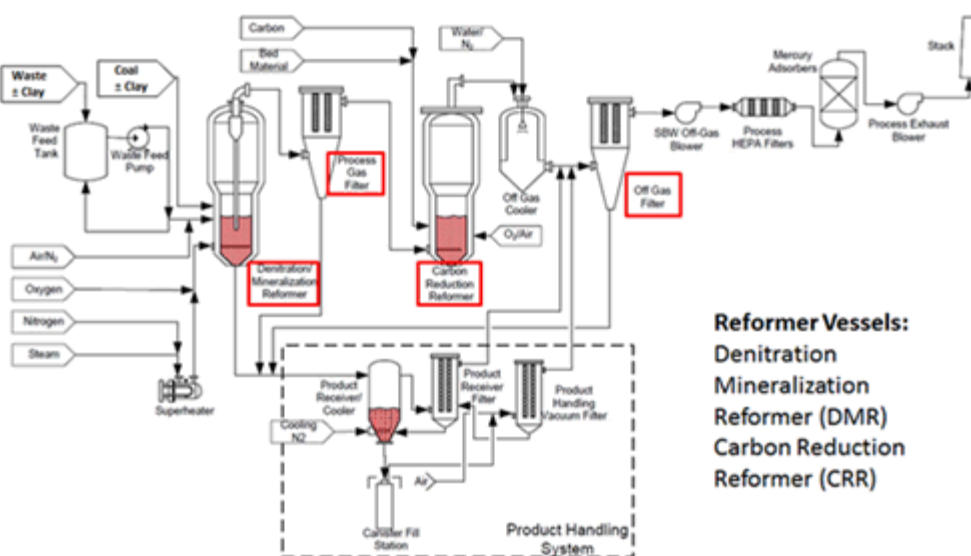
The IWTU underwent an Operational Readiness Review (ORR) in March 2014. From late 2014 through January 2015, the initial non-radioactive IWTU start-up campaign, referred to as the TI-102 campaign, processed over 60,000 gallons of non-radioactive simulated SBW. The facility is currently in restart after a planned outage for inspection of the equipment. The IWTU will resume processing simulated waste feed and perform another shutdown/inspection before beginning to process additional simulants and/or 900,000 gallons of radioactive SBW. The SBW will be made into a granular FBSR product (carbonate based) for eventual disposal in the Waste Isolation Pilot Plant (WIPP) in New Mexico.

During the 2015 TPR-8023 (1&2) campaign, wall scale, commonly referred to as "bark" due to its vertical tree-bark-like appearance, unexpectedly formed on the internal surfaces of the DMR and plugged the auger grinder. Bark had previously formed in the 2014-2015 non-radioactive campaign known as TI-102. No wall scale had formed during pilot-scale demonstrations (2003-2004) of the carbonate FBSR flow sheet with simulated SBW at the Science Applications International Corporation-Science and Technology Applications Research (SAIC-STAR) facility in Idaho Falls, Idaho. Those pilot scale tests were performed by a team of SAIC-STAR, INL, and THOR® Treatment Technologies (TTT) personnel. In 2006, wall scale had been observed as SBW was being processed into the solid carbonate product at Hazen Research Inc. (HRI) in Golden, Colorado. During the 2006 INTEC Carbonate Product

engineering-scale campaigns (CP-1 and CP-2) carried out by TTT.   SRNL and HRI performed an extensive investigation into the cause of the 2006 wall scale, identified three causes, and made recommendations to control wall-scale formation.   The conditions that caused the 2006 wall-scale formation at HRI do not exist in the IWTU.   The observance of wall scale during the IWTU TI-102 campaign and again during the TPR-8023 (1&2) campaign was therefore unexpected.   Interestingly the TPR-8023 (1&2) (November/December 2015) campaign did not form $NaAlO_2$ like the TI-102 campaign but formed two different polymorphs of $Al(OH)_3$ (gibbsite and boehmite).   While the Hazen CP-1/CP-2 campaigns made $NaAl_{11}O_{17}$ preferentially.

This report transmits the results of the SRNL analyses requested by IWTU on the products from the various IWTU vessels and the unwanted materials deposited in the IWTU during the TPR-8023 (1&2) (November/December 2015) campaign.   The TPR-8023 (1&2) November/December 2015 campaign produced a bark that was purer in composition than previous bark studied.   The bark in the DMR and auger grinder were the same.   Analysis of this simpler bark allowed the following to be determined:

Excess NaOH-KOH was found in the IWTU DMR bed products and likely participates in the bark formation.   The following analytic findings confirm the existence of a NaOH-KOH solid solution:

- excess Na in soluble mass balance for which there are no other anions other than OH available (DMR bed product and DMR and auger grinder bark)
- presence of faujasite in the drum #2 sample and in the auger grinder compressed material (faujasite needs NaOH to form)
- TGA and DSC's indicate the presence of NaOH-KOH mixture at ~250-300°C
- The TGA and DSC proved that only NaOH-KOH is involved and not eutectics with NaOH and Na_2CO_3, Na_2SO_4, or $NaNO_3$.

The excess NaOH-KOH is a very small mass amount and cannot be observed in a dry heating experiment.   The presence of NaOH-KOH is due to insufficient CO_2 in regions of the DMR and the chemistry involved is discussed in this report.

The presence of NaOH-KOH can also be responsible for the glassy phase formation when the hydroxides interact with the coal fly ash.   The following analytic findings confirm the existence of a glassy phase or partially crystallized glassy phase of the approximate composition $(Na,K)_2Si_2O_5$:

- excess sodium/potassium silicate in the insoluble mass balance
- identification by XRD – broad d-spacings in the bark XRD spectra hovering around the composition of partially crystalline $Na_4Mg_3Si_5O_{10}$ where $Na_2Si_2O_5$-$Na_4Mg_3Si_5O_{10}$ form a solid solution with likely substitution of Fe^{2+} for Mg both of which come from the coal ash
- identification of the glassy phase by Infrared Spectroscopy (IR), Fourier Transform Infrared Reflectance (FTIR) and Raman Spectroscopy

A similar glassy phase of $(Na,K)_2Si_2O_5$, with substitution of Ca, was found in all three FBSR tests of the INTEC SBW simulant, i.e. HRI 2006 ESTD, IWTU TI-102, and the current IWTU TPR-8023 (1&2).   For the HRI campaigns Ca was substituted in the glassy phase.   For the IWTU TPR-8023 (1&2) impurities likely included Ca, Mg, and Fe^{2+}.   Therefore, the chemistry of the glassy phase in all the SBW FBSR campaigns is considered relatively constant except for the substitution of a variety of impurities.   The presence of NaOH and Na_2SO_4 and possibly halides may catalyze the glass forming reaction(s). Therefore, experiments with fly ash, sodium carbonate, and these impurities in the presence of steam are being pursued at the SRNL to determine the mechanism of formation of the glassy phase in the bark.

SRNL-TR-2016-00172
Revision 0

The analyses provided in this report allow the following conclusions to be drawn regarding the original task questions posed regarding bark formation:

1. The glassy phase was present in the 2015 TI-102 bark, the Hazen CP-1/CP-2 bark and the current TPR-8023 (1&2) bark.
2. The binder in the bark is NaOH-KOH mixed with $(Na,K)_2CO_3$ bed product and a glassy phase of $(Na,K)_2Si_2O_5$.
3. The melting point of the bark is between 250-300°C as identified by TGA and DSC.
4. The rocks in the coal are typical sedimentary rocks found in coal formations and are unremarkable. The rocks do not participate in bark formation.
5. Additional CO_2 will "lock out" the NaOH-KOH component of the wall scale bark and may prevent the formation of the glassy phase as well. Additional testing is needed to confirm the relationship between the NaOH-KOH and the glassy phase.
6. Dilution of the feed will not inhibit the bark. What other operating changes might help prevent wall scale – DMR operating temperature, DMR operating temperature control, waste feed rate, NAR, superheated steam velocity (SSV), CO_2? More CO_2 can likely inhibit the NaOH that is likely causing the bark formation. Addition of a higher melting alumina containing component may also help.

TABLE OF CONTENTS

LIST OF TABLES

LIST OF FIGURES

LIST OF ABBREVIATIONS AND ACRONYMS

AG	Auger Grinder
BEA	Battelle Energy Alliance
CAA	Clean Air Act
CP	Carbonate Product
CRR	Carbon Reduction Reformer
CWI	CH2M-WG Idaho
DMR	Denitration and Mineralizing Reformer
DOE-EM	Department of Energy-Environmental Management
DSC	Differential Scanning Calorimetry
EDAX	Energy Dispersive Analysis by X-ray
E&CPT	Environmental & Chemical Process Technology
ESTD	Engineering Scale Test Demonstration
FBSR	Fluidized Bed Steam Reformer
FTIR	Fourier Transform Infrared Reflectance
HRI	Hazen Research Inc.
HTXRD	High Temperature X-ray Diffraction
IC	Ion Chromatography
ICP-AES	Inductively Coupled Plasma-Atomic Emission Spectroscopy
INL	Idaho National Laboratory
INTEC	Idaho Nuclear Technology and Engineering Center
IR	Infrared Reflectance
IWTU	Integrated Waste Treatment Unit
LHS	Left Hand Side
MACT	Maximum Achievable Concentration Technology
MS	Mass Spectroscopy
NAR	nozzle-to-atomizing
OGC	off-gas cooler
OGF	Off Gas Filter
ORR	Operational Readiness Review
OST	Operations Support Team
PGF	Process Gas Filter
PSAL	Process Science Analytical Laboratory
REDOX	REDuction/OXidation
RHS	Right Hand Side
SAIC-STAR	Science Applications International Corporation- Science and Technology Applications Research
SBW	Sodium Bearing Waste
SEM	Scanning electron microscopy
SRNL	Savannah River National Laboratory
SSV	Superficial Space Velocity
TGA	Thermo Gravimetric Analysis
TIC	Total Inorganic Carbon
TTT	THOR® Treatment Technologies
WIPP	Waste Isolation Pilot Plant
XRD	X-ray Diffraction

1.0 INTRODUCTION

1.1 PREVIOUS PILOT SCALE TESTING OF SBW CARBONATE FLOW SHEET

In the Fluidized Bed Steam Reforming (FBSR) process, calcined coal is used to create a CO_2 fugacity to force the waste species to convert to carbonate species. The carbonate and aluminosilicate FBSR flow sheets were demonstrated with simulated sodium-bearing waste (SBW) at the Science Applications International Corporation-Science and Technology Applications Research (SAIC-STAR) facility in Idaho Falls, Idaho. The pilot-scale tests were performed on Idaho National Laboratory (INL) SBW [1,2,3] by a team from SAIC-STAR, INL, and THOR® Treatment Technologies (TTT) in 2003-2004. In 2006, TTT demonstrated the carbonate and aluminosilicate FBSR flow sheets in the Engineering Scale Test Demonstration (ESTD) facility using Idaho Nuclear Technology and Engineering Center (INTEC) SBW. The ESTD was run at Hazen Research Inc. (HRI) in Golden, Colorado.[4] The differences in the pilot scale and engineering scale test facilities and operation are summarized in Table 1-1.

Table 1-1. Pilot-scale and Engineering-scale FBSR Testing for Carbonate Flow Sheet with INTEC SBW Simulant

Facility	Scale	FBSR Column Diameter	Externally or Autothermally Heated	Dual or Single Reformer Flow Sheet?	Reductant of Choice	Catalyst
SAIC-STAR 2003-2004	Pilot	6"	external and autothermal with coal	Single	BB* charcoal	No
TTT ESTD 2006	Engineering	15"	autothermal with coal	Dual	BB* charcoal and General Carbon (GC-CRB) coal	Yes

* Berger Brothers

Wall scale was not observed in the SAIC-STAR pilot scale testing of the SBW waste.[1, 2]

In the ESTD engineering scale tests, wall scale formation was observed on the internal surfaces of the Denitration and Mineralization Reformer (DMR) at the end of the first Carbonate Product (CP) scoping tests (CP-1) on January 14, 2006. Wall scale was sampled after the shutdown of the CP-1 production tests on January 21, 2006, and after the final shutdown of the CP-2 production tests (June 2006).[5] The CP-1 scale was 1-6 mm (1/16-1/4") thick on the DMR wall but heavier on the downcomer and corrosion coupons. After the CP-2 production test was concluded, wall scale deposits of 1-6 mm were also discovered in the DMR on the inside metal and refractory surfaces. TTT reported that the internal surfaces of the DMR, from the normal bed high level to just below the fluidizing gas distributors, were

coated with a thin layer of hard deposits. Deposit thickness was reported to range from ~1/4" on the bottom edge of the corrosion coupons to ~ 1/16" on the downcomer pipe. Deposit thickness on the refractory walls appeared to be 1/16" to 1/8" in the lower portions of the bed with thinning deposits up the walls with deposits extending up to the enlarged diameter section in the freeboard. TTT also reported that the deposits could be manually broken off the refractory and metal surfaces to which they adhered and the deposits were determined to be water soluble. The deposits were reported to be gray in color and have the appearance of ripples as if they formed from a flowing film. The deposits had the appearance of tree bark. The CP-2 scale was similar in appearance to the CP-1 scale.[5] It should be noted that wall scale was not formed during the subsequent SBW aluminosilicate mineralizing runs.

Three causes of the CP-1/CP-2 deposits were identified [6], which were
- The use of Mulcoa 70$^\circledR$ (a crystalline and glassy mixture of mullite) as a bed additive which reacted with the potassium in the SBW
- The use of PureOX which is mostly Fe_2O_3 as a bed additive
- The use of a high sulfur containing coal (Berger Bros. P6) which caused $SO_4^=$ salts to form at 640°C and complex with other alkali salts in the SBW to form low melting eutectic phases that can cause agglomerations and/or initiate attack on any silicates or refractory present.

1.2 PREVIOUS IWTU TESTING OF SBW CARBONATE FLOWSHEET

From late 2014 through January 2015, the initial non-radioactive IWTU start-up campaign, referred to as the TI-102 campaign, processed over 60,000 gallons of non-radioactive simulated SBW. During the 2014-2015 TI-102 campaign, wall scale, commonly referred to as "bark" due to its vertical tree-bark-like appearance as described above, unexpectedly formed on the internal surfaces of the DMR and plugged the auger grinder. The bark was thicker toward the bottom of the DMR near the fluidizing rails.

During the IWTU 2014-2015 TI-102 campaign neither Mulcoa 70$^\circledR$ nor PureOX were used. The IWTU DMR is not refractory lined as was the DMR at HRI. In addition, a low sulfur containing coal, Bestac coal, was used at the IWTU per the coal procurement specification that requires a range of S between 0-0.7 wt%. These precautions should have prevented any scale formation in the IWTU during the TI-102 campaign. However, the bauxite bed material being used at IWTU in the DMR during TI-102 and in the CRR does contain mullite, the main ingredient in Mulcoa 70$^\circledR$, and the bauxite contains a significant quantity of Fe_2O_3 impurities as is shown by the analyses presented in Reference.[7]

The high sulfur containing coal used in the CP-1/CP-2 campaigns at HRI was General Carbon (GC-CRB) coal (Table 1-1), which contained 3.71 wt% S [26], while the Bestac coal used by TTT in 2007 and 2009 contained only 0.16-0.32 wt% S and the Bestac coal being used by IWTU contains only 0.2 to 0.24 wt% S.[8] However, when ashed the coal contains 6.16-8.96 wt% ash and the ash contains 6.80-7.80 wt% SO_4 which converts to 0.41-0.70 wt% SO_4 in the coal ash.

The use of bauxite was considered as a possible reason that the TI-102 campaigns made copious amounts of bark. However, the findings in Reference 8, as summarized in Table 1-2, suggest that stable operations were not achieved in the TI-102 campaign. Specifically it appeared that the waste simulant had been overfed, that coal had been overfed, that the nozzle-to-atomizing ration (NAR) was too high, indicating that the DMR residence times were not long enough for particle growth and complete reaction, i.e. NaOH was present which formed a low melting eutectic with either Na_2CO_3 (the product) and/or $NaNO_3$ (the feed). The presence of NaOH in the bark and in the DMR bed product meant that the CO_2 fugacity was insufficient in the DMR. An entire chapter in Reference 8 is devoted to the multiple lines of evidence for NaOH formation.

Table 1-2. Findings, Potential Cause(s) and Suggested Operational Remediation for Bark Formation in INTEC TI-102 SBW Campaigns (from Reference 8)

Finding	Potential Cause	Operational Remediation
Shard-like Na_2CO_3 particles Average active bed DMR particle size ~15 micron with bauxite bed compared to Hazen ~300-382 micron with alumina start-up bed and not undissolved solids in the simulant	Nozzle-to-atomizing (NAR) ratio too high Little particle growth on bauxite bed	Reduce NAR to increase DMR residence times, allow particle size growth, i.e. stable operations Change bed to Al_2O_3
High concentration of coal ash in IWTU canister product	Overfeeding coal to DMR	Do not overfeed coal
Excess Na_2O in mass balance of DMR active beds and trace in the canister	Presence of NaOH over all other alkali anions	Increase residence time in DMR, i.e. stable operations Do not overfeed the waste, i.e. stable operations Increase CO_2 fugacity in DMR
Presence of $NaAlO_2$ in canister products and elsewhere	$NaAlO_2$ is formed commercially (Bayer aluminum process) by treating $Al(OH)_3$ (the main component of bauxite) with NaOH.	
Presence of megakalsilite on underside of bark attached to the metal vessel wall	Megakalsilite cannot form except in the presence of NaOH	
Presence of the mineral faujasite	Faujesite cannot form except in the presence of coal fly ash and NaOH	
Presence of $NaNO_3$ in the DMR active beds and canister	Denitration reactions incomplete; carbonation reactions insufficient; lack of sufficient residence time in DMR	
Presence of NaCl in the DMR active beds and canister	Carbonation reactions insufficient; CO_2 fugacity in DMR insufficient	
OGF solids	Mostly CRR bed carryover (77-80% coke, 12-13% bauxite, 7-10% coal ash)	Lower attrition rates; Reduce off-gas velocities

1.3 IWTU PROCESS FLOW SHEET

The IWTU process flow sheet is shown in Figure 1-1. The THOR® FBSR mineralizing technology uses reformers to pyrolyze organics, if any are present, in the presence of a fluidization media of steam. Steam reforming, as a chemical conversion process, has been used for >100 years on gaseous fuels. Mineralizing FBSR's can be externally heated or internally heated or a combination of the two heating methods. Externally heated FBSR's are normally limited to a diameter in the 6-8" range while coal or another reductant such as sugar can be used to assist in the denitration reactions. Coal is used to auto-thermally heat larger reformers (>8" diameter). FBSR flow sheets can be single reformer or dual reformer. The DMR is a fluidized bed but it uses calcined coal as its fuel source and operates at ~650°C for making carbonate products at ~725-750°C to make primarily Na_2O-Al_2O_3-SiO_2 (NAS) minerals. In the latter case, the feed is mixed with kaolin to promote the formation of the durable NAS minerals. Organics not pyrolyzed in the DMR and excess H_2 are oxidized in the second reformer known as the

Carbon Reduction Reformer (CRR). The CRR is a fluidized bed that uses petroleum coke as its fuel source and operates at a higher temperature (950°C) and is more oxidizing than the DMR.

Off-gases from the CRR are cooled by direct water injection in an off-gas cooler (OGC) vessel and are then filtered in the off-gas filter (OGF). The off-gas then goes through a set of high-efficiency particulate air (HEPA) filters so that the primary emissions released to the atmosphere from the process are carbon dioxide and water vapor (there are no liquid effluents from the process). The off-gas from the DMR contains fine particulates that pass through an internal cyclone system which returns relatively larger and/or heavier particles back to the DMR. Particles that are small and/or light enough pass through the internal cyclones and travel via a pipe duct system where they are removed via Inconel® sintered metal candle filters in the Process Gas Filter (PGF) vessel. An eductor system removes the flyash material from the bottom of the PGF vessel. The samples analyzed in this report are from material in the DMR, the PGF, the CRR, and the OGF vessels.

The FBSR process is Clean Air Act (CAA) compliant. The FBSR technology has also been shown, during pilot-scale and engineering scale testing to be Hazardous Waste Combustor (HWC) Maximum Achievable Control Technology (MACT) compliant for Hg, Cl, CO, total hydrocarbons, and heavy metals [1,2]. A significant benefit of the FBSR process is that it produces zero-liquid releases. All water is released as water vapor.
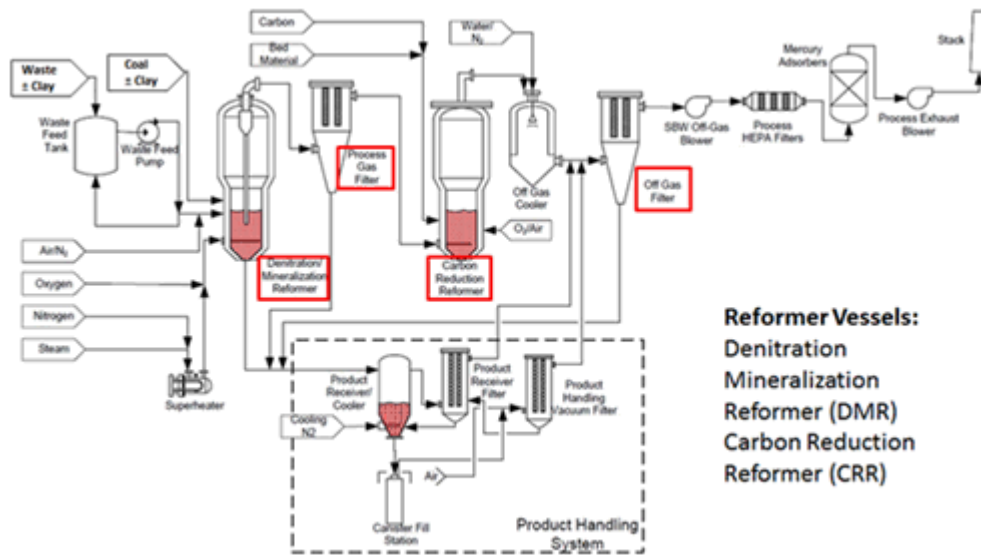
Figure 1-1. *IWTU FBSR Process Flow sheet with major vessels identified.*

1.4 IWTU SBW TPR-8023 (1&2) SIMULANT COMPARED TO IWTU TI-102 and 2006 ESTD SIMULANT

From late 2015 through January 2016, the second and third non-radioactive IWTU start-up campaigns, referred to as TRP-8023-1 and TRP-8023-2, processed 8,600 and 30,500 gallons more simulant respectively, under more restrictively controlled feed rate and NAR ratios. Less bark was produced and the bark was simpler in compositional makeup to previous bark samples facilitating analysis and mechanistic understanding of bark formation.[9]

The IWTU TI-102 campaign, the initial non-radioactive startup campaign, was composed of two batches of simulant. Batch 1 was a simulant containing only two components, $NaNO_3$ and $Al(NO_3)_3$. The Batch 2 simulant contained the sodium and aluminum nitrates and in addition it contained KNO_3 and K_2SO_4. The potassium salts and the sulfate salts had been added at the request of the DOE-EM Operations Support Team (OST) as SRNL had identified these components in 2006 [10] as participating in wall scale formation and they are components of the radioactive SBW.

Table 1-3 provides a comparison of the simulants used in the 2006 ESTD demonstrations (columns 3 and 4) and in the 2014-15 IWTU TI-102 campaigns (columns 6 and 7). The IWTU simulant is based on the measured 2007 compositional analyses of the INTEC tank contents. Therefore, the concentrations are somewhat different between the ESTD and IWTU facility demonstrations. However, all the major constituents (at >0.02 wt%) are accounted for in the IWTU simulant except Cl and PO_4. Since the IWTU simulant was made up with process water, Cl was present in the simulant in unknown amounts until analyzed (see Table 1-3, column 8) by SRNL.

The SRNL analyses (Table 1-3, column 6) indicate that the Al, Na, NO_3 and SO_4 in the TI-102 simulant are on target but the K concentrations are only 70% of the target values in M/L. The Cl impurities in M/L from the process water are 0.0032 M/L. Trace amounts (in the fifth decimal) were quantified for Ti, Ni, Cr and Si but not reported in Table 1-3.

The most recent IWTU simulant (TPR-8023) is based on the 2007 compositional analyses of the INTEC tank contents (Table 1-3 Columns 7 and 8) that became available after the 2006 ESTD pilot scale campaigns. Therefore, the concentrations in Table 1-3 are somewhat different between the ESTD (columns 3 and 4) and IWTU facility demonstrations (columns 5, 6, 10, 11). However, the major constituents (>0.02M) were all accounted for in the TI-102 IWTU simulant except F and Cl. Since the TI-102 IWTU simulant was made up with process water, Cl was present in the simulant in unknown amounts until analyzed (see Table 1-3) by SRNL.

The May 2015 IWTU simulant had Cl doped into the simulant at the reference tank concentrations and the simulant was made up with deionized water. The analysis of the May 2015 simulant is given in Table 1-3. The May 2015 IWTU simulant is just within specification of 0.7±0.1 as the analyzed value in column 9 of Table 1-3 is just over 0.80 M/L at 0.81 M/L. The total NO_3 comes from the $Al(NO_3)_3.9H_2O$, $NaNO_3$ and the HNO_3 (Acid) and small amounts from the KNO_3 as shown in column 10 of Table 1-3. Using the maximum and minimum values specified for all the nitrates in column 10 of Table 1-3, the allowable total nitrate concentration can vary from 5.816-7.864 M/L. The SRNL total NO_3 value measured in M/L is 7.48 M/L and was NO_3 7.29 M/L when re-measured. These NO_3 values are toward the high side of the allowable NO_3 but still within range. The minor constituents such as K, Cl, and SO_4 are all within the specification range.

The cations were analyzed by Inductively Coupled Plasma Emission Spectroscopy (ICP-ES) and the anions were analyzed by Ion Chromotography (IC). The SO_4 concentration in M/L is taken from the ICP-ES data and not from the IC data as a large dilution was necessary to get the NO_3 concentrations in range for the IC measurement of anions and this can add error to the analysis.

Table 1-3. Comparison of the IWTU and the ESTD SBW Simulants (Elemental Basis)

1.	2.	3.	4.	5.	6.	7.	8.	9.	10.	11.
Element (M/L)	Component added	CP1 (2006)* Table 4-2 [5] (M/L)	CP2 (2006)* Table 4-2 [5] (M/L)	IWTU TI-102 Simulant Batch 2 Recipe [8] (gmol/L)	IWTU TI-102 Simulant Batch 2 [8] (gmol/L)	High Range of Tank Compositions WM-187 WM-188 WM-189	Average Tank Compositions WM-187 WM-188 WM-189	Component added	IWTU Simulant Recipe, SOW-308, R.4 (5/18/15) (gmol/L)	IWTU May 2015 Simulant Analyses (gmol/L)
Al	$Al(NO_3)_3.9H_2O$	0.719	0.719	0.7026	0.7598	0.59-0.85	0.69	$Al(NO_3)_3.9H_2O$	0.7±0.1	0.8099
B	H_3BO_3	0.0217	0.0217	---	---	0.010-0.024	0.017	Not added	---	---
Ca	$Ca(NO_3)_2.4H_2O$	0.0731	0.0731	---	0.0016	0.046-0.083	0.065	Not added	---	0.0010
Fe	$Fe(NO_3)_3.9H_2O$	0.0217	0.0217	---	0.0002	0.020-0.031	0.025	Not added	---	0.0002
Mg	$Mg(NO_3)_2.6H_2O$	0.0257	0.0257	---	0.0020	Not Analyzed	Not Analyzed	Not added	---	0.0018
Mn	$Mn(NO_3)_2$ (50 wt% sol'n, ρ=1.54)	0.0152	0.0152	---	---	0.015-0.020	0.017	Not added	---	BDL
K	KNO_3	0.225	0.225	0.1174	0.1572	0.174-0.25	0.210	KNO_3 and K_2SO_4	0.24±0.024	0.2444
K	K_2SO_4	---	---	0.0549						
Na	$NaNO_3$ for majority of Na	2.20	2.20	2.0029	1.9508	1.76-2.04	1.84	$NaNO_3$	2.0±0.2	2.127
SO₄	Na_2SO_4	0.107	0.107	---	0.0597	0.054-0.068	0.054	K_2SO_4	0.059±0.006	0.0627 (ICP-ES)
Cl	NaCl	0.0334	0.0334	---	0.0032	0.0170-0.0359	0.0219	NaCl	0.031±0.003	0.0297 (IC)
F	HF (28.9 M sol'n)	0.0506	0.0506	---	---	0.0075-0.015	0.0066	Not added	---	BDL[t]
PO₄	$Na_3PO_4.12H_2O$	0.0138	0.0138	---	---	BDL[t]	BDL[t]	Not added	---	BDL[t]
Acid	HNO_3	3.06	3.06	2.3663	---	---	---	HNO_3	2.5±0.5	---
NO₃	Total NO_3 (nitrates + 69 wt% soln HNO_3)	7.53	7.53	6.594	6.758	5.31-7.57 by MEB[#]	5.474 analyzed 6.66 by MEB[#]	Total NO_3 (nitrates + HNO_3)	5.816-7.864 (min minus max values)	7.48 (IC) 7.29 (IC replicate)
pH	---	---	---	---	1.78	1.87-3.31	2.52	pH	---	2.09
Density (g/cc)	---	---	1.30	1.30	---	1.3065	1.29-1.34	1.30	Density (g/cc)	---	1.3206

*CP means Carbonate Product
[t]BDL is Below Detection Limit
MEB means Mass and Energy Balance

1.5 PHASE FORMATION IN SBW CAMPAIGN TI-102 AND THE ROLE OF NaOH

The identification of phases in the various vessels and deposits is an important part of understanding if the FBSR carbonate flow sheet is working as intended and to compare these products to the identification of phases in the 2006 ESTD CP-1 and CP-2 campaigns. The simple simulant composition given in Table 1-3 (column 10) should make primarily Na_2CO_3 and K_2CO_3 FBSR products. While the mineral dawsonite ($Al_2(CO_3)_3$) is known in nature, the synthetic $Al_2(CO_3)_3$ is not known.[11] Therefore, the Al in the IWTU simulant will likely couple with the Na and form $NaAlO_2$ (see additional discussion below). Performing a simple mass balance for the two alkali carbonates, sodium sulfate, and sodium aluminate provides the theoretical IWTU FBSR species weight percent (Table 1-4). If aluminate phases form that do not couple with Na, i.e. Al_2O_3, then more Na_2CO_3 will be formed.

However, with alumina, silica, calcium, and other species, including more sulfate, available from the coal ash it is anticipated that minerals such as $NaAlSiO_4$ (nepheline) and $KAlSiO_4$ (kalsilite) will form. The amount of Si in a given chemical analysis of the DMR product is an indication of how much coal ash is being produced and how much coal is being consumed (ashed) in the FBSR process. The Bestac coal is 7.40 wt% ash (see Reference 7) and the ash contains 61.01-63.69 wt% SiO_2 and 17.90-23.64 wt% Al_2O_3.

Table 1-4. Ideal TI-102 Batch 2 Simulant Product Phases in Weight %

Component	Wt%
Na_2CO_3	36.7
K_2CO_3	11.51
$NaAlO_2^*$	46.02
Na_2SO_4	5.72

*Note that in CP-1 and CP-2 $NaAl_{11}O_{17}$ was formed preferentially.

Note that $Al_5(CO_3)(OH)_{13}\bullet 5H_2O$ (scarbroite), $Al_{14}(CO_3)_3(OH)_{36}\bullet nH_2O$ (hydroscarbroite), and $NaAlCO_3(OH)_2$ (dawsonite) are not predicted to form in Table 1-4 because phases such as dawsonite are not stable above ~350°C. In particular, dawsonite decomposes, the structure collapses, the hydroxyl groups are lost, and a large portion of the carbonate is lost at >350°C. The dawsonite like material that remains is amorphous and continues to lose CO_2 with increased temperature until crystalline $NaAlO_2$ is formed at 600-670°C.[12] Further evidence of this is indicated in Table 1-5 as $NaAlO_2$ was the only alkali aluminate phase (as sodium aluminate) observed during TI-102 SBW campaigns except for alkali aluminosilicates (sodium aluminosilicates and potassium aluminosilicates) that formed from the silica available from the Bestac coal ash.

Table 1-5 lists all of the mineral phases found by X-ray Diffraction (XRD) during the analysis of the IWTU vessel contents and unwanted deposits. The paragenesis of a few of the various mineral phases listed in Table 1-5 will be discussed briefly as the mechanism by which these mineral phases form and the locations in which they were observed in the IWTU flow sheet suggest the mechanism by which the DMR bark may have formed. The presence of certain minerals ($NaAlO_2$, megakalsilite, and the zeolite known as faujasite) indicate that free NaOH was present during the TI-102 campaign.

The most notable evidence for free NaOH during the TI-102 campaign was the fact that the mass balance performed on the active DMR beds contained 4.29 and 5.28 wt% excess Na_2O while the wall bark contained 1.59 wt% excess Na_2O.[8] The product canister only contained 0.19% excess Na_2O. Excess NaOH is reported as Na_2O in the samples analyzed over the amount of sodium that could not be accounted for as $NaAlO_2$, $NaNO_3$, $NaNO_2$, Na_2SO_4, or Na_2CO_3. The only anion that could not be

analyzed was OH$^-$ and so it is believed that the excess Na$_2$O existed as NaOH vapor at the operating temperature of the DMR.[8]

The phases in the TI-102 bark were analyzed by XRD when the bark was ground up. The phases in the bark top surface (facing the DMR chamber) and under side of the bark (attached to the vessel wall) were also analyzed by XRD and Scanning Electron Microscopy which is discussed below. A major component of the ground up bark sample was NaAlO$_2$ of varying stoichiometry including traces of SiO$_2$. It is important to recognize that the decomposition of dawsonite discussed above occurs at the DMR processing temperatures. So if dawsonite does form as a metastable phase, it will be decomposing to NaAlO$_2$ at the DMR processing temperatures. Alkalized alumina processes are used in gas purification where combinations of dawsonite and NaAlO$_2$ are activated at 649°C to form a high surface area, high porosity, solid which has been used to remove SO$_2$ from flue gases at lower temperatures.[13] This may serve to explain the high S concentrations observed in the wall bark as noted in the SEM of the top surface of the DMR bark and elemental scans in Reference 8.

The presence of NaOH is also indicated by the presence of the sodium aluminate in all the FBSR vessels of the IWTU TI-102 campaign. Sodium aluminate was never found as a phase in the ESTD CP-1 and CP-2 carbonate product campaigns (see Table 3-3). Sodium aluminate is manufactured by the dissolution of aluminum hydroxide in a caustic soda (NaOH) solution. Aluminium hydroxide (gibbsite which was the main component of the DMR bauxite bed during TI-102) can be dissolved in 20–25% aqueous NaOH solution at a temperature near the boiling point. The use of more concentrated NaOH solutions leads to a semi-solid product. The process is usually carried out in steam-heated vessels of nickel or steel which is a similar environment to the DMR.

Both kalsilite and megakalsilite are different structural types of KAlSiO$_4$ (Table 1-5). Kalsilite was found on the upper side of the DMR bark that faced the inside of the DMR by XRD analysis. The kalsilite on the upper side of the bark was a major phase.[8] Kalsilite found on the underside of the bark, i.e., the surface that touched the metallic components of the DMR, was a minor phase while the megakalsilite polymorph of KAlSiO$_4$ was the major phase.[8] Megakalsilite cannot form except in the presence of NaOH [14] which indicates that a thin film of NaOH may have been present on the DMR wall at the initial time the wall scale formed.

The mineral, faujasite, which is a zeolite, was only found in the TI-102 DMR bark and the auger grinder bark after the sample was ashed at 750°C. It was not found in the DMR bark nor the auger grinder bark in the as-received samples, nor after leaching. Faujasite was found in the TI-102 DMR bed and can samples (all 3 samples) but not in the PGF nor in any other vessels. Faujesite is a zeolite that can form during geopolymerization from reaction of fly ash and NaOH.[15] Researchers in Australia examined geopolymers made from various fly ash compositions by Synchrotron radiation-based infrared microscopy.[15] In general, fly ash was found to be composed of reactive components such as 36.6% amorphous SiO$_2$ and 15.3% amorphous Al$_2$O$_3$ with the remainder being unreactive crystalline mullite, quartz, and iron oxide phases. These reactive amorphous flyash compositions, can only form faujasite when alkali activated with NaOH.[15]

Table 1-5. Phases Identified in Various IWTU Vessels and Deposits During TI-102
(from Reference 8)

Phase*	Generic Phase	Mineral Name	Powder Diffraction File (PDF) Identification
C	Carbon	Graphite	00-056-0159
C		Graphite-2H	00-041-1487
$NaNO_3$	Nitrate	Nitratine	00-136-1474
$Na_2CO_3 \bullet H_2O$	Carbonates	Thermonatrite	00-008-0448
$CaCO_3$		Calcite	00-047-1743 00-005-0586
Fe_2O_3	Iron Oxides	Hematite	00-033-0664
Fe_2O_3		Maghemite-Q	04-008-3650
Fe_3O_4		Magnetite	00-019-0629
$MgFe_2O_4$		Magnesioferrite	04-002-8204
Fe_2TiO_5	Titanium Oxides	Pseudobrookite	00-041-1432
$Al(OH)_3$	Alumina Oxides	Bayerite	00-020-0011
Al_2O_3		Corundum	00-010-0173
SiO_2	Silica Oxide	Quartz	00-045-1045
$Al_6Si_2O_{13}$	Aluminosilicate	Mullite	00-010-0776
$Na_{1.75}Al_{1.75}Si_{0.25}O_4$	$NaAlO_2$ with varying traces of SiO_2	Sodium Aluminate	00-049-0004
$Na_{0.975}Al_{0.975}Si_{0.025}O_2$		Sodium Aluminate	04-010-3958
$Na_{1.95}Al_{1.95}Si_{0.05}O_4$		Sodium Aluminate	00-049-0003
$NaAl_{11}O_{17}$	Beta Alumina	Diaoyudaoite	00-045-1451
$Na_2Al_2Si_4O_{12} \bullet 12H_2O$	Hydrated Sodium Aluminosilicate	Faujasite (zeolite)	00-039-1380
$NaAlSiO_4$	Sodium Aluminosilicates	Nepheline	00-035-0424
$NaAlSi_2O_6$		Jadeite	00-022-1338
$KAlSiO_4$	Potassium Aluminosilicates $KAlSiO_4$	Megakalsilite	14-014-5043
$KAlSiO_4$		Kalsilite	00-011-0579
$KAlSiO_4$		Kaliophilite	00-011-0313

*any minor phase present at 2-5 wt%, like sulfate phases, cannot be detected by XRD analysis.

The findings from TI-102 indicated that the residence time of the waste in the DMR may have been too short and thus conversion of feed alkali to the desired product (carbonates) was incomplete. Results have demonstrated that the presence of non-carbonate alkali compounds like NaOH will contribute to phase assemblages with undesirably low melting points in the DMR system.[8] Eliminating the potential for these low melting phases requires knowledge of reaction rates between the alkali in the system and species in the gas phase. Control of these reaction rates includes a diffusion rate component and the inherent chemical reaction rates for alkali with these gaseous species. In order to understand the competing rates of the carbonation reactions (desired) and alkali reactions with other gaseous species (undesired), the inherent gas solid chemical reaction rates must be measured. As these become available, they can be added to overall rate equations to develop means to promote alkali carbonation and suppress other alkali/gas phase reactions that may be controlling bark formation.[8]

1.6 SUMMARY OF CURRENT TESTING OF SBW CARBONATE FLOW SHEET

From November/December 2015 through January 2016, the second and third non-radioactive IWTU start-up campaigns, referred to as TRP-8023-1 and TRP-8023-2, processed 8,600 and 30,500 gallons more simulant respectively, under more restrictively controlled feed rate and NAR ratios than campaign TI-102. Less bark was produced than in TI-102 and unidentified rocks were found to be a component of the coal. The contractor sent eleven samples to SRNL for analyses and requested that the following questions be answered:

1. Identify the chemical constituents of the bark 2015 vs bark 2014 vs bark Hazen.
2. What is the binder (potassium or other element) in the bark?
3. What is the melting point of the bark?
4. Are the rocks in the coal a factor in the bark?
5. Is there an additive that will lock out the binder from the reaction that causes the wall scale?
6. Can the feed be diluted so the binder in the bark is less effective or made innocuous?
7. What other operating changes might help prevent wall scale – DMR operating temperature, DMR operating temperature control, waste feed rate, NAR, superheated steam velocity (SSV), CO_2?

The scope of analyses was split between Idaho National Laboratory Battelle Energy Alliance (INL-BEA) and SRNL according to Table 1-6. This report summarizes results of the SRNL analyses listed in Table 1-6. The INL-BEA analysis results are reported separately.

Table 1-6. Analyses to be performed at the INL and SRNL

Analysis	Laboratory	
	INL-BEA	SRNL
Crush/grind prior to analysis	X	X
Scanning Electron Microscopy/Energy Dispersive Analysis by X-ray (SEM/EDAX). Elemental mapping (cross-section bark samples, bed particle samples (mount/grind/polish bed samples to enable particle cross-sections)		X
Optical microscopy to see magnified particles	X	
SEM/EDAX for elemental composition and morphology	X	
Softening/melting point	X	X
Thermo Gravimetric Analysis (TGA) in air	X	X
X-ray Diffraction (XRD)		X
Wet chemistry for anions and cations	X	X
Soluble/Insoluble Wet chemistry of anions and cations		X
Differential Scanning Calorimety (DSC)	X	X
Fourier Transform Infrared Spectroscopy (FTIR)		X
Infrared Reflectance (IR)		X
Raman Spectroscopy		X

Eleven samples were received and were pre-numbered so that INL-BEA and SRNL used the same sample numbers (Table 1-7). Samples were from the DMR during shut down, from the Auger Grinder (AG), from the product receipt drums, and rocks from the raw coal.

Table 1-7. Analyses Performed by SRNL on Various Samples

Sample Number	Sample ID	Sample Analyses Performed by SRNL
1	DMR bed media Dec15	XRD/Wet Chemistry
2	DMR bed media Dec15 (more product)	XRD/Wet Chemistry
3	DMR bark 19Dec15	XRD/Wet Chemistry/SEM-EDAX/DSC/FTIR/TGA/IR/Raman Spectroscopy
4	DMR rocks 17Dec15	XRD
5	Coal rocks from bed 19Dec15	XRD
6	Rocks from coal Dec15	XRD
7	DMR drum 1 vacuumed thru downcomer 16Dec15	XRD
8	DMR drum 2 vacuumed thru downcomer 16Dec15	XRD
9	DMR scale sifted from DMR auger 19 Dec15	XRD
10	AG material 19Dec15	XRD/Wet Chemistry/SEM
11	AG compressed product 19Dec15	XRD

The phase identification of every sample was determined by XRD. When rocks from the DMR and/or raw coal had different colors, multiple XRD's were performed to see the variation in the rock components. Whole element chemistry was determined by dissolution and wet chemistry of the vessel contents, the bark deposits, and the AG deposits. The soluble portion of the vessel contents and deposits were dissolved in water at 80°C for 2 hours (1g solid/100mL deionized water). The water soluble portions of the deposits are believed to be the low melting phase(s) that act as the "glue" for the bark adhering to the DMR walls and the glue that entrains the DMR bed contents. The water insoluble contents of the vessel contents and deposits were dissolved by fusion in acid or sodium peroxide at elevated temperatures and then analyzed. The soluble and insoluble analyses were combined to get whole element chemistries for each sample. The soluble and insoluble portions were weighted by the amount of each determined during the hot water dissolution to get the whole element chemistry. Whole element chemistry included cations (Al, Ca, Cr, Fe, K, Mg, Mn, Na, Ni, P, S, Si, Ti), anions (F, Cl, NO_2, NO_3, SO_4 and PO_4) including Total Inorganic Carbon (TIC) and moisture content measured at 107°C.   The coal content of the entire sample, which was mainly in the insoluble fraction, was determined by ashing at 525°C in air which removes the coal contribution but not the sulfur [16] and/or the alkali carbonate product phases. Mass balance was performed using the phases identified by XRD analyses. The details of the mass balance are given in Appendix I.

Neither particle size, $Fe^{2+}/\Sigma Fe$ REDOX (REDuction/OXidation) ratio, nor sample density were measured. Analyses concentrated on additional testing of the bark and included, TGA, DSC, FTIR, and IR to assist with the determination of the soluble and insoluble fractions of the bark. All the analyses performed on

the vessel contents, the unanticipated deposits, and the coal rocks are documented in this study. These analyses are then used to determine the cause of the chemical scale and deposits.

2.0 DMR BED PRODUCT ANALYSES

2.1 DMR BED PRODUCT PHASE ANALYSES BY XRD (Samples #1 & #2)

The DMR product bed Sample #1, as analyzed by XRD, was mostly Al_2O_3 startup bed and coal ash products (SiO_2 as quartz and $Al_6Si_2O_{13}$ as mullite). The fines contained $NaAl_{11}O_{17}$ (Diaoyudaolite) and FeO (wustite) as well (Table 2-1).

The DMR product bed Sample #2, as analyzed by XRD, contained the desired product phase $Na_2CO_3.H_2O$ (thermonatrite) and $KAlSiO_4$ (kalsilite) along with startup bed Al_2O_3 (corundum) and coal ash SiO_2 (quartz) (Table 2-1). The presence of $NaAlSi_2O_6$ (jadeite), which is a high pressure mineral phase, is puzzling as $NaAlSiO_4$ (nepheline) should have formed preferentially from the sodium in the feed and the aluminosilicate in the fly ash. Jadeite was not found in the DMR rocks (Sample #4), nor in the coal rocks found in the bed (Sample #5), nor in the rocks from the bags of coal (Sample #6) as discussed in Section 4.0.

Table 2-1. X-ray Identification of Phases in DMR Bed Product

Sample Location	Sample Color/Description	XRD Phases Identified	ICDD (Intl. Centre for Diffraction Data)*
DMR Bed Media (#1)	Fines	Al_2O_3 (corundum) SiO_2 (quartz) $NaAl_{11}O_{17}$ (Diaoyudaolite) FeO (wustite)	00-010-0173 00-046-1045 00-021-1096 00-006-0615
	Gray	SiO_2 (quartz) $Al_6Si_2O_{13}$ (mullite)	00-046-1045 00-015-0776
DMR Bed Media (more Product) (#2)	Composite	Al_2O_3 (corundum) $Na_2CO_3.H_2O$ (thermonatrite) $NaAlSi_2O_6$ (jadeite) $KAlSiO_4$ (kalsilite) SiO_2 (quartz)	00-010-0173 00-008-0448 00-022-1338 00-044-0579 00-046-1045

2.2 DMR BED PRODUCT SOLUBLE/INSOLUBLE CHEMICAL ANALYSES (Samples #1 & #2)

The physical characteristics of the DMR bed products (Sample #1 & #2) are shown in Figure 2-1. The DMR bed products were dissolved in 80°C deionized ASTM-Type I water. Three grams of solid were dissolved in 300 mL of water for 2 hours. The insoluble solids were analyzed by XRD and the soluble solids were determined by the difference between the XRD analyses of the as-received sample (Table 2-1) and the insoluble solids sample.

The dissolution water was analyzed so a mass balance could be performed of the soluble and insoluble phases. In the soluble mass balance, the anions and cations are balanced on the soluble phases determined by the difference in XRD analyses mentioned above. Once the analyzed anions are balanced

against the cations, there is often excess alkali which is reported as $Na_2O(ex)$. Note that this excess sodium is calculated as sodium oxide in the mass balance which is performed on room temperature samples but that the excesss Na is likely NaOH at the DMR operating temperature.

The insoluble solids were dissolved in acid and analyzed so a mass balance could be performed against the insoluble solid phases identified by XRD. The soluble and insoluble fractions were weighted by their mass fraction, which had been determined during the dissolution, so that a whole element chemistry could be determined. The mass balance for DMR Bed Sample #1 are given in Table 2-2 and for DMR Bed Sample #2 are given in Table 2-3. The raw data and the methodology used for calculation of the mass balance against the phases determined by XRD are given in Appendix I.

| Sample #1 DMR Bed Media December 15, 2015 (mm ruler divisions) | Sample #2 DMR Bed Media More Product December 15, 2015 (mm ruler divisions) |
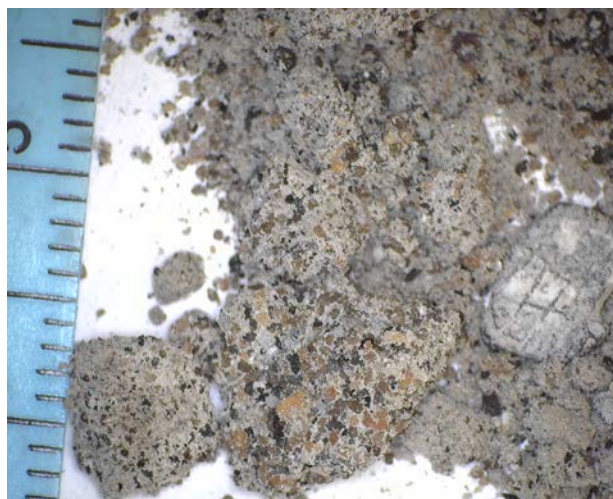
Figure 2-1. DMR Bed Media Sample #1 and Sample #2.

Table 2-2 demonstrates that Sample #1 was mostly 96 wt% insoluble startup bed composed of Al_2O_3, a minimal coal content of 0.78 wt%, and flyash components such as SiO_2 and Al_2O_3. There was only 0.07 wt% Na_2CO_3 bed product and little to no excess $Na_2O(ex)$ over the anions used for mass balance. Table 2-3 demonstrates that Sample #2 has only 60.61 wt% insoluble startup bed composed of Al_2O_3 and a coal content of 14.37 wt%. Coal ash, alumina and silica species, account for another 12 wt%. Bestac coal ash from 2008 was measured to be $0.57Al_2O_3 \bullet 2.64SiO_2$ while the IWTU Bestac coal from 2014 was measured [7] to contain $0.48Al_2O_3 \bullet 2.79SiO_2$ indicating that the coal ash is richer in silica than alumina. The Na_2CO_3 to K_2CO_3 bed product accounts for an additional 11.19 and 1.99 wt% of the DMR bed. Excess Na over the anions analyzed is small accounting for 0.11 wt%. This is likely present at the DMR operating temperature in the high steam fugacity as NaOH (or KOH) and the presence of this phase in TPR-8023 (1&2) was much lower than in the previous TI-102 campaigns.

Table 2-2. Soluble/Insoluble Species Mass Balance for DMR Bed Media Sample #1

Chemical Species by XRD	SAMPLE #1 DMR Bed Media Dec 15 Soluble	SAMPLE #1 DMR Bed Media Dec 15 Insoluble	SAMPLE #1 DMR Bed Media Soluble and Insoluble
% Soluble vs Insoluble Used in Calculations (3 g/300mL)	0.001	99.999	100
Al_2O_3		95.95	95.95
$Al(OH)_3$	17.91		0.02
CaO			
$CaCO_3$	24.61		0.03
Cr_2O_3			
Fe_2O_3		0.36	0.36
K_2O			
K_2CO_3			
MgO			
$MgCO_3$			
MnO			
$NaAlO_2$			
Na_2O (sil)		0.15	0.14
Na_2O (ex)	0.62		0.001
Na_2CO_3	70.65		0.07
NaCl			
$NaNO_3$			
NiO			
P_2O_5			
Na_2SO_4			
SiO_2		3.47	3.47
TiO_2			
F, Cl, NO_2,NO_3, SO_4,PO_4 all below detection limits			
Whole Sample Coal by wt loss at 525°C		0.78	0.78
Sum	113.79	99.93	100.91
pH	9.55		
XRD As-received	Al_2O_3 (corundum) SiO_2 (quartz), $NaAl_{11}O_{17}$ (diaoyudaolite), FeO (wustite), $Al_6Si_2O_{13}$ (mullite)		
XRD Insoluble Phases	Al_2O_3 (corundum) SiO_2 (quartz), $NaAl_{11}O_{17}$ (diaoyudaolite), FeO (wustite), $Al_6Si_2O_{13}$ (mullite)		
Soluble Phases by Difference	None		

Table 2-3. Soluble/Insoluble Species Mass Balance for DMR Bed Media Sample #1

Chemical Species by XRD	Sample 2 DMR Bed Media (More Product) Soluble	Sample 2 DMR Bed Media (More Product) Insoluble	Sample 2 DMR Bed Media (More Product) Soluble and Insoluble
% Soluble vs Insoluble Used in Calculations (3 g/300mL)	17.24	82.76	100
Al_2O_3		73.23	60.61
$Al(OH)_3$	35.55		6.13
CaO			
$CaCO_3$	0.265	0.33	0.32
Cr_2O_3		0.01	0.01
Fe_2O_3		2.13	1.76
K_2O		0.078	0.06
K_2CO_3	11.53		1.99
MgO		0.14	0.12
$MgCO_3$			
MnO		0.07	0.06
$NaAlO_2$			
Na_2O (sil)		0.53	0.44
Na_2O (ex)	0.635		0.11
Na_2CO_3	64.92		11.19
NaCl			
$NaNO_3$			
NiO			
P_2O_5		0.03	0.02
Na_2SO_4	2.55		0.44
SiO_2	1.96	6.72	5.90
TiO_2		0.11	0.09
F, Cl, NO_2, NO_3, PO_4 all below detection limits-SO_4 only anion found			
Whole Sample Coal by wt loss at 525°C		14.37	14.37
Sum	117.41	97.75	103.62
pH	11		
XRD As-received	Al_2O_3 (corundum), $Na_2CO_3 \cdot H_2O$ (thermonatrite), $NaAlSi_2O_6$ (jadeite), $KAlSiO_4$ (kalsilite), SiO_2 (quartz)		
XRD Insoluble Phases	Al_2O_3 (corundum), SiO_2 (quartz), $NaAl_{11}O_{17}$ (diaoyudaolite), FeO (wustite), $KAlSiO_4$ (kalsilite), $Ca(Mg,Al)(Si,Al)_2O_6$ (diopside)		
Soluble Phases by Difference	$Na_2CO_3 \cdot H_2O$ (thermonatrite)		

3.0 BARK ANALYSES FROM DMR WALL (Sample #3), DMR SCALE SIFTED FROM AG (Sample #9), AG (Sample #10 & #11), AND DMR SCALE VACUMMED THROUGH DOWNCOMER INTO DRUMS (Samples #7 & #8)

Samples of bark taken on December 19, 2015 from the DMR were received (Sample #3 shown in Figure 3-1). DMR scale was also vacuumed through the downcomer into drums (Drum #1 and #2) and are shown in Figure 3-2a and Figure 3-2b and are labelled Samples #7 and #8. More DMR scale was sifted from the AG on December 19, 2015 and is shown in Figure 3-2c and Figure 3-2d and labelled as Sample #9.

Samples from the AG were also received (Sample #10) and a sample of the compressed AG material (Sample #11). The AG samples are discussed in this section in order to determine if the AG material or AG compressed samples were enriched in bark components. The AG material (Sample #10) is shown in Figure 3-3 and looks bark like visually. Close up photographs of the AG material (Sample #10) and the compressed AG material (Sample #11) are shown in Figure 3-4 and appear very granular in nature.

(a)   DMR Bark Sample #3 Top Face Exposed to DMR Chamber
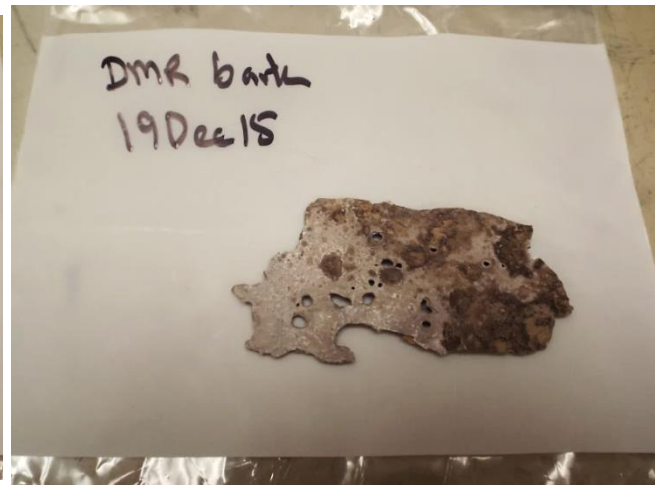
(b) DMR Bark Sample #3 Attached to DMR Metallic Wall

Figure 3-1. DMR Bark from December 19, 2015

(a)   DMR Drum #1 Vacuumed through Downcomer Sample #7 December 16, 2015

(b) DMR Scale Sifted from DMR Auger Sample #8 December 19, 2015

(c)   DMR Scale Sifted from DMR Auger Sample #9 December 19, 2015

(d) DMR Scale Sifted from DMR Auger Sample #9 December 19, 2015

Figure 3-2. Auger Grinder Material from DMR Bed and Drums (Samples #7, #8, #9)
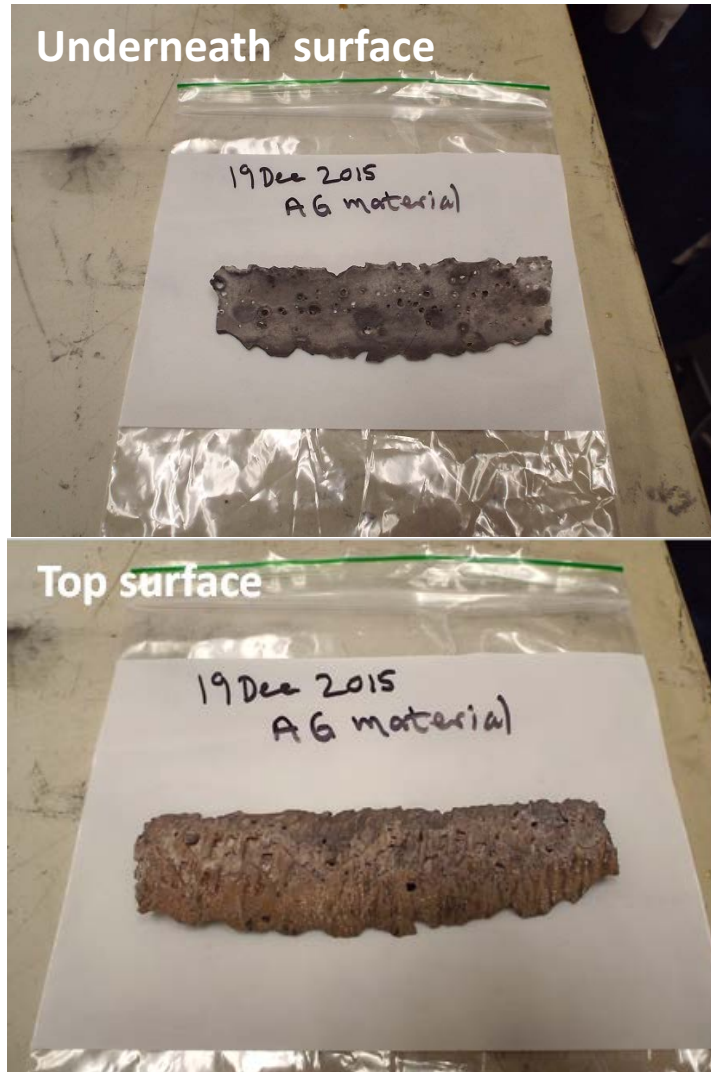
Figure 3-3. AG material (Sample #10) top and bottom surfaces.

(a)   AG Material Sample #10 December 19, 2015

(b) AG Compressed Material Sample #11 December 19, 2015
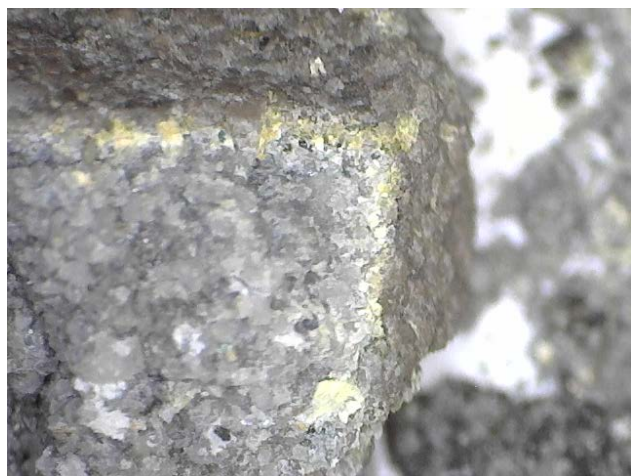
(c)   AG Compressed Material Sample #11 December 19, 2015
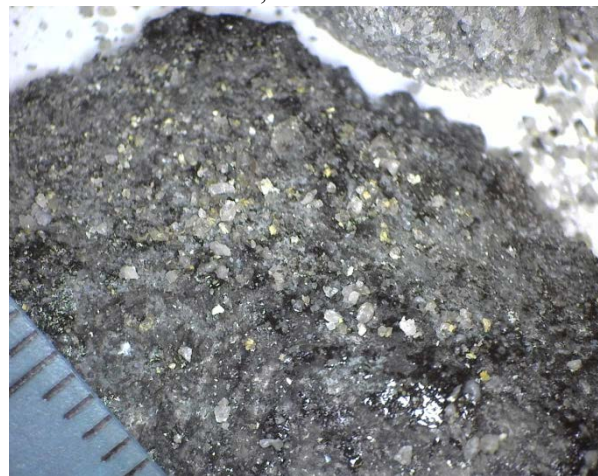
(d) AG Compressed Material Sample #11 December 19, 2015

Figure 3-4. Auger Grinder Material (Samples #10 & #11).

3.1 DMR BARK PHASE ANALYSES BY XRD (Sample #3)

Samples of wall bark from the DMR (Sample #3) were analyzed by XRD as a ground up composite and the top and bottom surfaces were analyzed by XRD. The ground composite and top of the bark, the portion facing into the DMR chamber were composed of only two crystalline phases, i.e. the product Na_2CO_3 and $Na_4Mg_2Si_3O_{10}$ (Table 3-1). The same two phases were found on the bottom of the bark, the portion that adhered to the metal wall of the DMR. In addition, the bottom surface had two different polymorphs of $Al(OH)_3$ known as bayerite and gibbsite.

The most important part of the phase analysis of the DMR bark were the XRD spectra themselves and the identification of $Na_4Mg_2Si_3O_{10}$ (sodium magnesium silicate). For the DMR wall bark (Sample #3) the peaks of the composite sample are relatively sharp indicating crystalline phases and there is no amorphous hump in the spectra (Figure 3-5). The XRD pattern of the top surface of the bark (Figure 3-6a) exhibits a broad amorphous hump in the spectra characteristic of a glassy amorphous phase and broad peaks as indicated by the double headed arrow superimposed on the spectra. Broad peaks indicate

that the crystalline phase, the $Na_4Mg_2Si_3O_{10}$, is partially amorphous and poorly crystallized. Figure 3-6b which is the XRD spectra of the bottom surface of the bark (attached to the DMR wall) indicates that the material is more crystalline and there is less glass, i.e. the glass that may have been there initially has started to crystallize.

There is no Mg in the IWTU simulants (Table 1-3) but there is 0.25-1.23 wt% MgO in the Bestac coal ash and 2.03-22.70 iron oxide which is reported on an Fe_2O_3 weight percent basis.[7] However, at the oxygen fugacity of the IWTU [8] most of the iron will be FeO which can substitute for MgO easily in a glassy or partially crystalline phase. Moreover, crystalline $Na_4Mg_2Si_3O_{10}$ is known to crystallize from a glass in the binary phase system of the $Na_2O \bullet 2SiO_2 - 2(MgO \bullet Na_2O \bullet 1.5SiO_2)$ where $Na_2O \bullet 2SiO_2$ is $Na_2Si_2O_5$.[17]

The phases identified in the TPR-8023 (1&2) bark are not the same as those found in the TI-102 bark (Table 3-2), i.e. $NaAlO_2$ is absent and megakalsilite is absent. The phases in the TPR-8023 (1&2) bark are similar to those identified in the CP-1/CP-2 campaigns (Table 3-3). Note that in Table 3-3 $Na_4Mg_2Si_3O_{10}$ was also found by x-ray analysis even though the bark was more complex. The CP-1 bark also had kyanite, mixed alkali alkaline earth carbonates $(Na_2Mg(CO_3)_2)$ (Table 3-3) and mixed alkali sulfates $(K_3Na(SO_4)_2)$ which the TI-102 and TPR-8023 (1&2) bark did not have (Table 3-2 and Table 3-1 respectively). In addition, the CP-1 bark had trace amounts of $NaNO_2$ (Table 3-3) and the TI-102 bark had none (Table 3-2). The CP-1 bark may have been formed by the same or similar mechanisms but these mechanisms were confounded because in CP-1, glassy Mulcoa had been added to the DMR as well as PurOX (Fe_2O_3) a denitration catalyst. Therefore, the presence of the kyanite from the Mulcoa and the PurOX obscured the actual bark formation mechanism. The 2015 DMR bark is chemically simpler but the formation is still complex. The TPR-8023 (1&2) is compositionally the simplest bark produced in the DMR to date and this should facilitate understanding the formation mechanism.

3.2 AG BARK AND COMPRESSED MATERIAL PHASE ANALYSES BY XRD (Sample #10 & #11)

The AG bark (Sample #10) was also analyzed as a composite and found to contain the Na_2CO_3, $Na_4Mg_2Si_3O_{10}$, and gibbsite (Table 3-1). The top and bottom surfaces were analyzed separately and found to contain only sodium carbonate and alkali magnesium silicate by XRD analysis. The most important part of the phase analysis of the AG bark were the XRD spectra themselves and the identification of $Na_4Mg_2Si_3O_{10}$ (sodium magnesium silicate). For the AG bark (Sample #10) the peaks of the composite sample are relatively sharp indicating crystalline phases and there is no amorphous hump in the spectra (Figure 3-7). The XRD pattern of the top surface of the bark (Figure 3-8a) exhibits a broad amorphous hump in the spectra characteristic of a glassy amorphous phase and broad peaks as indicated by the double headed arrow superimposed on the spectra. This is identical to what was seen in Figure 3-6 for the DMR bark. Broad peaks indicate that the crystalline phase, the $Na_4Mg_2Si_3O_{10}$, is partially amorphous and poorly crystallized. Figure 3-8b which is the XRD spectra of the bottom surface of the bark (attached to the DMR wall) indicates that the material is more crystalline and there is less glass, i.e. the glass that may have been there initially has started to crystallize.

The AG compressed material (Sample #11), which was thought to be compressed bark and bed product and contained gray and black colored material (Figure 3-4). The black colored material was indeed compressed bark and bed material and contained $Na_{1.95}Al_{1.95}Si_{0.05}O_4$ (sodium aluminate), startup bed Al_2O_3 (corundum), and the bed products Na_2CO_3 (natrite) and $Na_4Mg_2Si_3O_{10}$ (sodium magnesium silicate) (Table 3-1). The black material also contained $Na_2Al_2Si_4O_{12} \bullet 8H_2O$, the mineral faujasite, which cannot form unless NaOH is present (see discussion in Section 1.5). The gray material was primarily SiO_2 (quartz), $CaCO_3$ (calcite), and a trace of $Al(OH)_3$ (gibbsite) and $Ca(OH)_2$ (portlandite) (Table 3-1). Since there is no calcium in the simulant, the calcium has to come from the coal ash and the presence of calcium in the compressed AG material indicates that the fly ash is reacting with DMR gases, i.e. steam or NaOH

as a source of OH and forming cementitious like materials, portlandite, in the AG (see components of fly ash in Reference 7).

3.3 DMR BARK PHASE ANALYSES BY XRD (Sample #7, #8, #9)

Samples of bark of different colors were analyzed by XRD analysis from the drums that had been filled by vacuuming the DMR through the downcomer (Samples #7 & #8) and by sifting DMR scale from the DMR auger (Sample #9). These samples contain bark of various colors (red, orange, and gray as shown in Figure 3-2). The samples contained the bark components, mostly Na_2CO_3, and $Na_4Mg_2Si_3O_{10}$ with $Al(OH)_3$ (bayerite or gibbsite) and some Al_2O_3 startup bed and SiO_2 (quartz) (Table 3-1). The samples also contained hydrated $Na_2CO_3 \bullet H_2O$ and $(K,Na)AlSiO_4$ bed product which was to be expected (Table 3-1). The $Na_4Mg_2Si_3O_{10}$ is ubiquitous and there is a noted absence of $NaAlO_2$.

Table 3-1. X-ray Identification of Phases in Bark from DMR, AG, and Drums

Sample Location	Sample Color/Description	XRD Phases Identified	ICDD (Intl. Centre for Diffraction Data)*
DMR Bark (#3)	Ground composite	$Na_4Mg_2Si_3O_{10}$(sodium magnesium silicate) Na_2CO_3 (natrite)	00-033-1265 00-037-0451
	Top (facing DMR chamber) peaks not sharp	$Na_4Mg_2Si_3O_{10}$ (sodium magnesium silicate) Na_2CO_3 (natrite)	00-033-1265 00-037-0451
	Bottom (touching DMR metal)	$Na_4Mg_2Si_3O_{10}$ (sodium magnesium silicate) Na_2CO_3 (natrite) $Al(OH)3$ (bayerite) $Al(OH)3$ (gibbsite)	00-033-1265 00-037-0451 00-020-0011 00-033-0018
DMR-Drum 1- Vac thru Downcomer Bark (#7)	White	SiO_2 (quartz) $KAlSi_3O_8$ (microcline)	00-046-1045 00-019-0926
	Red Bark Like	$Na_2CO_3 \bullet H_2O$ (thermonatrite) Na_2CO_3 (natrite) $Al(OH)_3$ (bayerite) $Na_4Mg_2Si_3O_{10}$ (sodium magnesium silicate) $NaAlSiO_4$ (nepheline)	00-008-0448 00-037-0451 00-020-0011 00-033-1265 00-035-0424
	Orange Bark Like	$Na_2CO_3 \bullet H_2O$ (thermonatrite) $Al(OH)_3$ (bayerite) $Na_4Mg_2Si_3O_{10}$ (sodium magnesium silicate) $NaAlSiO_4$ (nepheline) $KAlSiO_4$ (kalsilite)	00-008-0448 00-020-0011 00-033-1265 00-035-0424 00-011-0579
	Light Orange Bark Like	$Na_2CO_3 \bullet H_2O$ (thermonatrite) $Al(OH)_3$ (bayerite) $Na_4Mg_2Si_3O_{10}$ (sodium magnesium silicate) $NaAlSiO_4$ (nepheline) $KAlSiO_4$ (kalsilite)	00-008-0448 00-020-0011 00-033-1265 00-035-0424 00-011-0579
	Gray with Light Brown Pellet	SiO_2 (quartz) $KAl_3Si_3O_{11}$ (potassium aluminosilicate) $(Ca,Na)(Al,Si)_2Si_2O_8$ (anorthite)	00-046-1045 00-046-0741 00-020-0528
	Gray Bark	$Na_2CO_3 \bullet H_2O$ (thermonatrite) Na_2CO_3 (natrite) $Al(OH)_3$ (bayerite) $Na_4Mg_2Si_3O_{10}$ (sodium magnesium silicate) $NaAlSiO_4$ (nepheline)	00-008-0448 00-037-0451 00-020-0011 00-033-1265 00-035-0424
	Gray Bark	$Na_2CO_3 \bullet H_2O$ (thermonatrite) $Al(OH)_3$ (bayerite) $Na_4Mg_2Si_3O_{10}$ (sodium magnesium silicate) $NaAlSiO_4$ (nepheline) $KAlSiO_4$ (kalsilite)	00-008-0448 00-020-0011 00-033-1265 00-035-0424 00-011-0579
	Black	SiO_2 (quartz) and amorphous	00-046-1045

Sample Location	Sample Color/Description	XRD Phases Identified	ICDD (Intl. Centre for Diffraction Data)*
DMR-Drum 2- Vac thru Downcomer Bark (#8)	Bark	$Na_4Mg_2Si_3O_{10}$ (Sodium Magnesium Silicate) $Na_2CO_3 \cdot H_2O$ (thermonatrite) $KAlSiO_4$ (kalsilite) $NaAlSiO_4$ (nepheline)	00-033-1265 00-008-0448 00-011-0579 00-035-0424
	Black chunk	Graphite-3R (carbon)	00-026-1079
	Gray chunk	SiO_2 (quartz) $KAl_3Si_3O_{11}$ (dehydroxylated K-Al Silicate) $(Ca,Na)(Al,Si)_2Si_2O_8$ (Anorthite)	00-046-1045 00-046-0741 00-020-0528
	Black	$Na_{1.95}Al_{1.95}Si_{0.05}O_4$ (sodium aluminate) Al_2O_3 (corundum) Na_2CO_3 (natrite) $Na_4Mg_2Si_3O_{10}$ (sodium magnesium silicate) $Na_2Al_2Si_4O_{12} \cdot 8H_2O$ (faujasite) $NaAl_{11}O_{17}$ (diaoyudaoite) Al_2SiO_5 (andalusite)	00-049-0003 00-010-0173 00-037-0451 00-033-1265 00-039-1380 00-045-1451 00-039-0376
Auger Grinder Bark (#10)	Composite Ground	$Na_4Mg_2Si_3O_{10}$ (sodium magnesium silicate) Na_2CO_3 (natrite) $Al(OH)_3$ (gibbsite)	00-033-1265 00-037-0451 00-033-0018
	Front piece of bark (peaks not sharp)	$Na_4Mg_2Si_3O_{10}$ (sodium magnesium silicate) Na_2CO_3 (natrite)	00-033-1265 00-037-0451
	Back of bark (peaks not sharp)	$Na_4Mg_2Si_3O_{10}$ (sodium magnesium silicate) Na_2CO_3 (natrite)	00-033-1265 00-037-0451
Auger Grinder Material Compressed Material (#11)	Gray	SiO_2 (quartz) $CaCO_3$ (calcite) $Al(OH)_3$ (gibbsite-trace) $Ca(OH)_2$ (portlandite-trace)	00-046-1045 00-005-0586 00-033-0018 00-004-0733
	Black	$Na_{1.95}Al_{1.95}Si_{0.05}O_4$ (sodium aluminate) Al_2O_3 (corundum) Na_2CO_3 (natrite) $Na_4Mg_2Si_3O_{10}$ (sodium magnesium silicate) $Na_2Al_2Si_4O_{12} \cdot 8H_2O$ (faujasite) $NaAl_{11}O_{17}$ (diaoyudaoite) Al_2SiO_5 (andalusite)	00-049-0003 00-010-0173 00-037-0451 00-033-1265 00-039-1380 00-045-1451 00-039-0376

Figure 3-5. Ground up composite of DMR Bark sample #3.
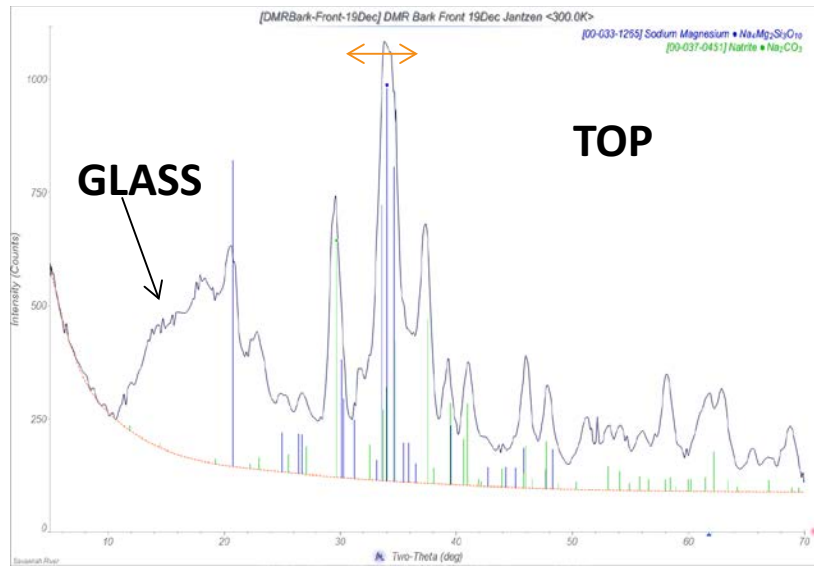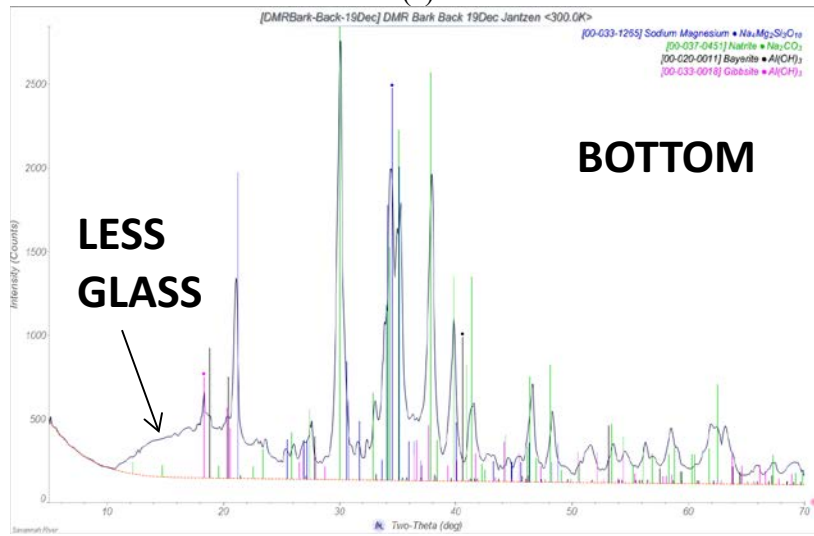
Figure 3-6. Top and Bottom Surfaces of DMR Bark sample #3.

Table 3-2. X-Ray Diffraction of the 2015 IWTU TI-102 Wall Bark Top and Bottom Surfaces, Crushed Wall Bark and Auger Grinder Bark

Phase*	Mineral Name	Relative Amount
XRD Top Bark Surface (As Received)		
$KAlSiO_4$	Kalsilite	Major
$CaCO_3$	Calcite	Major
$Na_2CO_3 \bullet H_2O$	Thermonatrite	Major
$Na_{0.975}Al_{0.975}Si_{0.025}O_2$	Sodium Aluminate	Minor
$MgFe_2O_4$	Magnesioferrite	Minor
XRD Bottom Bark Surface (As Received)		
$KAlSiO_4$	Megakalsilite	Major
$Na_{1.75}Al_{1.75}Si_{0.25}O_4$	Sodium Aluminate	Major
$Na_{0.975}Al_{0.975}Si_{0.025}O_2$	Sodium Aluminate	Major
$KAlSiO_4$	Kalsilite	Minor
$Na_2CO_3 \bullet H_2O$	Thermonatrite	Minor
XRD Wall Bark Crushed (As Received)		
Al_2O_3	Corundum	Major
$Na_{0.975}Al_{0.975}Si_{0.025}O_2$	Sodium Aluminate	Major
$Na_{1.75}Al_{1.75}Si_{0.25}O_4$	Sodium Aluminate	Major
$Na_2CO_3 \bullet H_2O$	Thermonatrite	Major
$KAlSiO_4$	Kalsilite	Minor
$CaCO_3$	Calcite	Minor
Auger Grinder Bark (As Received)		
$Na_{0.975}Al_{0.975}Si_{0.025}O_2$	Sodium Aluminate	Major
$Na_{1.75}Al_{1.75}Si_{0.25}O_4$	Sodium Aluminate	Major
$Na_2CO_3 \bullet H_2O$	Thermonatrite	Minor
$KAlSiO_4$	Kalsilite	Minor

*any minor phase present at 2-5 wt%, like sulfate phases, cannot be detected by XRD analysis

Table 3-3. X-Ray Diffraction of the the CP-1 DMR Bark Phases

ID#	Date Analyzed	Location	Major Phase(s)*	Minor Phase(s)*
End of Scoping Test #1378	3/06	DMR Cyclone Scale	$Na_2Mg(CO_3)_2$ (eitelite), $Na_2(CO_3) \bullet H_2O$ (thermonatrite), $K_3Na(SO_4)_2$ (aphthitalite), $Al(OH)_3$ (bayerite)	$NaAlSiO_4$ (nepheline), Al_2SiO_5 (kyanite)
CP-1 #1378	2/07	DMR Cyclone Scale SURFACE	$Na_2(CO_3) \bullet H_2O$ (thermonatrite), $Al(OH)_3$ (gibbsite)	$NaNO_2$
CP-1 #1511	3/06	DMR Wall Scale WHITE/BLACK	Al_2O_3 (corundum) $NaAlSiO_4$ (nepheline-both hexagonal and cubic structured)	$Na_{1.95}Al_{1.95}Si_{0.05}O_4$ (sodium aluminate) SiO_2 (quartz), $Na_6[Al_6Si_6][1.86NaOH] \bullet 4 H_2O$ (hydroxyl-sodalite)*
CP-1 #1511	3/06	DMR Wall Scale BROWN	$Na_4Mg_2Si_3O_{10}$, Al_2SiO_5 (kyanite)	Al_2O_3 (Corundum), $Na_2(CO_3) \bullet H_2O$ (thermonatrite), $K_3Na(SO_4)_2$ (aphthitalite)
CP-1 #1512	3/06	DMR Free Flowing Bed With AGSCO Al_2O_3 – Bed Drain Product	$Na_2(CO_3) \bullet H_2O$ (thermonatrite), $NaAl_{11}O_{17}$ (Diaoyudaoite), $NaAlO_2$	$Al(OH)_3$ (bayerite), $FeOOH$ (goethite), $K_3Na(SO_4)_2$ (aphthitalite)

*any minor phase present at 2-5 wt%, like sulfate phases, cannot be detected by XRD analysis
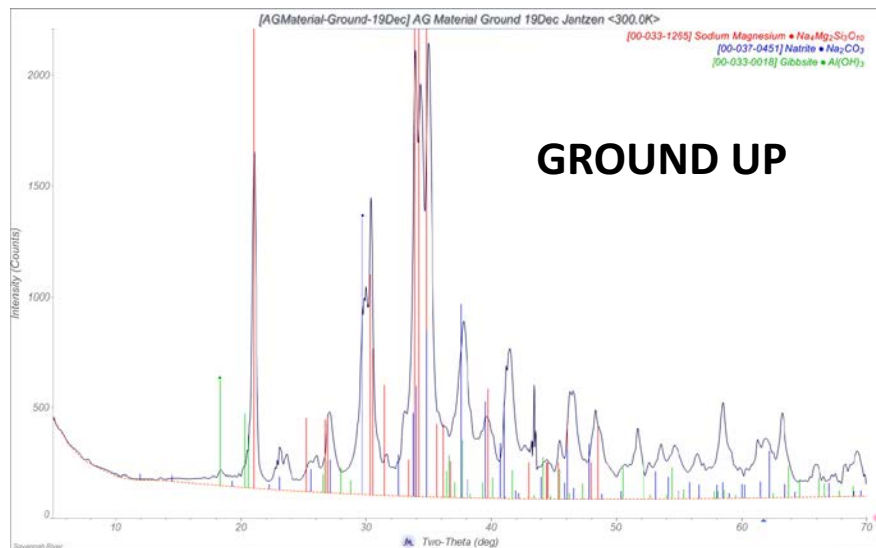
Figure 3-7. Ground up composite of AR Bark sample #10.

(a)

(b)
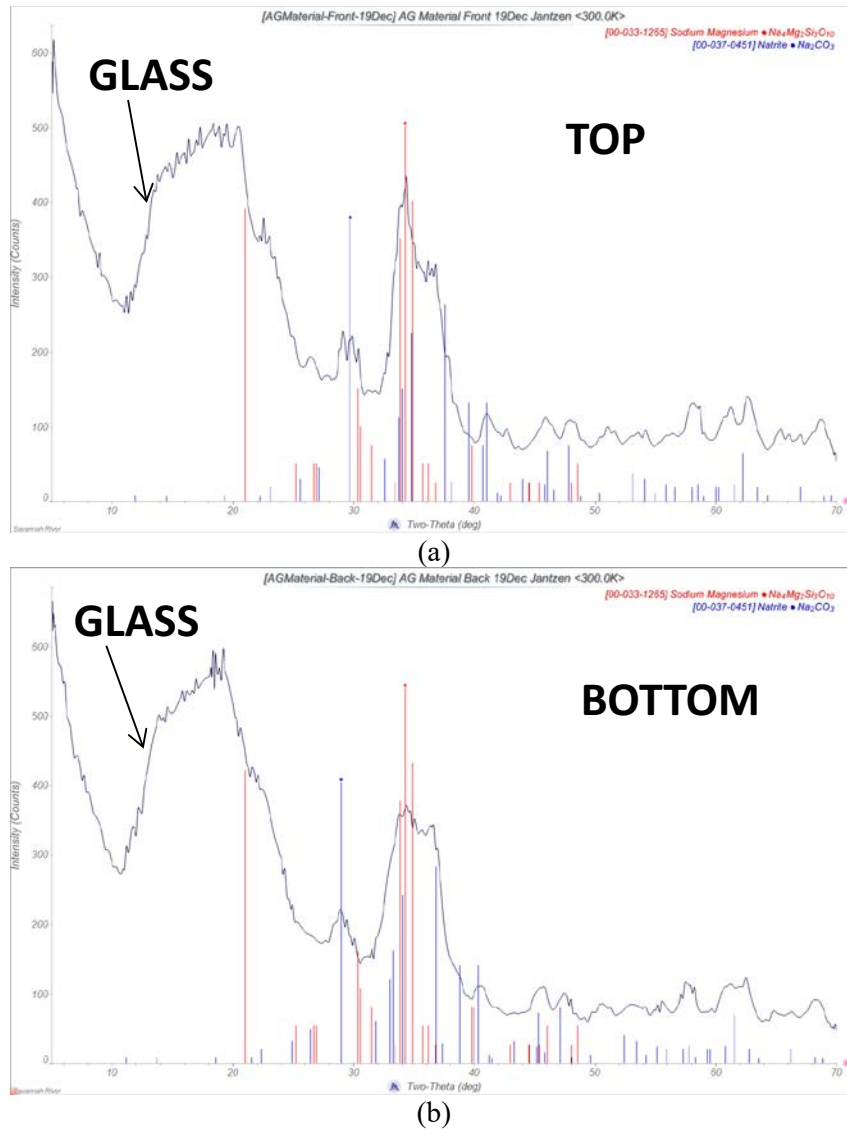
Figure 3-8. Top and Bottom Surfaces of DMR Bark sample #10.

3.4 BARK SOLUBLE/INSOLUBLE CHEMICAL ANALYSIS

Samples #3 (DMR Bark) and #10 (AG Bark) underwent more in depth analyses which included dissolution in 80°C deionized ASTM-Type I water. Three grams of solid were dissolved in 300 mL of water for 2 hours. The insoluble solids were analyzed by XRD and the soluble solids were determined by the difference between the XRD analyses of the as-received sample (Table 3-4 and Table 3-5) and the insoluble solids sample.

The dissolution water was analyzed so a mass balance could be performed against the soluble and insoluble phases. The insoluble solids were dissolved in acid and analyzed so a mass balance could be performed against the insoluble solid phases. The soluble and insoluble fractions were weighted by their mass fraction, which had been determined during the dissolution, so that a whole element chemistry could be determined. The mass balance for the DMR bark (Sample #3) are given in Table 3-4 and for the AG bark Sample #10 are given in Table 3-5. The raw data and the methodology used for calculation of the mass balance against the phases determined by XRD are given in Appendix I.

Table 3-4 demonstrates that Sample #3, the DMR bark, was ~61 wt% soluble Na_2CO_3 with only a small fraction of soluble K_2CO_3, i.e. 0.28 wt%. There is evidence of excess Na_2O in the soluble bark fraction, likely present at the DMR temperatures as NaOH of 0.39 wt%. This is less than observed in TI-102 mass balance but there is still excess NaOH present. The $Al(OH)_3$ polymorph gibbsite is found in the soluble solids. No $NaAlO_2$ is found in the soluble or insoluble solids as it was in previous IWTU campaigns.

Most of the potassium in the DMR bark appears to be in the insoluble solids along with calcium and magnesium (that could be present as insoluble $(Ca,Mg)CO_3$ or $(Ca,Mg)SiO_3$ (Table 3-4). The $Al(OH)_3$ polymorph known as bayerite is found in the insoluble solids. Entrained coal only contributes 1.30 wt% to the bark. The remaining insoluble solids are alkali (Na_2O=3.32 and K_2O=0.77) and silica (9.04) rich. The alkali silicates are much higher in the bark than in the bed media (compare Table 3-4 to Table 2-2 and Table 2-3). When the alkali and silica are converted to a mole % from the weight percent given in Table 3-4, the $(K,Na)_2O:SiO_2$ ratio is 0.42:1 which indicates a glassy or crystalline phase of $Na_2Si_2O_5$.

Table 3-5 demonstrates that Sample #10, the AG bark, was ~57 wt% soluble Na_2CO_3 with only a small fraction of soluble K_2CO_3, i.e. 0.36 wt%. There is evidence of excess Na_2O in the soluble bark fraction, likely present at the DMR temperatures as NaOH of 0.43 wt%. This is less than observed in TI-102 mass balance but there is still excess NaOH present. The $Al(OH)_3$ polymorph gibbsite is found in the soluble solids. No $NaAlO_2$ is found in the soluble or insoluble solids as it was in previous IWTU campaigns.

Most of the potassium in the AG bark appears to be in the insoluble solids along with calcium and magnesium (that could be present as insoluble $(Ca,Mg)CO_3$ or $(Ca,Mg)SiO_3$ (Table 3-5). The $Al(OH)_3$ polymorph known as bayerite and some gibbsite is found in the insoluble solids. Entrained coal only contributes 1.46 wt% to the bark. The remaining insoluble solids are alkali (Na_2O=3.05 and K_2O=0.55) and silica (7.43) rich. The alkali silicates are much higher in the bark than in the bed media (compare Table 3-5 to Table 2-2 and Table 2-3). When the alkali and silica are converted to a mole % from the weight percent given in Table 3-5, the $(K,Na)_2O:SiO_2$ ratio is 0.48:1 which indicates a glassy or crystalline phase of $Na_2Si_2O_5$. The DMR bark (Sample #3) and the AG bark (Sample #10) are chemically almost identical.

Table 3-4. Mass Balance of Soluble/Insoluble Species from DMR Bark

Chemical Species by XRD	SAMPLE 3 DMR Bark 19Dec15 Soluble	SAMPLE 3 DMR Bark 19Dec15 Insoluble	SAMPLE 3 DMR Bark 19Dec15 Soluble and Insoluble
% Soluble vs Insoluble Used in Calculations (3 g/300mL)	67.73	32.27	100.00
Al_2O_3			
$Al(OH)_3$	29.43	56.91	38.30
CaO			
$CaCO_3$	0.135	4.29	1.48
Cr_2O_3		0.03	0.01
Fe_2O_3		1.72	0.56
K_2O		2.40	0.77
K_2CO_3	0.42		0.28
MgO		0.45	0.15
$MgCO_3$			
MnO		0.03	0.01
$NaAlO_2$			0.00
Na_2O (sil)		10.28	3.32
Na_2O (ex)	0.58		0.39
Na_2CO_3	89.91		60.90
NaCl			
$NaNO_3$			
NiO		0.03	0.01
P_2O_5	0.21	0.12	0.18
Na_2SO_4			
SiO_2	0.47	27.04	9.04
TiO_2		0.26	0.08
F, Cl, NO_2,NO_3, SO_4,PO_4 all below detection limits			
Whole Sample Coal by wt loss at 525°C		1.30	1.30
Sum	121.15	104.86	116.77
pH	11.8		
XRD As Received	$Na_4Mg_2Si_3O_{10}$ (sodium magnesium silicate same structure as nepheline), Na_2CO_3 (natrite), $Al(OH)_3$ (bayerite), $Al(OH)_3$ (gibbsite)		
Insoluble XRD Phases	$NaAlSiO_4$ (nepheline), $CaCO_3$ (calcite), SiO_2 (quartz), $Al(OH)_3$ (bayerite)		
Soluble XRD Phases	Na_2CO_3 (natrite), $Al(OH)_3$ (gibbsite)		

*all Na_2CO_3 is $Na_2CO_3 \bullet H_2O$ (thermonatrite) in XRD

Table 3-5. Mass Balance of Soluble/Insoluble Species from AG Bark

Chemical Species by XRD	SAMPLE 10 Auger Grinder Bark 19Dec15 Soluble	SAMPLE 10 Auger Grinder Bark 19Dec15 Insoluble	SAMPLE 10 Auger Grinder Bark 19Dec15 Soluble and Insoluble
% Soluble vs Insoluble Used in Calculations (3 g/300mL)	70.54	29.46	100
Al_2O_3			0.00
$Al(OH)_3$	30.86	57.77	38.79
CaO			0.00
$CaCO_3$	0.16	3.93	1.27
Cr_2O_3		0.04	0.01
Fe_2O_3		2.06	0.61
K_2O		1.87	0.55
K_2CO_3	0.51		0.36
MgO		0.45	0.13
$MgCO_3$			0.00
MnO		0.04	0.01
$NaAlO_2$			0.00
Na_2O (sil)		10.34	3.05
Na_2O (ex)	0.615		0.43
Na_2CO_3	80.48		56.77
NaCl			0.00
$NaNO_3$			0.00
NiO		0.02	0.01
P_2O_5	0.195	0.13	0.18
Na_2SO_4	2.55	0.00	1.80
SiO_2	0.455	24.13	7.43
TiO_2		0.22	0.06
F, Cl, NO_2,NO_3,PO_4 all below detection limits except SO_4			
Whole Sample Coal by wt loss at 525°C		1.46	1.46
Sum	115.83	102.46	112.92
pH	11.8		
XRD As Received	$Na_4Mg_2Si_3O_{10}$ (sodium magnesium silicate same structure as nepheline), Na_2CO_3 (natrite), $Al(OH)_3$ (gibbsite)		
Insoluble XRD Phases	$NaAlSiO_4$ (nepheline), $CaCO_3$ (calcite), SiO_2 (quartz), $Al(OH)_3$ (bayerite), Al_2O_3 (corundum), $Al(OH)_3$ gibbsite		
Soluble XRD Phases	Na_2CO_3 (natrite), $Al(OH)_3$ (gibbsite)		

*all Na_2CO_3 is $Na_2CO_3 \bullet H_2O$ (thermonatrite) in XRD

3.5 DMR BARK MATERIAL (Sample # 3) AND AG BARK MATERIAL (Sample #10) BY SEM
   ANALYSIS

The DMR bark (Sample #3) and AG bark (Sample #10) were further studied by SEM analyses coupled with elemental mapping by Energy Dispersive Analysis by X-ray (EDAX). The DMR sample will be discussed in Section 3.5.1 and 3.5.2 while the AG sample will be discussed in Section 3.5.3.

3.5.1 DMR BARK MATERIAL (Sample #3) SEM OF SIDE FACING DMR CHAMBER

Figure 3-9a shows an optical image of the front face of the DMR bark at an increased magnification compared to Figure 3-1a, i.e. the bark facing the interior of the DMR chamber. The dashed line in Figure 3-9a show flow lines and the box indicates the portion of the sample that is shown in Figure 3-9b. The areas in Figure 3-9b that are marked with an M appear to have been molten causing the flow lines shown in Figure 3-9a. The areas marked with a C appear to be crystalline.
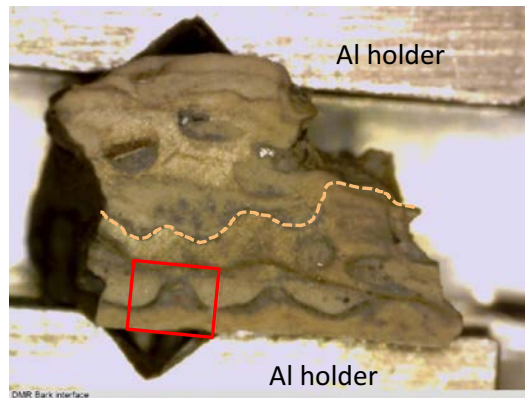
(a) Molten flow lines (dashed line) and box showing area
   from which image (b) was taken
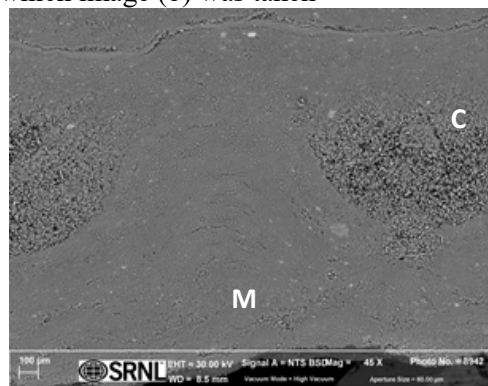
(b) SEM Secondary Electron Image.

Figure 3-9. Optical (a) and SEM (b) images of the DMR Bark Facing the Vessel. Areas labelled M appear to have been molten. Areas labelled C appear to be crystalline.

Figure 3-10 shows the same region of the DMR bark sample as shown in Figure 3-9. SEM elemental maps were used to examine the chemical variation of the surface of the bark. When a given color shows brightly in an elemental map it is enriched in that element compared to the darker/duller regions of the SEM micrograph. Both Na and K are enriched in the molten phase and Na is enriched in the crystalline

phase. Si is also enriched in the crystalline phase and so is carbon. Al is slightly enriched in the crystalline phase. So the molten phase is primarily Na and K and likely NaOH-KOH mixture as there are no other anions or cations present. There is no involvement of Cl, Fe, P, Ca, S, or Ti as elemental maps were taken of all these species and showed nothing. The crystalline phase, which could be a glassy phase that is partially crystalline is Na, Si, K, Al and C rich which indicates that it may be a glassy phase formed by interaction of the coal ash with the NaOH-KOH.

(a) SEM Back Scattered Electron Image   (b) Elemental Map of Na for same area

(c) Elemental Map of Si for same area   (d) Elemental Map of Al for same area

(e) Elemental Map of K for same area   (f) Elemental Map of C for same area
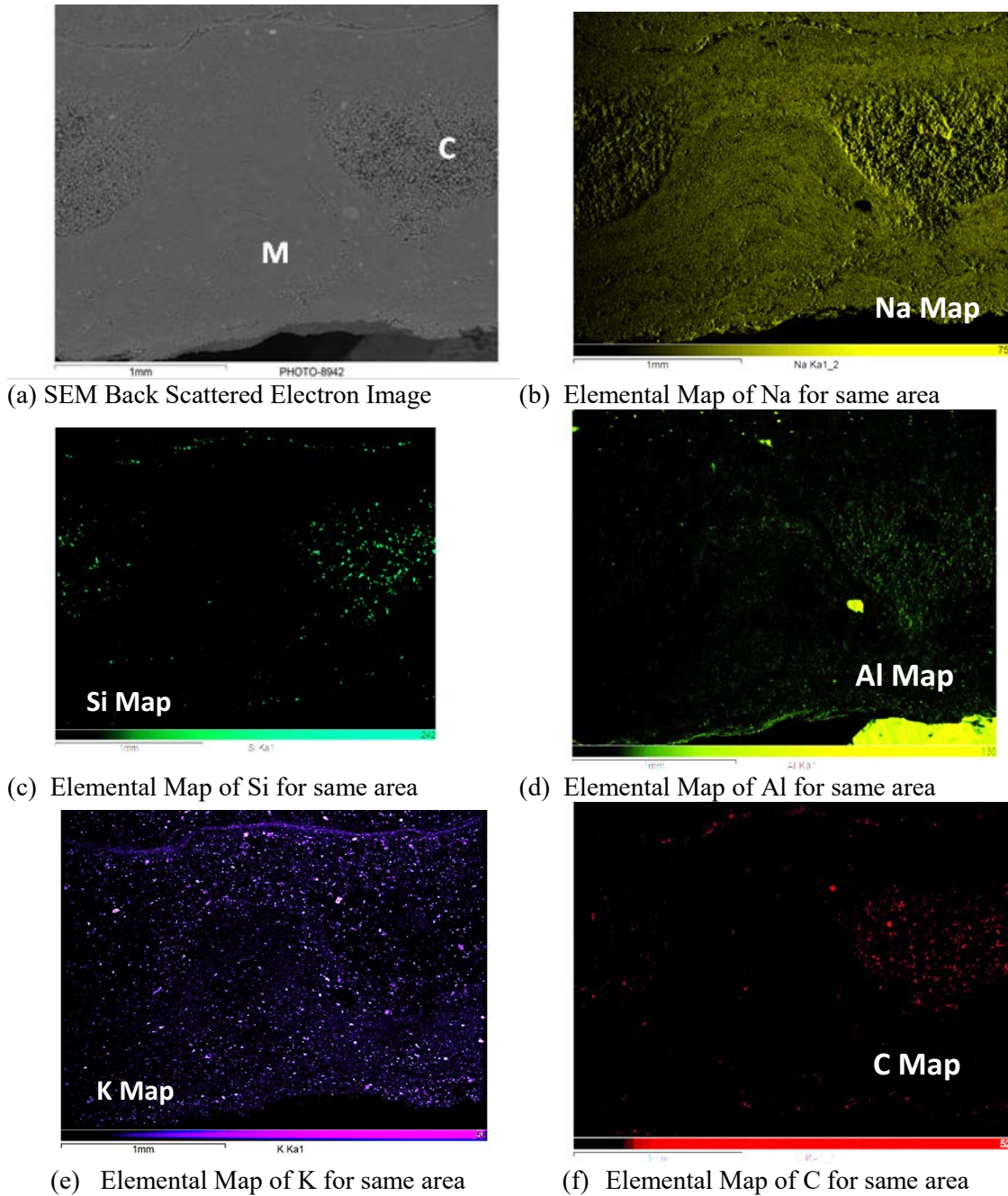
Figure 3-10. SEM elemental maps of the DMR Bark Facing the interior of the vessel. Same area mapped as shown in Figure 3-9.

Figure 3-11a shows a different area of the same sample shown in Figure 3-9. This portion of the DMR bark also shows molten and crystalline regions (Figure 3-11b). The elemental maps corresponding to Figure 3-11b are shown in Figure 3-12. The oxygen elemental map (Figure 3-12a) indicates more oxygen in the molten matrix phase than in the crystallized regions. Figure 3-12b and e shows more Na and K in the molten phase than in the crystallized regions but it also shows participation of K in the crystalline phase which was not observed in the first area of this sample examined. Carbon is higher in the crystalline regions (Figure 3-12f) as is Si (Figure 3-12c). The distribution of Al is interesting as the Al appears to participate in both the molten and crystalline phases (Figure 3-12d). This portion of the bark samples shows the same distributions of elements as the first sample: Na, K, C, Si, Al and less oxygen in the glassy/partly crystalline phase and Na,K,Al in the molten phase. As with the first sample examined this indicates that it may be a glassy phase formed by interaction of the coal ash with the NaOH-KOH.
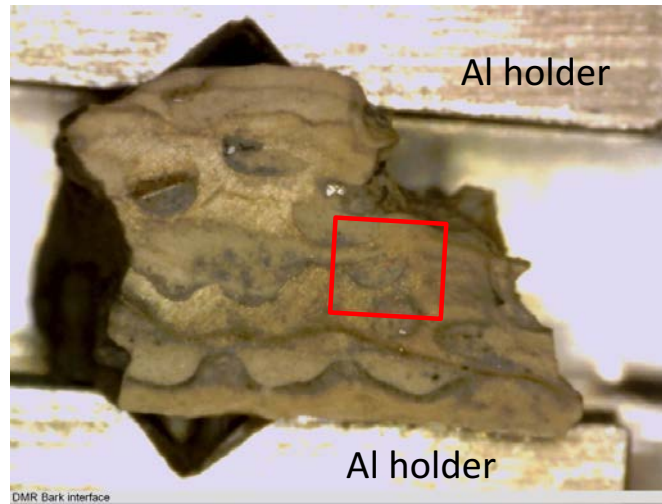
(a) Different area of the bark sample from Figure 10. Box showing area from which image (b) was taken
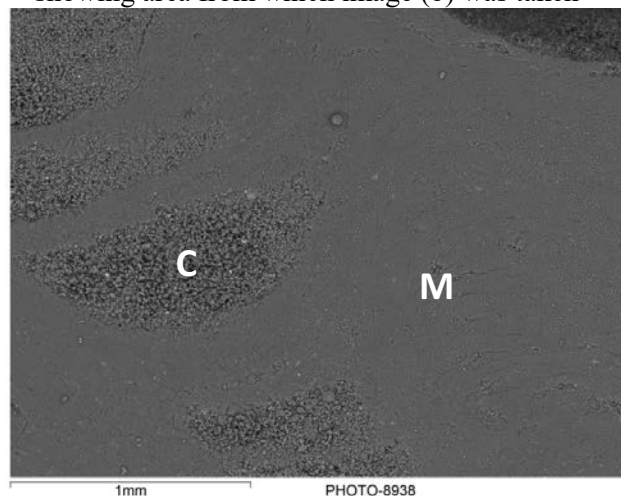
(b) SEM Backscattered Electron Image

Figure 3-11. Optical (a) and SEM (b) images of the DMR Bark Facing the Vessel. Areas labelled M appear to have been molten. Areas labelled C appear to be crystalline. Image b corresponds to Figure 3-12 elemental maps.

(a) Elemental Map of Oxygen

(b) Elemental Map of Na

(c) Elemental Map of Si for same area

(d) Elemental Map of Al

(e) Elemental Map of K
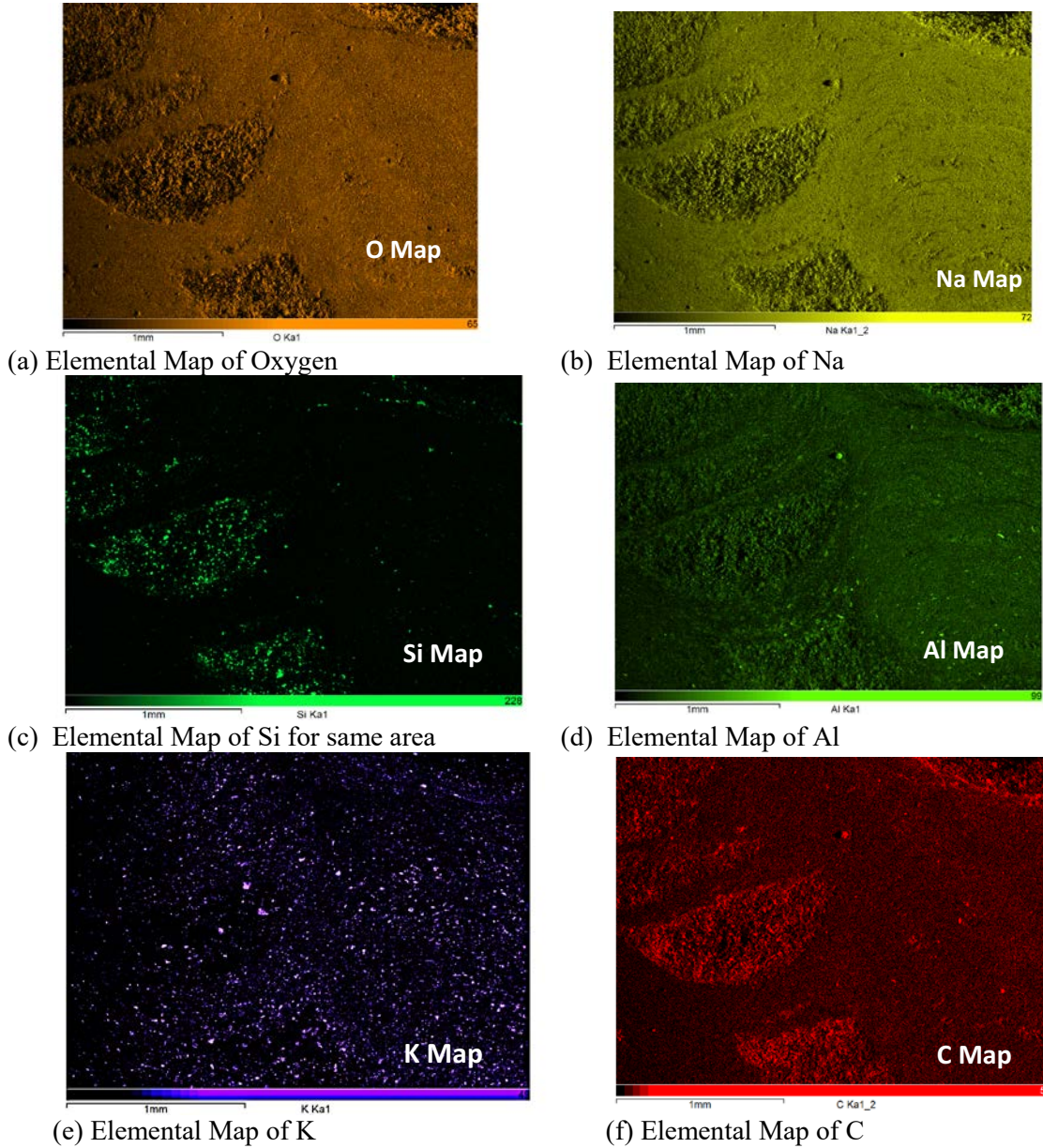
(f) Elemental Map of C

Figure 3-12. SEM elemental maps of the DMR Bark Facing the interior of the vessel. Sample corresponds to the area shown in Figure 3-11.

3.5.2 DMR BARK MATERIAL (Sample #3) SEM CROSS SECTION AND ELEMENTAL MAPS

The DMR bark was also examined in cross section by SEM and elemental mapping. Figure 3-13a and b show the cross section of the bark at different scales. Figure 3-13a is an SEM back scattered electron image that corresponds to the elemental maps in Figure 3-14. Note the partially digested "foot" of crystalline material in the molten flowable regions of Figure 3-13a and b. Figure 3-13 shows that the flow areas contain embedded micro particulates.

The elemental maps shown in Figure 3-14 of the bark in cross section show enrichment of carbon, oxygen, aluminum and sulfur on the side of the bark facing the DMR chamber. The bark is depleted in C

and S with depth (Figure 3-14 f and g). Flow areas are outlined with particulates rich in Al and Si (Figure 3-14c
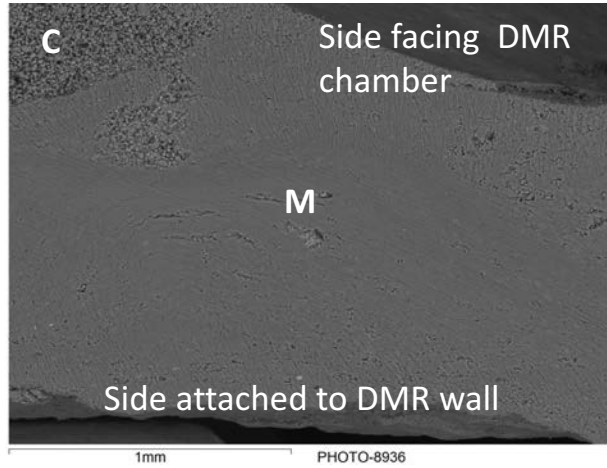
(a)   Cross section of DMR bark.
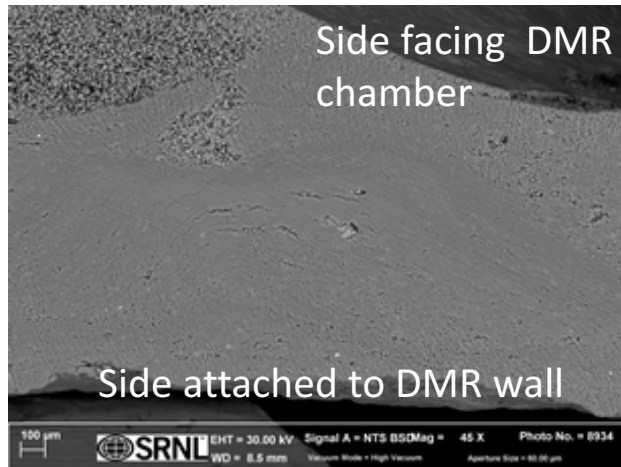
(b) SEM Backscattered Image of a Thin Cross Section.
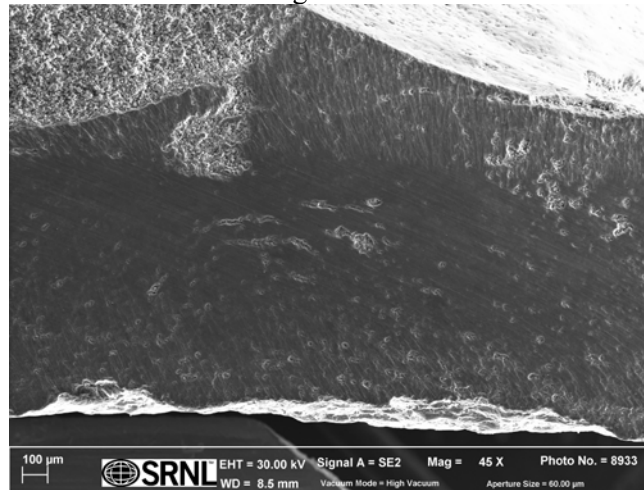
(c) SEM Secondary Electron Image.

Figure 3-13. SEM images of the DMR bark in cross section. Note the partially digested "foot" of crystalline material that protrudes into the molten flow regions. Areas labelled C appear to be crystalline. Image b corresponds to Figure 3-14 elemental maps.

(a) Elemental Map of Oxygen

(b) Elemental Map of Na

(c) Elemental Map of Si for same area

(d) Elemental Map of Al

(e) Elemental Map of K

(f) Elemental Map of C

(g) Elemental Map of S

(h) Elemental Map of Fe
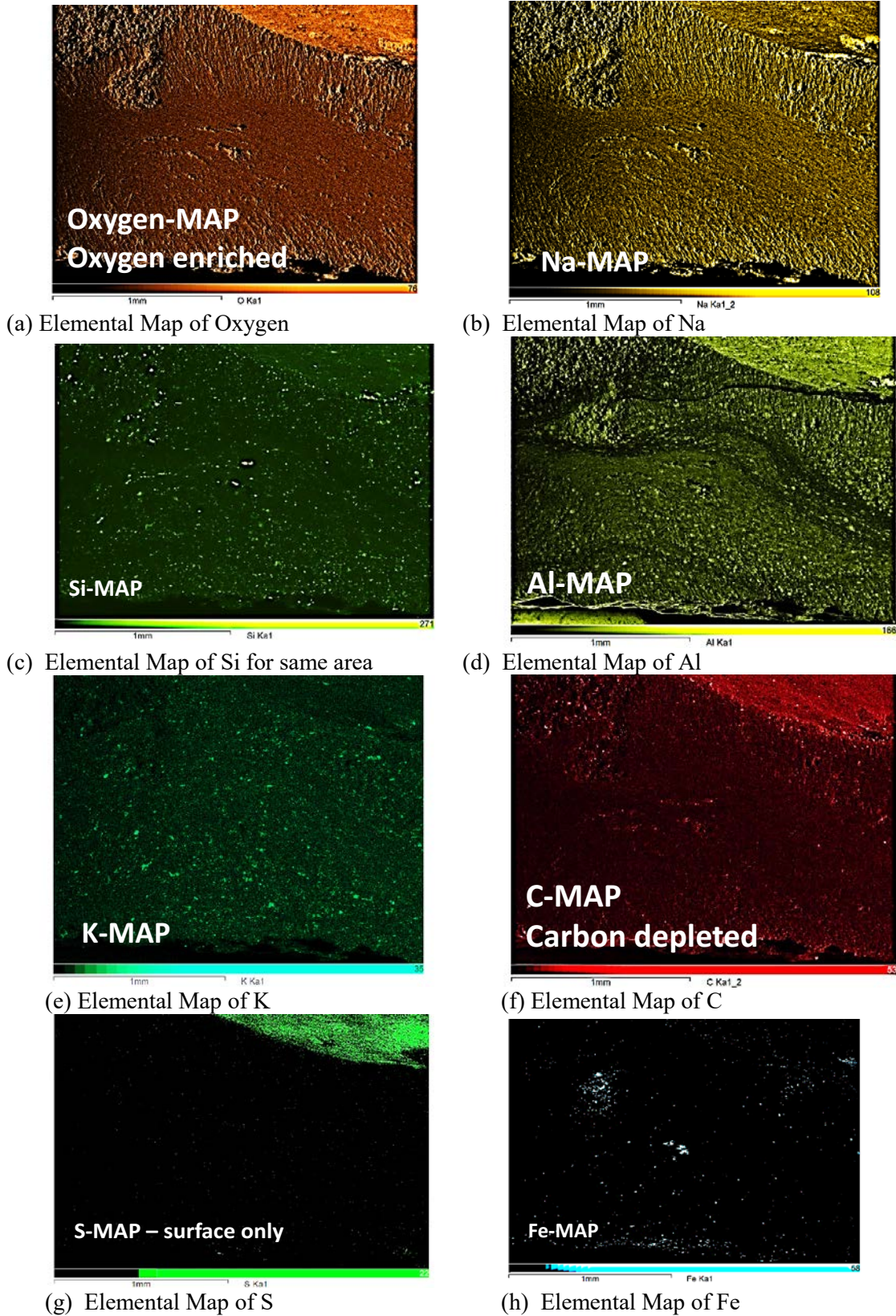
Figure 3-14. SEM elemental maps of the DMR Bark in Cross Section. Sample corresponds to the area shown in Figure 3-13c.

and d). Regions enriched in Fe are observed (Figure 3-14h) and Na and K are ubiquitous (Figure 3-14b and e). The sodium and oxygen are enriched in layers just beneath the top surface and bottom surface of the bark (Figure 3-14a and b). There is little involvement of S, Cl, Fe, P, Ca or Ti.

3.5.3 AG BARK MATERIAL (Sample #10) SEM OF SURFACES AND ELEMENTAL MAPS

The samples labelled AG material that looked bark like (Sample #10) in Figure 3-3 were examined by SEM analyses, elemental scans, and elemental mapping. Figure 3-15 (top) shows a backscatter electron image that clearly shows the AG material appears to have flow lines and contain large particulates and crescent shaped regions of smaller particulates with reaction rims along the edges of the crescent as if the particles are being consumed. This can also be seen in the SEM secondary electron image in Figure 3-15 (bottom).
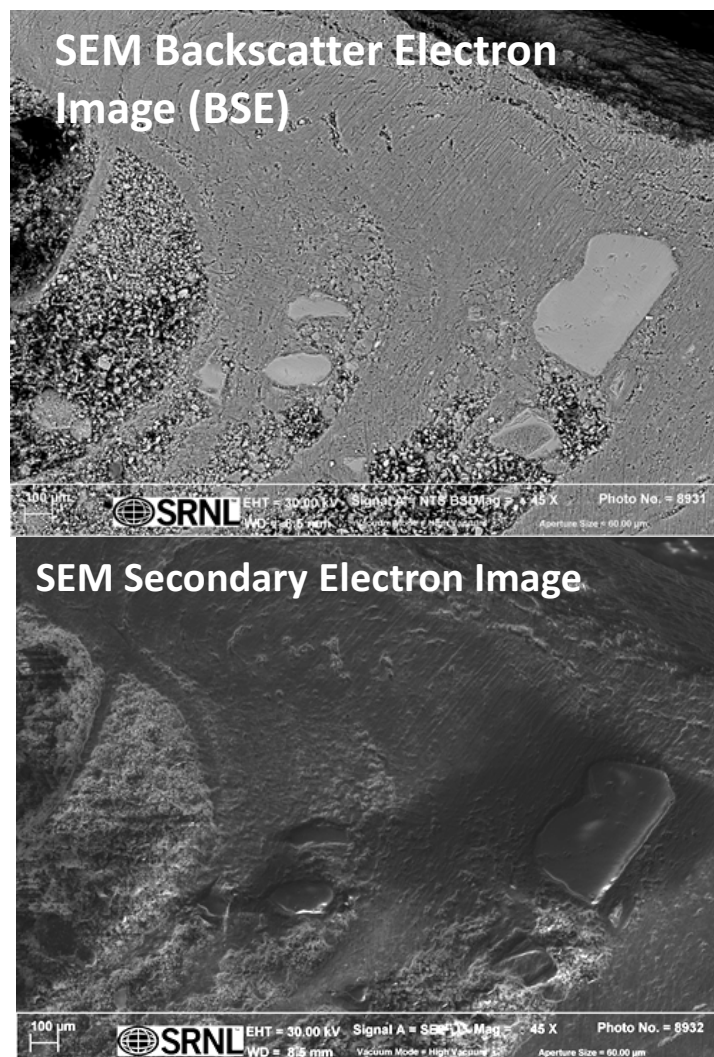
Figure 3-15. SEM of the AG Bark (Sample #10).

Figure 3-16a numbers the different phases seen in the SEM scan. Each of these different phases were analyzed by EDAX. Phases #1, 5, 6, 7, 8 and 9 were primarily $NaAlO_2$ with traces of S and Ca and other species. Phases #2, 3, and 4 were Al_2O_3 startup bed. Scans of phases #1, 5, and 7 are given in Figure 3-16 as examples. Phases #8 and 9 are aluminosilicates with a little more involvement of S, Ca, and K. Scans of phases #8 and 9 are given in Figure 3-16 as examples.
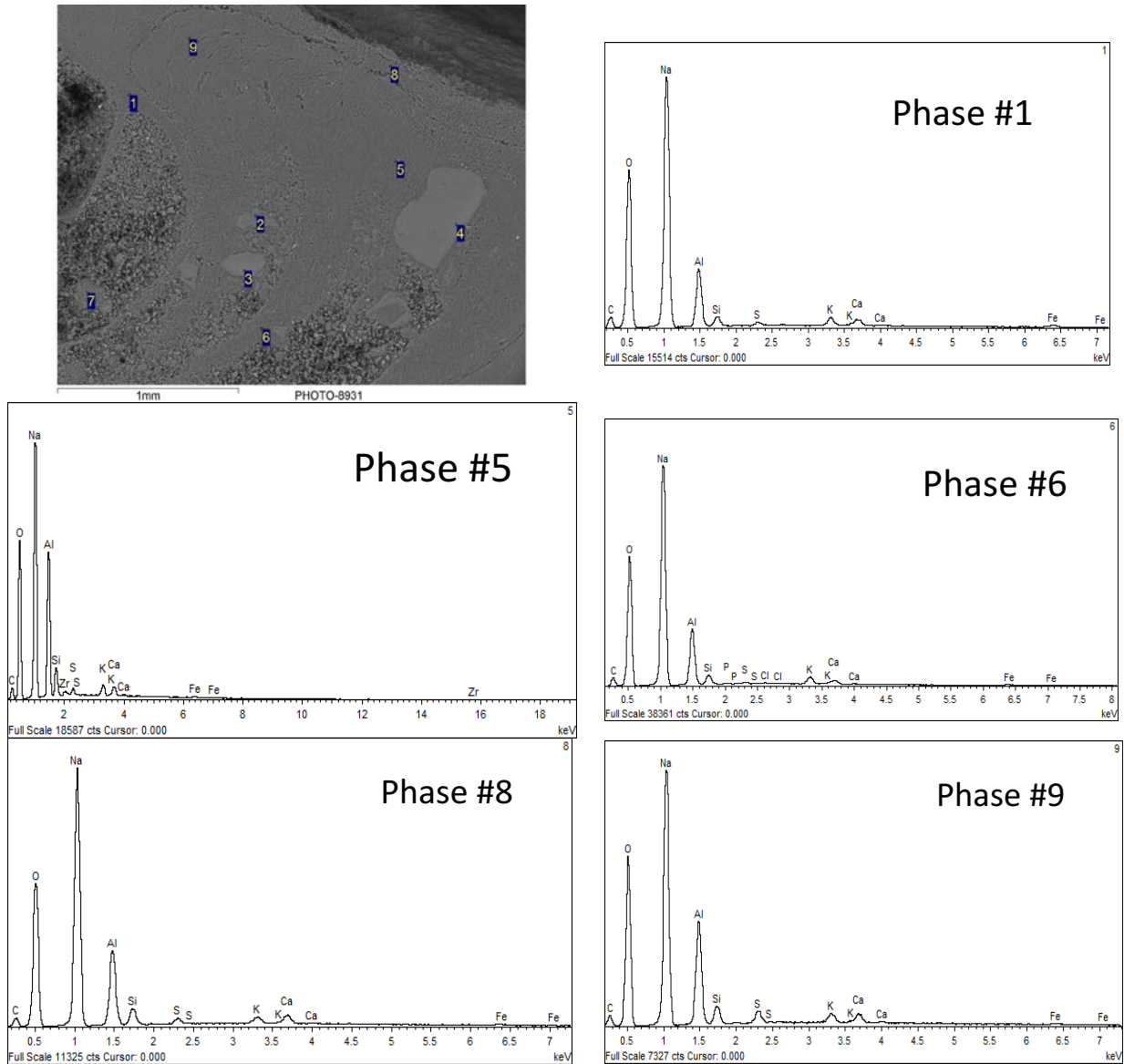
Figure 3-16. SEM elemental scans of AG material (Sample #10).

Figure 3-17 shows the elemental maps for the AG bark material (Sample #10). It is oxygen enriched and carbon depleted. It is sodium rich and the potassium is evenly distributed in the sodium matrix. Alumina rich particles are distributed in the entire sample but silica is enriched only along cracks and voids indicating that it may be fluid when deposited.
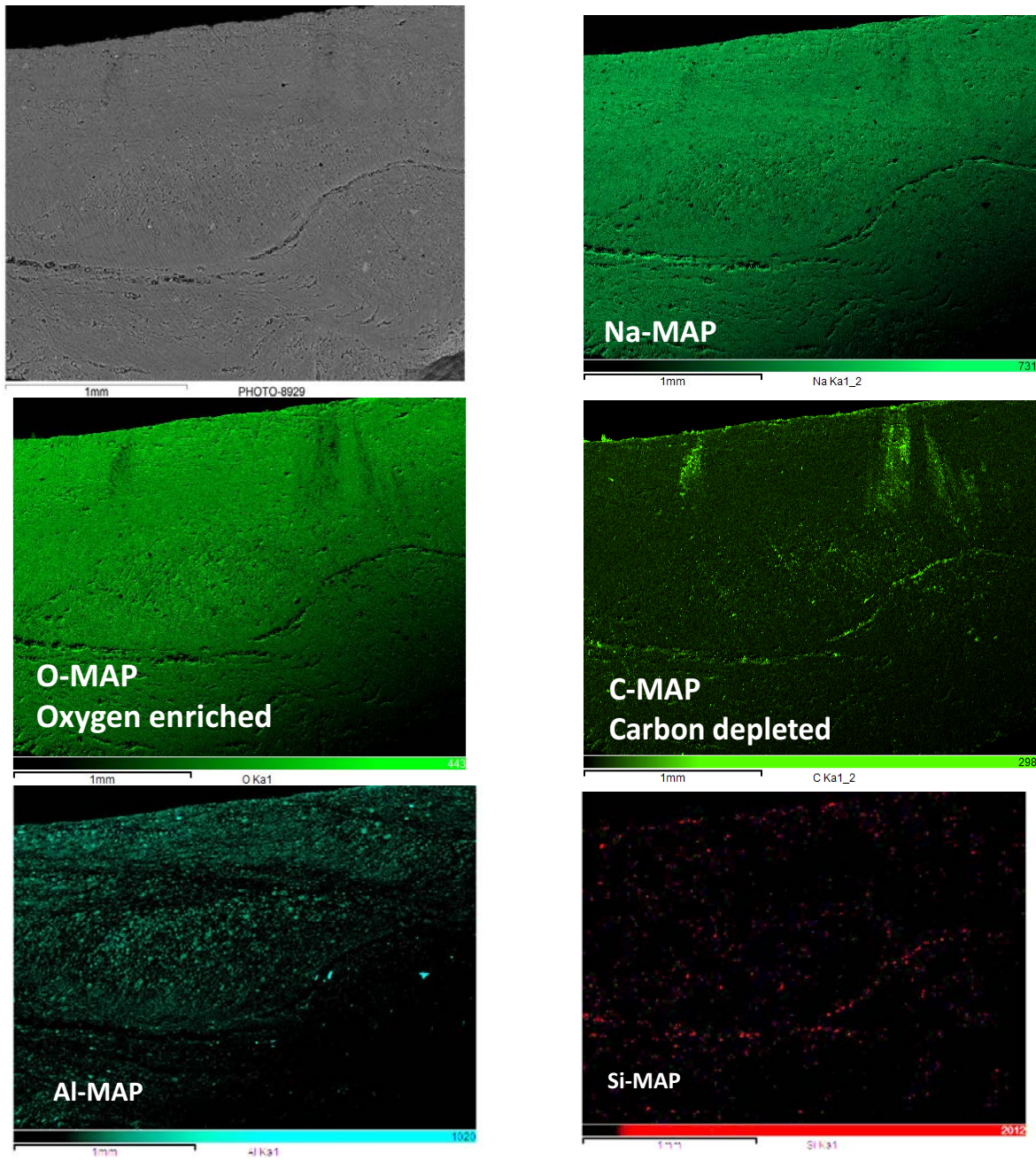
Figure 3-17. SEM elemental maps of AG material (Sample #10)

3.6 DMR BARK MATERIAL By HIGH TEMPERATURE XRD (HTXRD)

The HTXRD analysis in argon included an initial XRD at room temperature which revealed the presence of $Na_4Mg_2Si_3O_{18}$ which is believed to have crystallized from a glassy phase (see Section 7.2) and Na_2CO_3 DMR product. This may indicate that the carbonate gets stuck or embedded in the liquid phase.

From the initial heat treatment hold at 200°C to 325°C the $Na_4Mg_2Si_3O_{18}$ and Na_2CO_3 are still present along with a slightly silica enriched $NaAlO_2$ phase, i.e. $Na_{1.95}Al_{1.95}Si_{0.05}O_4$.

After the 325°C heat treatment the sample was allowed to cool back to room temperature and was reanalyzed by XRD. At this point the $NaAlO_2$ phase is no longer observed and $KAlSiO_4$ is observed instead. (Table 3-6) This may suggest a dynamic equilibrium between $(Na,K)AlO_2$ and $(K,Na)AlSiO_4$ where sodium is the main constituent of the alkali aluminate and potassium is the main constituent of $(K,Na)AlSiO_4$ since $KAlSiO_4$ and $NaAlSiO_4$ exhibit a limited solid solution.

Table 3-6. Phases Identified in HTXRD of DMR Bark

Temperature (°C)	Dwell Time (minutes)	Phases Identified	
		Name	Chemical Formula
25	30	Sodium Magnesium Silicate Natrite	$Na_4Mg_2Si_3O_{18}$ Na_2CO_3
200	30		
205	30		
210	30		
220	30		
225	30		
230	30		
235	30		
240	30		
245	30		
250	30		
255	30		
260	30	Sodium Magnesium Silicate	$Na_4Mg_2Si_3O_{18}$
265	30	Natrite	Na_2CO_3
270	30	Sodium Aluminate	$Na_{1.95}Al_{1.95}Si_{0.05}O_4$
275	30		
280	30		
285	30		
290	30		
295	30		
300	30		
305	30		
310	30		
315	30		
320	30		
325	30		
After Cooling		Sodium Magnesium Silicate Natrite Kalsilite	$Na_4Mg_2Si_3O_{18}$ Na_2CO_3 $KAlSiO_4$

3.7 DMR BARK MATERIAL (Sample #3) By DIFFERENTIAL SCANNING CALORIMETRY (DSC) COUPLED WITH MASS SPECTROSCOPY (MS) OF GASES EVOLVED

The DMR bark (Sample #3) was further studied by DSC analyses by two different analysts. Figure 3-18 indicates an early CO_2 evolution at 100-150°C and a second evolution at 664°C where Na_2CO_3 starts to decompose in argon. The DSC results show a significant deviation at the upper temperature, so the first derivative of the DSC results are given to emphasize where a change in heat input occurs.

Mass Spectrometry, Idaho Steam Reformer Sample, Non-rad (Jan. 2016)
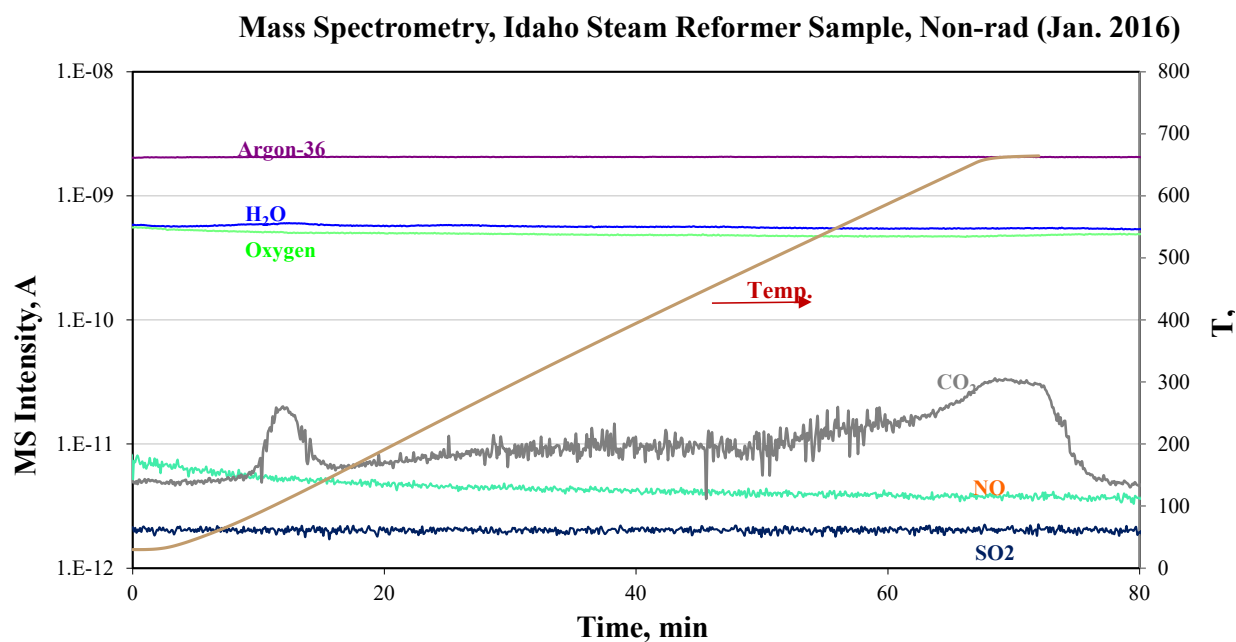
Figure 3-18. Differential Scanning Calorimetry (DSC) coupled with Mass Spectroscopy of the Gases Evolved for DMR Bark Sample #3.

Approximately 25 mg of the bark sample was placed in a heat flux TA calorimeter. Great care was taken to ensure intimate contact between the bark and the calorimeter detector. The sample was heated at 15 C/min to 500°C under Argon gas. The output signal from the calorimeter is shown in Figure 3-19. The output contains several peaks with peaks pointing downwards indicating an endothermic event and peak pointing upwards indicating an exothermic event. The peaks at 68°C and 120°C are due to water loss and bicarbonate decomposition (sodium). The broad peak at 250°C is due to dehydroxylation of aluminum hydroxide, and a possible melting peak. The exothermic followed by an endothermic peaks starting at 340°C are possibly due to the decomposition of aluminum oxyhydroxide and/or oxalate.[18]

The gases from the heating test in Figure 3-19 were analyzed with a mass Spectrometer (MS). The mass data is shown in the bottom graph of Figure 3-20. For easier evaluation, the upper graph includes Figure 3-19 as well as a second calorimetry scan of the bark that ran in Figure 3-19. An inspection of the bottom graph in Figure 3-20 show two water losses (peaks) accompanied by two CO_2 gas losses (peaks) with peak maximum at 68°C and 250°C. The corresponding weight losses were 0.2 and 0.5 wt% respectively. These reactions are associated with the small amount of crystalline material in the bark that contains both carbonates (bicarbonates) and sulfates.

None of the endothermic peaks were observed on re-heating the sample (see Figure 3-19) indicating these thermal events are irreversible. The endotherms indicate a decomposition at ~250°C. The fact that only one endothermic peak is seen at ~250°C indicates that it may be the decomposition of a solid solution of NaOH and KOH that exists in the bark. Since NaOH melts at 318°C and KOH melts at 360°C and there is a single endotherm at 250°C is consistent with the RHS of the NaOH-KOH phase diagram (see circled region in Figure 3-21, Reference 19) where only one endotherm exists instead of the LHS of the NaOH-KOH diagram where two endotherms would have to exist. Furthermore, the broadness of the 250°C endotherm peak is further evidence indicating that the composition of the solid solution mixture of NaOH and KOH is at or higher than (to the right of) the 50 mole% NaOH in the NaOH-KOH phase diagram.[19]

Other components that might form in the bark such as Na_2CO_3-$NaNO_3$, $NaNO_3$-Na_2SO_4, $NaNO_3$-NaOH, NaOH-Na_2CO_3 and NaOH-Na_2SO_4 (see Figure 3-22 and Figure 3-23) can't explain the single broad endotherm either because their eutectic temperatures are higher than 250°C or they melt with at least two endotherms.[20,21,22] Therefore, the NaOH-KOH binary eutectic is the only eutectic that is consistent with the DSC analysis.
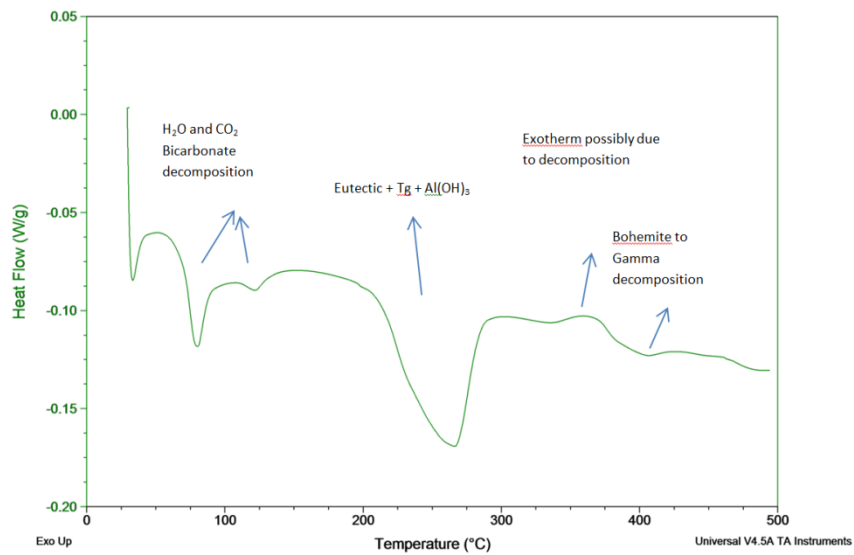
Figure 3-19. Differential Scanning Calorimetry (DSC) for DMR Bark Sample #3.
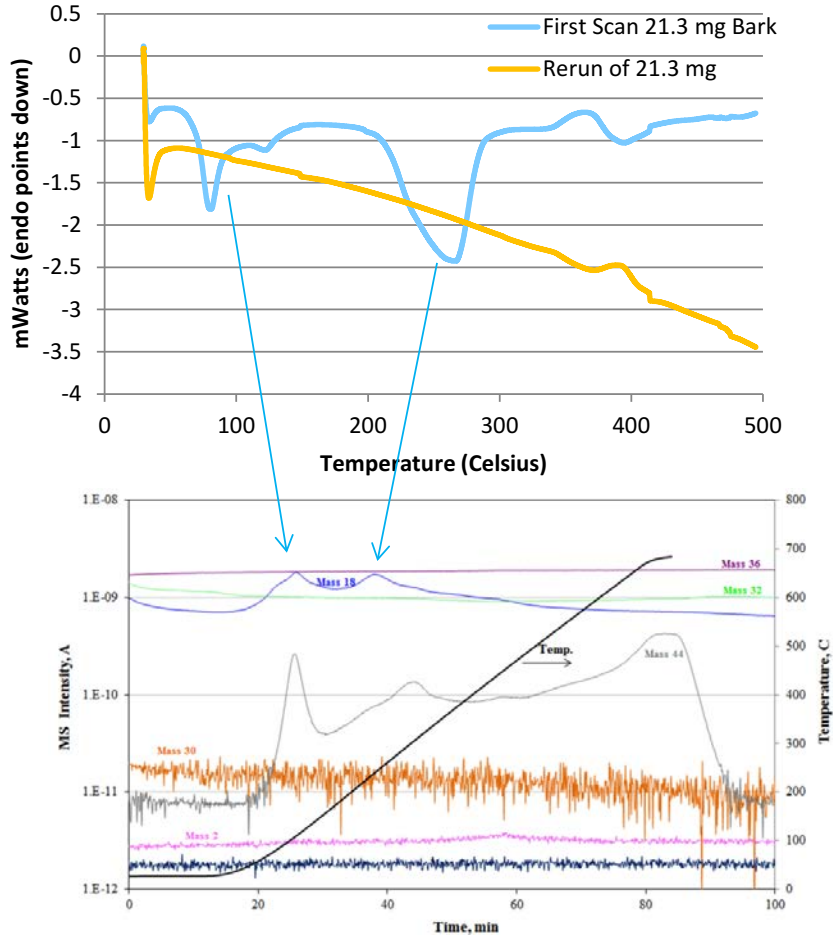
Figure 3-20. Differential Scanning Calorimetry (DSC) for DMR Bark Sample #3.
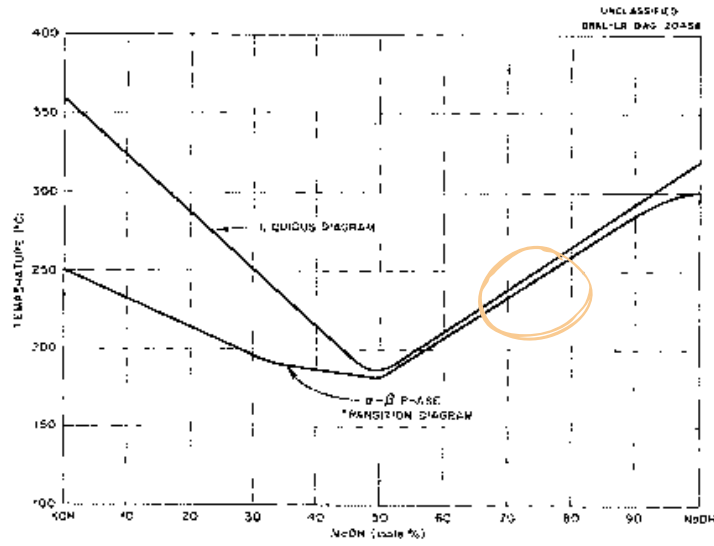
Figure 3-21. Binary phase diagram between NaOH-KOH.[19]
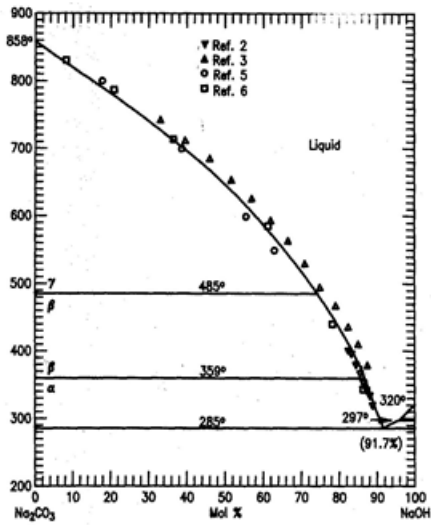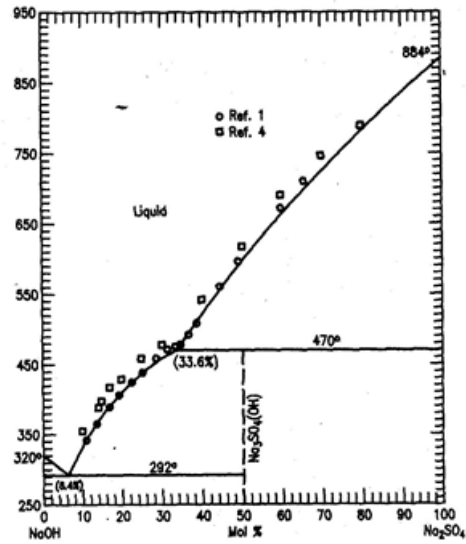
(a) from Reference 20   (b) from Reference 21

Figure 3-22. Known phase diagrams between NaOH-Na₂CO₃ and NaOH-Na₂SO₄.
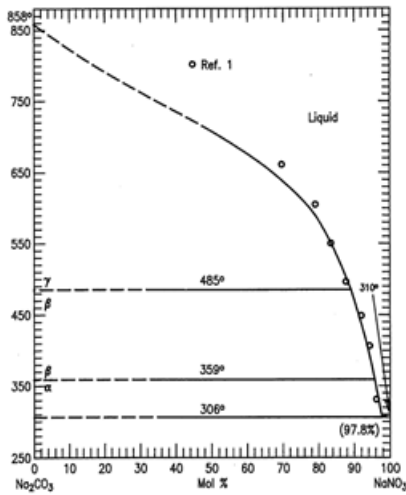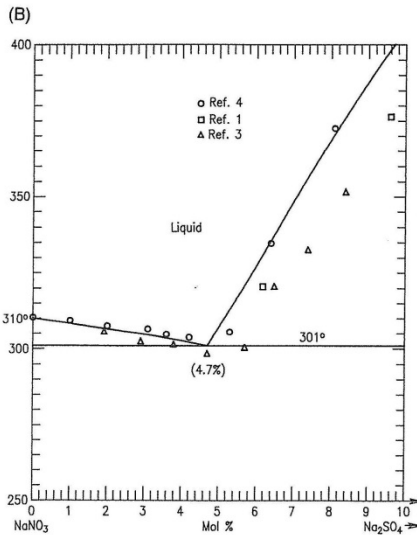
(a) From Reference 22   (b) From Reference 23   (c) from Reference 20
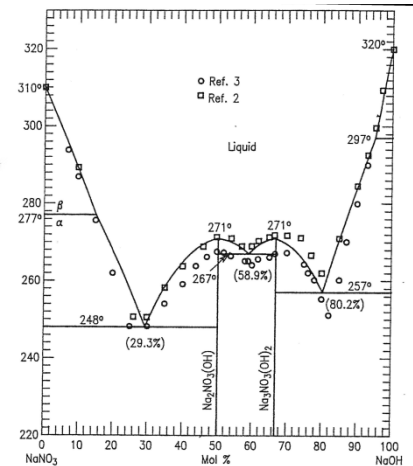
Figure 3-23. Known phase diagrams between Na₂CO₃-NaNO₃, NaNO₃-Na₂SO₄, and NaNO₃-NaOH.

3.8 DMR BARK MATERIAL (Sample #3) by THERMO GRAVIMETRIC ANALYSIS (TGA) WITH MASS SPECTROSCOPY (MS) OF GASES EVOLVED

A closer look at the TGA data from the bark (Figure 3-24 and Figure 3-25) reveals that the weight loss at 250°C is about 0.2 wt% or twice that of the weight loss at 100°C. The DSC indicates the heat loss at 250°C is about three times that of the endotherm at 100°C indicating the excess heat loss at 250°C is due

to the melting of the NaOH-KOH solid solution that probably reacted right after melting. The water loss (or OH loss) at 250°C is more consistent with a 50:50 or 75:25 NaOH:KOH mixture. No NO_x was observed.
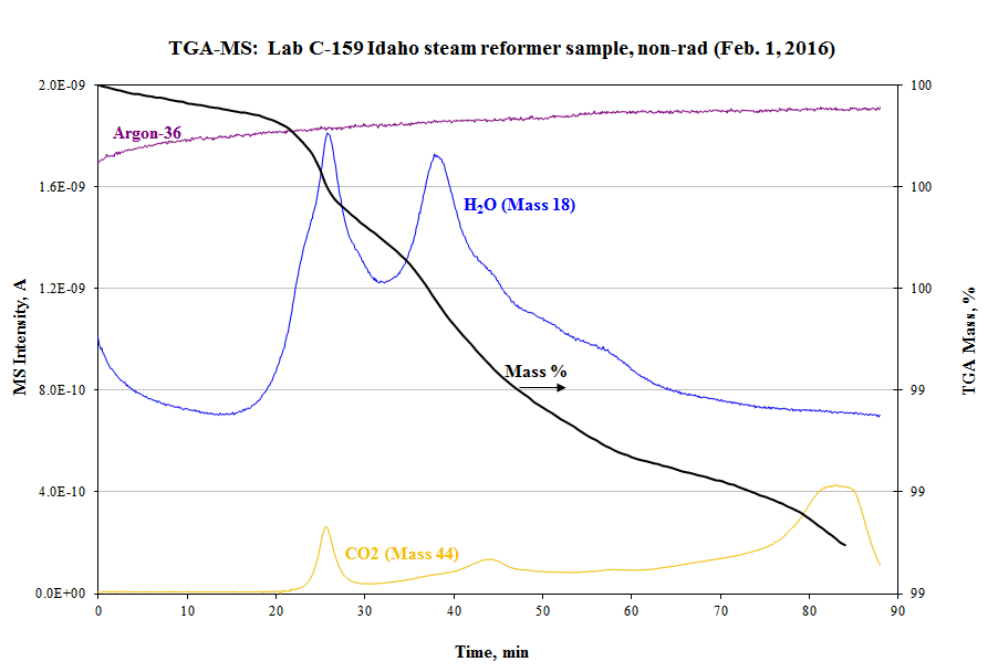
(a)
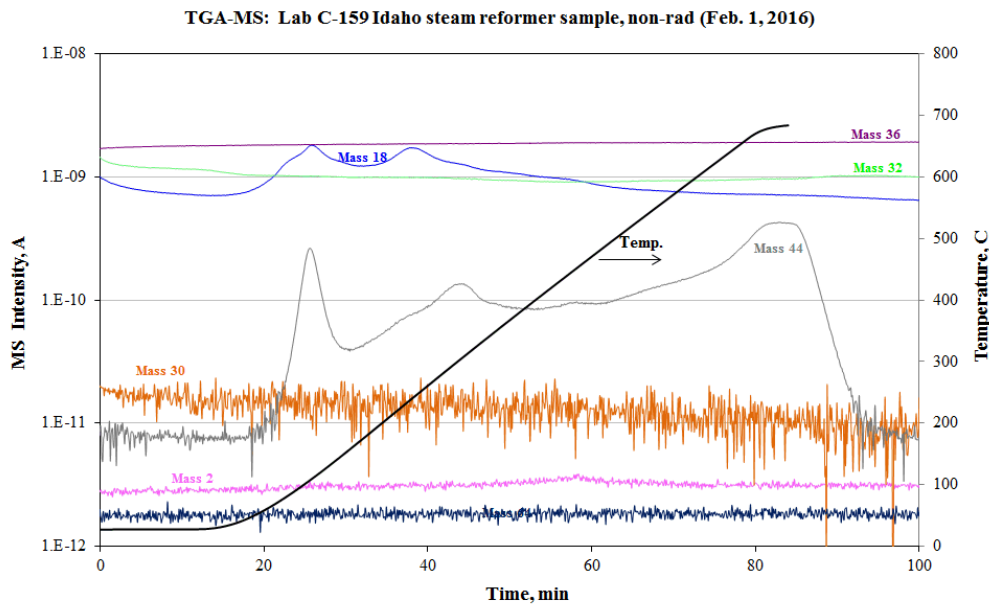
(b)

Figure 3-24. Thermal Gravimetric Analysis of DMR Bark (Sample #3) with Mass Spectroscopy of Gases Evolved.

TGA-MS: Lab C-159 Idaho steam reformer sample, non-rad (Feb. 1, 2016)

Due to buoyancy issue, the mass loss above 600 C may have been slightly greater than shown.

(a)

TGA-MS: Lab C-159 Idaho steam reformer sample, non-rad (Feb. 1, 2016)

Ten-minute isothermal hold with dry argon purge caused mass loss at low temperature.

Due to buoyancy issue, the mass loss above 600 C may have been slightly greater than shown.

(b)

Figure 3-25. TGA of DMR Bark (Sample #3).

3.9 DMR BARK MATERIAL (Sample 3) BY FTIR AND RAMAN SPECTROSCOPY

A portion of the bark sample (a 3 mm thick square) was sectioned perpendicular to the sample. A 20 micron infrared beam was focused on the cross section (through the thickness) of the sample and collected infrared spectra from the bark's sample surface to its interior (40 microns away from the

surface). The FTIR spectra clearly show (see Figure 3-26) the bark sample is heterogeneous through its thickness (as well as spatially). The FTIR data indicates the surface is mostly composed of silica and aluminosilicate with minor concentrations of sulfates and carbonates. The FTIR data from the interior of the sample indicate a relatively large concentration of carbonate and aluminum hydroxide relative to the glassy silica. Also shown in Figure 3-26 is the FTIR spectrum of an insoluble material found after acid leaching the bark that is mostly silica and aluminosilicate.
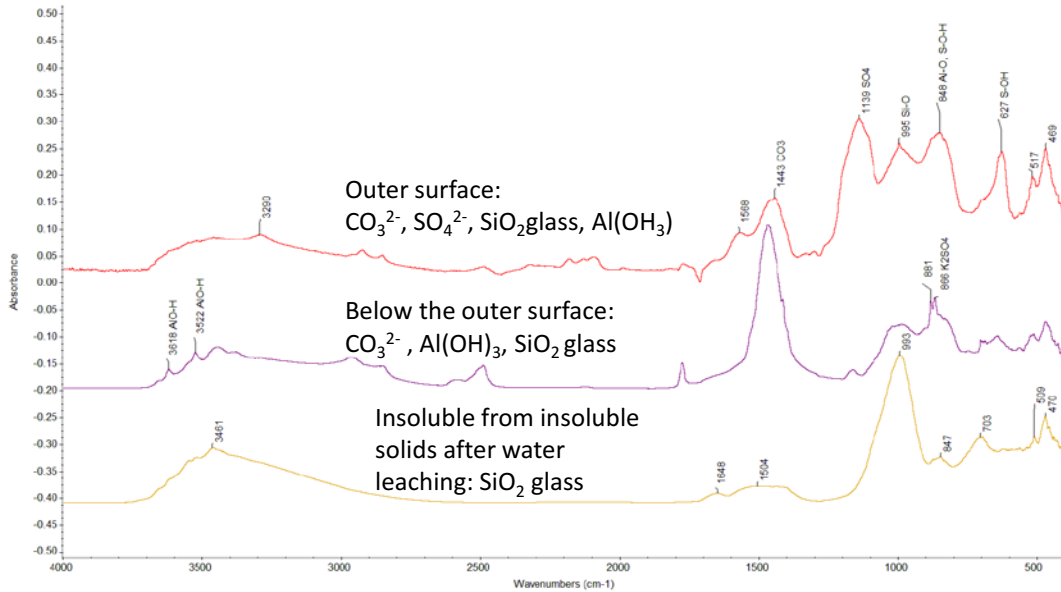
Figure 3-26. FTIR Spectra of SiO$_2$ Glassy Phase.

FTIR was also performed on the surface of the bark facing the DMR chamber after the bark was heat treated to 500°C (Figure 3-27 top). This spectra shows mostly carbonate bed material. After removing the top 200 microns of the bark it was again looked at with FTIR and Al(OH)$_3$ (gibbsite) and an aluminosilicate were identified (Figure 3-27 middle). The FTIR of the bark surface that adhered to the DMR vessel wall was primarily AlOOH (boehmite) and a hydrated silica which may be a gelatinous. Since silica can only come from the fly ash there may be interactions between the nitric acid in the feed and the silica that creates a gelatinous silica that may eventually become the crystallized Na$_4$Mg$_2$Si$_3$O$_{18}$ glassy phase. Experimentation is underway to determine if this mechanism is active in the DMR.
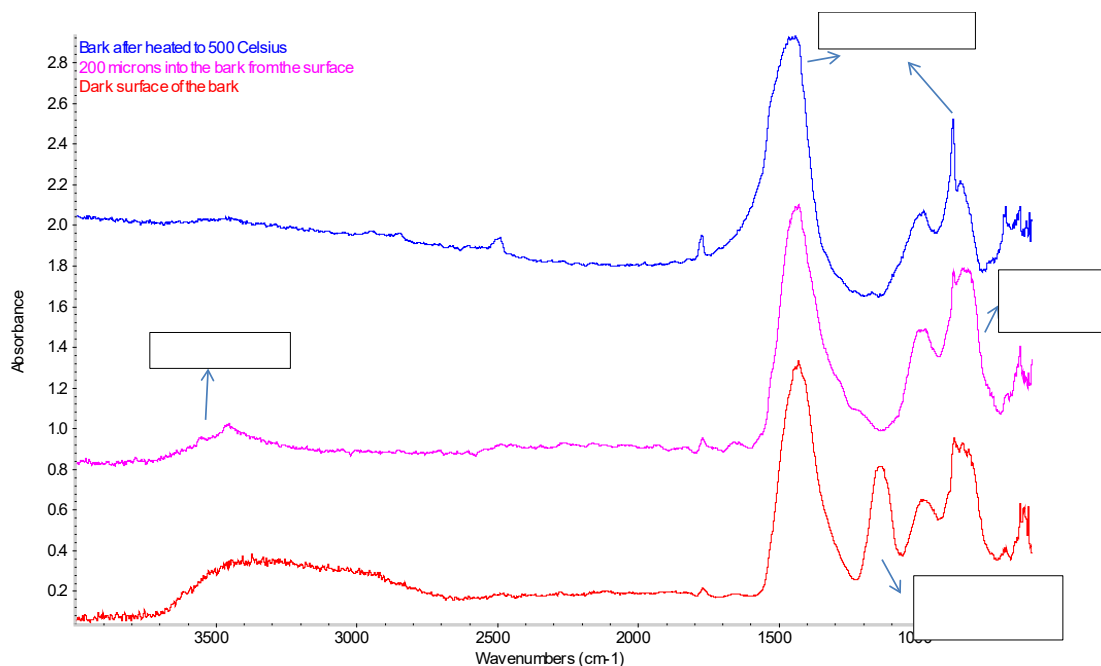
Figure 3-27. FTIR of DMR Bark (Sample #3) after heating.

Top image is the surface facing the DMR chamber. Middle Image is 200 microns into the
bark from the DMR surface. Bottom image is the bark attached to the wall of the DMR.

A Raman analysis of the surface of the bark sample (Figure 3-28) indicates the bark surface is very heterogeneous. Figure 3-28 reveals the presence of the carbonaceous material that includes ordered graphite (1586 cm^{-1}) and disordered graphite (1400 – 1220 cm^{-1}). The peak at 1220 cm^{-1} is from a polyalene like group in graphite. The Raman spectra in Figure 3-28 also indicate the graphite contains metal impurities. Also shown in Figure 3-28, is the presence of NaOH with peaks at 3250 cm-1 due to the O-H stretch and the 350 cm-1 peak due to the Na-OH stretch. The band at 998 cm^{-1} is due to sodium sulfate.   Overall, the findings from the Raman data are consistent with the rest of the findings in this study.
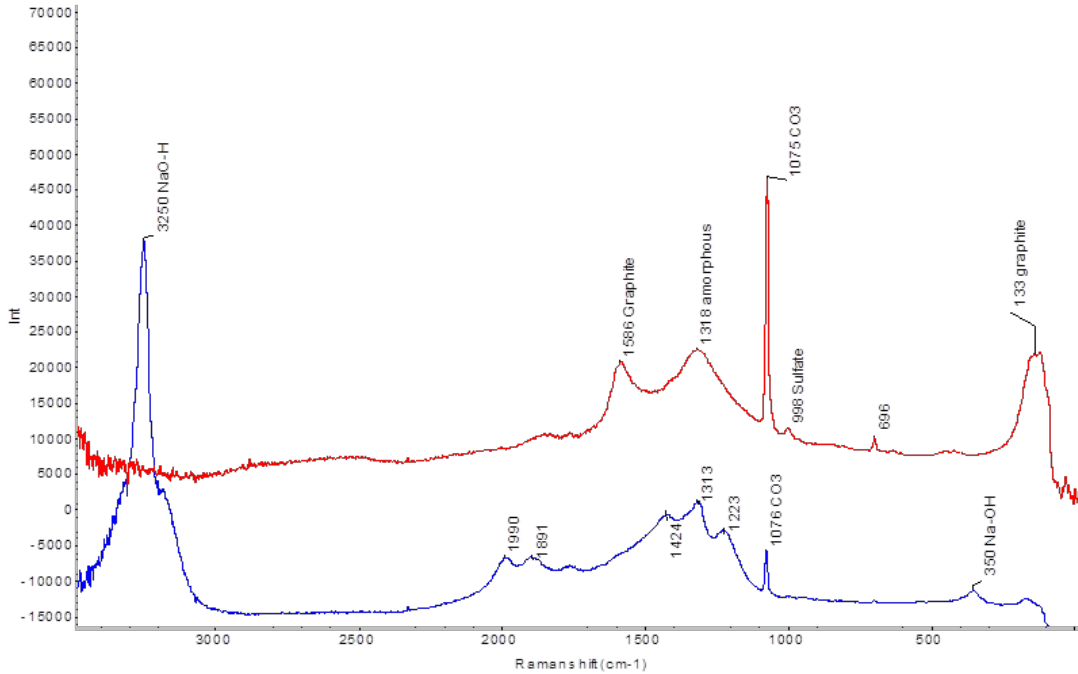
Figure 3-28. Raman Spectroscopy the DMR Bark (Sample #3).

3.10 DMR BARK MATERIAL (Sample #3) BY INFRARED REFLECTANCE (IR)

The DMR bark (Sample #3) was further studied by Infrared Reflectance analyses. The IR analysis indicates that sulfur is present as sulfate (SO_4) and not sulfide on the DMR/metal surface interface (Figure 3-29). The energy and mass balance for the IWTU also predicts SO_4 and not sulfide. The presence of sulfate was also confirmed by Fourier Transform Infrared Spectroscopy (FTIR). Therefore, it appears that SO_4 also plays a role in the bark and/or bark formation. Reference 13 alludes to the use of $NaAlO_2$ for sulfate removal from flue gases although no $NaAlO_2$ was identified in the DMR bark (Table 3-4).
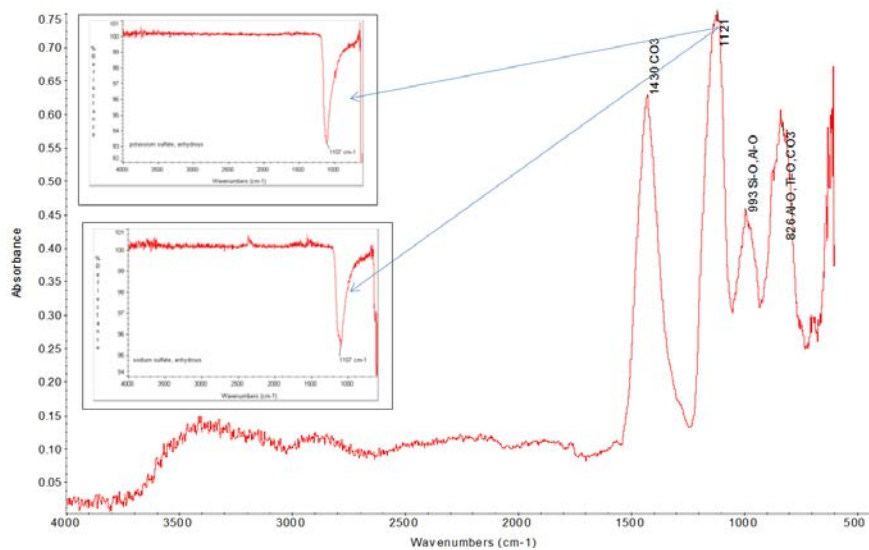
Figure 3-29. Infrared Reflectance Spectroscopy on Bottom of DMR Bark

4.0 ROCKS IN DMR AND COAL (Samples #4, #5, #6)

Three samples of rocks were received from IWTU. Samples #4 and #5 were rocks that had been picked out from or sifted from the DMR bed (Figure 4-1a and b). The remaining rocks were from the raw bags of coal (Sample #6-Figure 4-1c and d). The rock samples were gray, black, brown, and white. The rock samples were unremarkable and contained silicate species like anorthite and muscovite (a feldspar and mica of the composition $(Ca,Na)(Al,Si)_2Si_2O_8$ and $KAl_3Si_3O_{11}$, respectively), quartz (SiO_2), and kaolinite (Table 4-1). Some rocks had an amorphous component and some rocks were coated with bed product like Na_2CO_3, $KAlSiO_4$, $NaAlSiO_4$ and bark product like the $Na_4Mg_2Si_3O_{10}$ glassy phase. This was the only observance of $NaAlO_2$ and it was in the rocks from the unprocessed coal. Some organics, like natroxalate, were also found in the sample from the raw coal supersacs as that coal had not been thermally processed in the DMR. It does not appear that the rocks participate in the bark formation.

(a) DMR Rocks Sample #4 December 17, 2015

(b) DMR Rocks from coal in DMR Bed Sample #5 December 19, 2015

(c) Rocks from Bag of Coal Sample #6 side #1 December 15, 2015
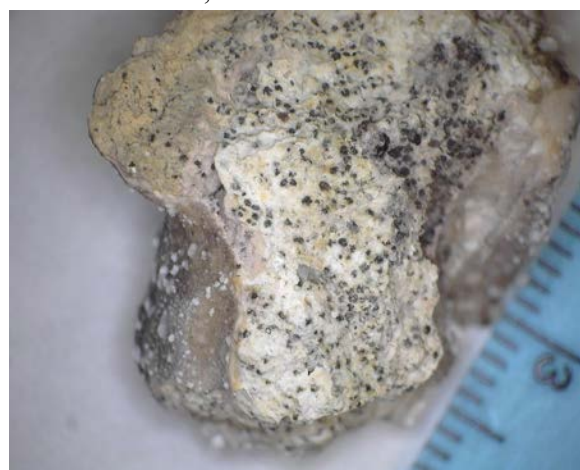
(d) Rocks from Bag of Coal Sample #6 side #2 December 15, 2015

Figure 4-1. Visual Appearance of Rocks in the DMR Bed and From the Raw Bags of Coal.

Table 4-1. Phase Identification of DMR and Raw Coal Rocks.

Sample Location	Sample Color/Description	XRD Phases Identified	ICDD (International Centre for Diffraction Data) No.
DMR Rocks (#4)	Black	C (carbon)	00-026-1076
	Gray with Black center	SiO_2 (quartz) $KAl_3Si_3O_{11}$ (muscovite)	00-046-1045 00-046-0741
	Light Brown	$Na_4Mg_2Si_3O_{10}$ (sodium magnesium silicate) $Na_2CO_3.H_2O$ (thermonatrite) $KAlSiO_4$ (kalsilite) $NaAlSiO_4$ (nepheline) $Al(OH)_3$ (bayerite)	00-033-1265 00-008-0448 00-011-0579 00-035-0424 00-020-0011
Rocks from Coal in Bed (#5)	White	SiO_2 (quartz) $KAl_3Si_3O_{11}$ (muscovite) $(Ca,Na)(Al,Si)_2Si_2O_8$ (Anorthite) $Na1.75Al1.75Si0.25O4$ (Sodium Aluminate)	00-046-1045 00-046-0741 00-020-0528 00-049-0004
	Gray	Amorphous and SiO_2 (quartz)	00-046-1045
	Brown	SiO_2 (quartz) $KAl_3Si_3O_{11}$ (muscovite) $(Ca,Na)(Al,Si)_2Si_2O_8$ (Anorthite)	00-046-1045 00-046-0741 00-020-0528
Rocks from Coal (#6)	Black	$Fe(CO_3)$ (siderite) SiO_2 (quartz) $CaMg(CO_3)_2$ (dolomite) $Al_2Si_2O_5(OH)_4$ (kaolinite)	00-012-0531 00-046-1045 00-011-0078 00-014-0164
	White	$Na_{1.95}Al_{1.95}Si_{0.05}O_4$ (sodium aluminate) $Na_2CO_3 \bullet H_2O$ (thermonatrite) $Al(OH)_3$ (bayerite) $KAlSiO_4$ (kalsilite) $Na_2C_2O_4$ (natroxalate) Al_2O_3 (corundum)-major	00-049-0003 00-008-0448 00-020-0011 00-011-0579 00-020-1149 00-010-0173

5.0 COMPARISON OF DMR CONTENTS TO WALL BARK CONTENTS

One can compare the composition of the DMR bark (Table 3-4) to the contents of the active DMR beds (Table 2-2 and Table 2-3) to see what elements are enriched in the bark, i.e. compare the total analyses (soluble plus insoluble) on a normalized 100 wt% basis. This summary is given in Table 5-1: a positive number (cells that are shaded in Table 5-1) indicates bark enrichment of that phase(s) with respect to the active DMR beds. The bark is enriched in the carbonates ($CaCO_3$ and Na_2CO_3) and $Al(OH)_3$. The bark is enriched in K_2O and SiO_2 and Na_2O silicate, i.e. glassy phases, over the DMR bed. The DMR and AG bark is enriched in excess Na_2O likely present at the DMR operating temperature as NaOH. The AG bark is enriched in alkali sulfate.

Table 5-1. Enrichment of Bark in Certain Components and Relative Density of DMR Bark and Bed

Chemical Species by XRD	Bark-DMR Bed (wt%)	AG Bark-DMR Bed (wt%)
Al_2O_3	-60.61	-60.61
$Al(OH)_3$	32.17	32.66
$CaCO_3$	1.16	0.95
Fe_2O_3	-1.21	-1.16
K_2O	0.71	0.48
K_2CO_3	-1.70	-1.63
MgO	0.03	0.02
Na_2O (sil)	2.88	2.61
Na_2O (ex)	0.28	0.32
Na_2CO_3	49.70	45.58
NiO	0.01	0.01
P_2O_5	0.16	0.15
Na_2SO_4 sulfate by IC	-0.44	1.36
SiO_2	3.14	1.53
Coal	-13	-13

6.0 COMPARISON OF SIMULANT TO DMR CONTENTS

Table 2-1 gives the theoretical phases that should form from the simulant given in Table 1-4. Comparisons of the theoretical values in Table 1-4 to the analyzed phase concentrations in the DMR as given in Table 2-2 and Table 2-3 indicate that $Al(OH)_3$ is forming instead of $NaAlO_2$. Note that $NaAlO_2$ had been found in TI-102 and $NaAl_{11}O_{17}$ had been found preferentially in the the Hazen CP-1/CP-2 campaigns (Table 1-5) but $Al(OH)_3$ was found in TPR-8023 (1&2).

7.0 POTENTIAL CAUSES OF BARK FORMATION AND REMEDIATION

Since the DMR was not run at steady state during TI-102 there is insufficient information to predict the exact DMR conditions that created the bark. Several possibilities are discussed in the sections below. The appearance of the bark indicates that a liquid or near liquid phase was present making the vertical rivulets observed in the DMR bark. Therefore, the discussions below concentrate on species that may have formed low melting (<640°C) eutectics in binary or ternary combinations with the alkali carbonates present in the DMR bed.

7.1 LOW MELTING EUTECTICS INVOLVING NaOH AND/OR KOH

NaOH can form in the DMR if the CO_2 fugacity is insufficient. During testing of the carbonate flow sheet for the SRS Tank 48 project, campaigns at the INL SAIC-STAR pilot scale FBSR produced bed deposits that were shown to be caused by excess NaOH in the DMR.[24] One of the authors of Reference 24 used

a thermodynamic code called HSC Chemistry and produced Figure 7-1 which shows that NaOH can form when the concentration of CO_2 in the DMR is not sufficient.
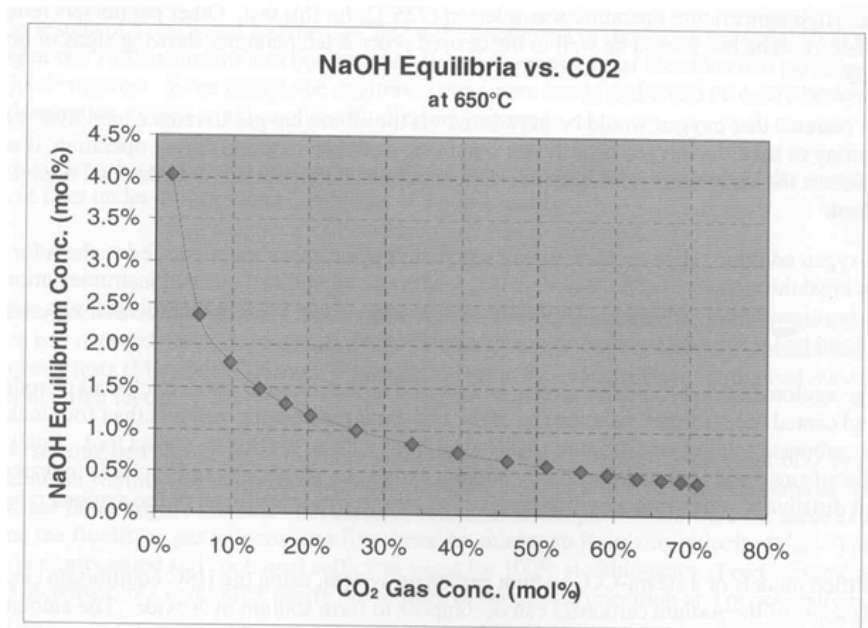
Figure 7-1. HSC Chemistry relationship between NaOH (mol%) and CO_2 gas (mol%) in the DMR at 650°C (from Reference 24)

The equilibria between NaOH and CO_2 can be reprented by the following equation [25]:

Equation 1. $$4NaOH + 2CO_2 \leftrightarrow 2Na_2CO_3 + 2H_2O$$
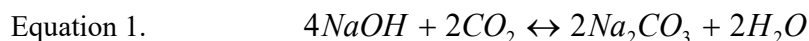
If NaOH was present as a vapor or liquid phase during the TI-102 and TPR-8023 (1&2) formation due to any of the processing consequences outlined in Section 1.2, this may have caused the NaOH-KOH low melting eutectic identified by wet chemistry mass balance of the soluble components, DSC, and TGA.

7.2 GLASSY PHASE IN TPR-8023 (1&2) AND PREVIOUS TESTING (CP1-CP2 AND TI-102)

In the CP1-CP2 testing in 2006, 3 grams of bark was dissolved in 90 mL of deionized water at 80°C for 2 hours. In the TI-102 testing and the November/December 2015 TRP-8023 testing, a more dilute concentration of bark in deionized water was used to avoid any saturation effects: 3 grams of bark was dissolved in 300 mL of deionized water at 80°C for 2 hours. For all the samples, both the soluble and insoluble fractions were analyzed. For the TI-102 and TRP-8023 runs, mass balances were performed on the soluble and insoluble fractions. The soluble mass balance suggested the presence of NaOH-KOH which has a low melting eutectic.[8,9] The insoluble mass balance of the TRP-8023 bark suggested the presence of an alkali silicate glass with a stoichiometry of $Na_2Si_2O_5$. [8,9]

RESULTS AND DISCUSSION
The chemical mass balance of the insoluble fraction of the bark solids formed at HRI (2006) and IWTU (2014/5 and 2015/6) are given in Table 7-1. The mass balance was performed against the phases identified by X-ray diffraction in References 8, 9 and 10. For the IWTU bark samples (TI-102 and TPR-

8023 (1&2)) the $SiO_2/(Na_2O+K_2O)$ wt% ratios are 1.07 for TI-102 and 2.13-1.98 for TPR-8023 (1&2) depending on whether the bark was from the DMR or had fallen into the Auger Grinder. Ratios of $SiO_2/(Na_2O+K_2O)$ between 3.22 to 1.0 are a sodium silicate glass known as water glass. Water glass has a composition of $Na_2O:SiO_2$ of 1:1 and can be formed by reacting sodium carbonate (the IWTU product) with silica in the presence of steam by the following reaction at temperatures of 1000°C:

$$Equation\ 2 \qquad Na_2CO_3 + SiO_2 \rightarrow Na_2O{\cdot}SiO_2 + CO_2$$
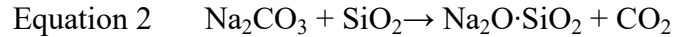
Equation 2 usually produces a glass of the composition $Na_2O{\bullet}6SiO_2$.[26]

Sodium metasilicate hydrate ($Na_2SiO_3{\bullet}9H_2O$) can be formed from reactive amorphous silica like rice husk ash (IWTU fly ash also contains ~60 wt% amorphous reactive silica) and sodium carbonate via Equation 3 or Equation 4 at temperatures of 500°C and steam pressures of 2.5 atm or 10 atm.[26] At 2.5 atm. the $Na_2SiO_3{\bullet}9H_2O$ is amorphous and at 10 atm the $Na_2SiO_3{\bullet}9H_2O$ is crystalline.[26]

$$Equation\ 3 \qquad Na_2CO_3 + SiO_2 + 10H_2O \rightarrow Na_2SiO_3{\bullet}9H_2O + H_2CO_3$$

$$Equation\ 4 \qquad 2NaOH + SiO_2 + 8H_2O \rightarrow Na_2SiO_3{\bullet}9H_2O$$
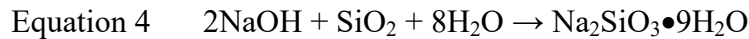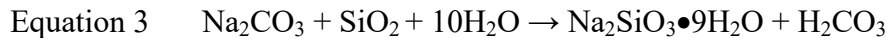
In Reference 26 the presence of NaOH, NaCl, and Na_2SO_4 were found to catalyze Equation 3. The latter two species are present in the IWTU waste and simulant (Table 1-3) and NaOH is created during FBSR processing using the carbonate flowsheet.[8,9]

Since water glass is fairly soluble in water, it is likely not the sodium silicate glassy phase present in the insoluble portion of the SBW bark samples. In the systems K_2O-SiO_2-CO_2 and Na_2O-SiO_2-CO_2 Niggli [27] found that the dilsilicates $K_2Si_2O_5$ and $Na_2Si_2O_5$ are more readily formed than K_2SiO_3 and Na_2SiO_3. In addition, the disilicates, $(K,Na)_2Si_2O_5$, form at lower temperatures than the metasilicates, $(K,Na)_2SiO_3$.[28]

A closer look at the molar ratios of $SiO_2/(Na_2O+K_2O)$ in the IWTU samples reveals that for TI-102 the glassy phase was $(Na,K)_{1.52}Si_2O_{4.76}$ while for TPR-8023 (1&2) it was $(Na,K)_{0.85}Si_2O_{4.42}$ for the DMR bark and $(Na,K)_{0.93}Si_2O_{4.47}$ for the auger grinder bark. Given that MgO and FeO as well as Fe_2O_3 can participate in the glassy phase, these are all nominally $(Na,K)_2Si_2O_5$ which was the glass compositions reported for the insoluble IWTU bark components in references 8 and 9.

Identification of the glassy phase composition in the 2006 HRI tests is more problematic due to the involvement of the LoAbrade refractory. The glassy phase composition given in Table 7-1 shows a large concentration of CaO in the insoluble solid portion of the bark, i.e. 35.98 wt% CaO. The LoAbrade refractory that lines the HRI DMR is a mixture of aluminosilicate aggregate (calcined fireclay which is calcined kaolinite) that was gunned onto the interior of the HRI DMR about 20 years ago. When kaolinite is calcined at temperatures of ~1400°C it forms mullite and an SiO_2 glass. This mullite-SiO_2 aggregate in the LoAbrade is held together by calcium aluminate cement – in this case CA ($CaO{\bullet}Al_2O_3$) and CA_2 ($CaO{\bullet}2Al_2O_3$). When the refractory is cured it forms C_3AH_6 ($3CaO{\bullet}Al_2O_3{\bullet}6H_2O$) and AH_3 ($Al_2O_3{\bullet}3H_2O$ or $Al(OH)_3$ known as gibbsite).[10]

If all of the Al_2O_3 in the HRI insoluble bark composition shown in Table 7-1 is assumed to be complexed as C_3AH_6, then the remaining CaO content available to participate in the glassy bark phase is only 10.19

wt% as shown by bold text in parentheses in Table 7-1. The molar calculations based on the 10.19 wt% CaO are also shown in bold in Table 7-1. The glassy phase in the bark is then calculated, on a mol% basis as $(Na,K)_{0.15}Ca_{1.06}Si_2O_{5.14}$ which is a CaO rich variant of $(Na,K)_2Si_2O_5$.

As identified in Reference 5 for the HRI SBW carbonate campaigns, there is a low melting eutectic (695°C) between $K_2Si_2O_5$-$K_2Si_4O_9$-$K_2Al_2Si_6O_{16}$.[29] The presence of steam enhances the reactivity of the glass forming components and impurities such as Mg, Ca and Fe in the glassy phase lowers the eutectic temperature from the 695°C theoretical melt temperature. An example is shown in Figure 7-2 where Mg lowers the melt temperature of $Na_2Si_2O_5$ from 874°C to 725°C. Note that Mg can be substituted by Ca or Fe^{2+} and have the same effect. If multiple cations substitute into the $Na_2Si_2O_5$ glassy phase the melt temperature can be depressed even further. Crystalline $Na_4Mg_3Si_5O_{10}$ was identified in the TPR-8023 (1&2) bark and likely formed from a melt of the same or similar composition.[9]

In addition, glasses do soften above the glass transition temperature (T_g) and the T_g is normally 2/3-3/4 of the glass melt temperature (T_m). For $Na_2Si_2O_5$, the T_g is 456°C and, for $K_2Si_2O_5$, the T_g is 440°C.

Table 7-1. Chemical Compositions of Glassy Phases in "Bark" Samples Produced During FBSR of SBW with A Carbonate Flowsheet

Chemical Species by XRD	IWTU SAMPLE 3 TPR-8023 (1&2) DMR Wall Bark [9]	IWTU SAMPLE 10 TPR-8023 (1&2) Auger Grinder Bark [9]	IWTU TI-102 DMR Wall Bark [8]	Hazen Research (CP-1) DMR Wall Bark [5]
Insoluble Fraction	3 g/300mL at 80°C for 2 hours			3 g/90mL at 80°C for 2 hours
Al_2O_3			39.66	15.63
$Al(OH)_3$	56.91	57.77	30.43	
CaO				35.98 **(10.19)**
$CaCO_3$	4.29	3.93	2.17	
Cr_2O_3	0.03	0.04		0.52
Fe_2O_3	1.72	2.06	1.945	12.54
K_2O	2.40	1.87	4.78	1.53
MgO	0.45	0.45	0.34	1.39
MnO	0.03	0.04	0.945	5.82
Na_2O (insoluble)	10.28	10.34	4.99	0.57
NiO	0.03	0.02		0.37
P_2O_5	0.12	0.13	0.2845	2.71
SiO_2	27.04	24.13	10.45	20.48
TiO_2	0.26	0.22	0.24	0.58
Sum	103.56	101.00	95.48	98.12
Weight Ratios				
$SiO_2/(Na_2O+K_2O)^*$	2.13	1.98	1.07	0.52
$SiO_2/(Na_2O+K_2O+CaO)^*$	N/A	N/A	N/A	0.54 **(1.67)**
Molar Ratios				
CaO	N/A	N/A	N/A	0.182
Na_2O	0.166	0.167	0.081	0.009
K_2O	0.025	0.020	0.051	0.016
SiO_2	0.450	0.402	0.174	0.341
$(Na_2O+K_2O)/SiO_2$	0.424	0.465	0.759	0.073
$(Na_2O+K_2O+CaO)/SiO_2$	N/A	N/A	N/A	**0.607**
$(CaO)/SiO_2$	N/A	N/A	N/A	**0.533**
$(Na_2O+K_2O):SiO_2$	0.43:1	0.47:1.0	0.75:1	0.08:1
$(CaO):SiO_2$	N/A	N/A	N/A	**0.53:1**
Nominally $(Na,K)_2Si_2O_5$	$(Na,K)_{0.85}Si_2O_{4.42}$	$(Na,K)_{0.93}Si_2O_{4.47}$	$(Na,K)_{1.52}Si_2O_{4.76}$	$(Na,K)_{0.15}Ca_{1.06}Si_2O_{5.14}$

* Values of 3.22 to 1.0 are water glass
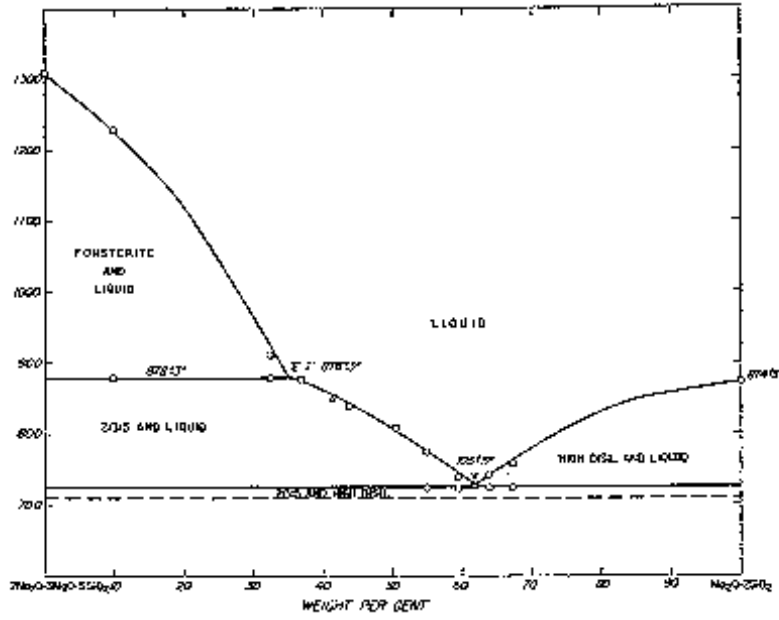
Figure 7-2. The system $Na_2Si_2O_5$-$Na_4Mg_3Si_5O_{10}$ where the presence of Mg or any divalent cation (Ca, Fe^{2+}) lowers the melt temperature of $Na_2Si_2O_5$ from 874°C to 725°C.[30]

8.0 CONCLUSIONS

To summarize, it can be concluded that excess NaOH-KOH is present in the IWTU DMR and likely participates in the bark formation. The following analytic findings confirm the existence of a NaOH-KOH solid solution:

- excess Na in soluble mass balance for which there are no other anions other than OH available
- presence of faujasite in the drum #2 sample (Sample #8) and in the AG compressed material (Sample #11)
- TGA and DSC's indicate the presence of NaOH-KOH mixture at ~250-300°C
- The excess NaOH-KOH is a very small mass amount and cannot be observed in a dry heating experiment
- The TGA and DSC proved that only NaOH-KOH is involved and not Na_2CO_3, Na_2SO_4, or $NaNO_3$.

The presence of NaOH-KOH is due to insufficient CO_2 in regions of the DMR as discussed in the body of this report.

The presence of NaOH-KOH can also be responsible for the glassy phase formation when the hydroxides interact with the coal fly ash. The following analytic findings confirm the existence of a glassy phase or partially crystallized glassy phase of the approximate composition $(Na,K)_2Si_2O_5$:

- excess sodium/potassium silicate in the insoluble mass balance
- identification by XRD – broad d-spacings in the bark XRD spectra hovering around the composition of partially crystalline $Na_4Mg_3Si_5O_{10}$ where $Na_2Si_2O_5$-$Na_4Mg_3Si_5O_{10}$ form a solid solution
- identification of the glassy phase by Infrared Spectroscopy (IR), Fourier Transform Infrared Reflectance (FTIR) and Raman Spectroscopy

In terms of the original task questions the following can be concluded

1. The glassy phase was present in the 2015 TI-102 bark and in the Hazen CP-1/CP-2 bark and in the current TPR-8023 (1&2) bark.
2. The binder in the bark is NaOH-KOH mixed with $(Na,K)_2CO_3$ bed product and a glassy phase of $(Na,K)_2Si_2O_5$.
3. The melting point of the bark is between 250-300°C as identified by TGA and DSC.
4. The rocks in the coal are typical sedimentary rocks found in coal formation and do not participate in bark formation. The rocks are unremarkable.
5. Additional CO_2 will "lock out" the NaOH-KOH component of the wall scale bark and may prevent the formation of the glassy phase as well. Additional testing is needed to confirm the relationship between the NaOH-KOH and the glassy phase.
6. Dilution of the feed will not inhibit the bark.
7. What other operating changes might help prevent wall scale – DMR operating temperature, DMR operating temperature control, waste feed rate, NAR, superheated steam velocity (SSV), CO_2? Only more CO_2 can inhibit the bark.

REFERENCES

1   Soelberg, N.R., D.W. Marshall, S.O. Bates, and D.D. Taylor, **"Phase 2 THOR Steam Reforming Tests for Sodium Bearing Waste Treatment"**, INEEL/EXT-04-01493, Rev. 1, Idaho National Engineering and Environmental Laboratory, Idaho Falls, Idaho (2004).

2   Marshall, D.W., N.R. Soelberg, and K.M. Shaber, **"THOR® Bench-Scale Steam Reforming Demonstration"**, INEEL/EXT.03-00437, Idaho National Laboratory, Idaho Falls, Idaho (2003).

3   Olson, A.L., N.R. Soelberg, D.W. Marshall, and G.L. Anderson, **"Fluidized Bed Steam Reforming of INEEL SBW Using THOR® Mineralizing Technology"**, INEEL/EXT-04-02564 Idaho National Laboratory, Idaho Falls, Idaho (2004).

4   Crawford, C.L. and C.M. Jantzen, **"Durability Testing of Fluidized Bed Steam Reformer (FBSR) Waste Forms for Sodium Bearing Waste (SBW) at INL"**, U.S. DOE Report WSRC-STI-2007-00319, Savannah River National Laboratory, Aiken, South Carolina (2007).

5   THOR® Treatment Technologies, **"Pilot Plant Report for Treating Sodium-Bearing Waste Surrogates Carbonate Flowsheet,"** Idaho Cleanup Project, Integrated Waste Treatment Unit, Project Number 28276, Document Number RT-ESTD-002, Rev. 1 (August 2006).

6   THOR® Treatment Technologies, **"IWTU Coal Specification,"** Idaho Cleanup Project, Integrated Waste Treatment Unit, Project Number 28266, Document Number RT-00-005, Rev. 0 (March 2010).

7   Jantzen, C.M., D.M. Missimer, C.P. Guenther, D. Shekhawat, D.T. VanEssendelft, **"Integrated Waste Treatment Unit Input Coal Analyses and Off-gas Filter (OGF) Content Analyses,"** SRNL-STI-2015-00015, Rev. 0 (2015).

8   Jantzen, C.M., D.M. Missimer, and C.L. Crawford, "**Analyses of Integrated Waste Treatment Unit (IWTU) Samples including Wall Scale Formed during Fluidized Bed Steam Reforming (FBSR) of Sodium Bearing Waste (SBW) into a Carbonate Form,"** SRNL-TR-2015-00258 (September 2015).

9   Jantzen, C.M., D.M. Missimer, H.M. Ajo, C.E. Brown, F.F. Fondeur, M. Crowder, P.R. Burket, **"Integrated Waste Treatment Unit (IWTU) Deposits: In Depth Look at the IWTU Bark and DMR bed products (02/08/16)," SRNL-STI-2016-00264 (2016).**

10 Jantzen, C.M., **"Recommendation for Remediation of Wall Scale Formation during Fluidized Bed Steam Reforming (FBSR) of Sodium Bearing Waste (SBW) into a Carbonate Form,"** Savannah River National Laboratory Memorandum SRNL-PSE-2007-00040 (May 2007).

11 Downs, A.J., **"Chemistry of Aluminium, Gallium, Indium, and Thallium,"** Springer, New York (1993).

12 Huggins, C.W., **"Thermal Decomposition of Dawsonite,"** Am. Mineralogist, 58, 548-550 (1973).

13 Kohl, A.L. and Nielsen, R., **"Gas Purification,"** Gulf Professional Publishing, Houston, TX, 900 pp. (1997).

14 McGuire, M.C., I. Bull, and G.M. Johnson, **"Synthetic Megakalsilite Via Hydrothermal Preparation,"** U.S. Patent 201402568 (September 2014).

15 Hajimohammadi, A., J.L. Provis, and J.S.J. van Devente, **"Effect of Alumina Release Rate on the Mechanism of Geopolymer Gel Formation"**, Chemistry of Materials, 22, 5199–5208 (2010).

16 Bullock, Jr., J.H; J.D. Cathcart, and W.J. Betterton, **"Analytical Methods Utilized by the United States Geological Survey for the Analysis of Coal and Coal Combustion By-products,"** US Geological Survey Open-File Report 02-389, Denver, CO (2002).

17 Schairer, J.F. and H.S. Yoder, Jr. Carnegie Inst Washington YB 1969-1970, p. 157-160.

18 A.H. Verdonk, **"Synthesis and Thermal Decomposition of Potassium Trioxalatoaluminate Hydrate,"** Thermochimica Acta, 4 (1972), 25-39.

19 VonHevesy, G. , **"The Binary Systems NaOH-KOH, KOH-RbOH, and RbOH-NaOH,"** Zeit. Physik. Chem. 73, 667-84 (1910).

20 Sangster, J. and A.D. Pelton, **"Critical Coupled Evaluation of Phase Diagrams and Thermodynamic Properties of Binary and Ternary Alkali Salt Systems,"** Special Report to the Phase Equilibrium Program, American Ceramic Society, Westerville, OH, 77-81 (1987) and Phase Diagrams for Ceramists Figure 7049.

21 Sangster, J. and A.D. Pelton, **"Critical Coupled Evaluation of Phase Diagrams and Thermodynamic Properties of Binary and Ternary Alkali Salt Systems,"** Special Report to the Phase Equilibrium Program, American Ceramic Society, Westerville, OH, 82-85 (1987) and Phase Diagrams for Ceramists Figure 7041.

22 Sangster, J. and A.D. Pelton, **"Critical Coupled Evaluation of Phase Diagrams and Thermodynamic Properties of Binary and Ternary Alkali Salt Systems,"** Special Report to the Phase Equilibrium Program, American Ceramic Society, Westerville, OH, 91-92 (1987) and Phase Diagrams for Ceramists Figure 7040.

23 Sangster, J. and A.D. Pelton, **"Critical Coupled Evaluation of Phase Diagrams and Thermodynamic Properties of Binary and Ternary Alkali Salt Systems,"** Special Report to the Phase Equilibrium Program, American Ceramic Society, Westerville, OH, 93-96 (1987) and Phase Diagrams for Ceramists Figure 7050.

24 Soelberg, N., D. Marshall, S. Bates, and D. Siemer, **"SRS Tank 48 Waste Steam Reforming Proof-of-Concept Test Results,"** U.S. DOE Report INEEL/EXT-03-01118, Rev. 1 (May 2004).

25 Lillo-Rodenas, M.A., D. Cazorla-Amoros, and A. Linares-Solano, **"Understanding Chemical Reactions Between Carbons and NaOH and KOH: An Insight Into the Chemical Activation Mechanism,"** Carbon, 41, 267-271 (2003).

26 Hussein, A.T., M. Abdel Maksoud, and S.M. Elwan, **"The Hydrothermal Preparation of Sodium Silicate,"** J. Appl. Chemical Biotechnology, 22, 659-665 (1972).

27 Niggli, P. **"The Phenomena of Equilibria Between Silica and the Alkali Carbonates,"** J. Am. Chem. Soc., 35, 1693-1727 (1913).

28 Morey, G. W. **"New Crystalline Silicates of Potassium and Sodium, Their Preparation and General Properties,"** J. Am. Chem. Soc., 36, 215-230 (1914).

29 Schairer, J.F. and N.L Bowen, **"The System K_2O-Al_2O_3-SiO_2,"** Am. Jour. Sci., 253, 681-746 (1955).

30 Schairer, J.F. and H.S. Yoder, Jr. Carnegie Inst Washington YB 1969-1970, p. 157-160.

APPENDIX I. DETAILS OF THE MASS BALANCE

The IWTU samples were leached in hot water (3g to 300mL of deionized water) at 80°C for 2 hours. The samples were shaken and then filtered through a Whatman #40 filter, which is an 8 micron filter paper. The filter papers were preweighed dry and then the solids and filter paper were reweighed after drying at 80°C in an oven overnight. The soluble filtrate was sent for whole element chemical analysis (cations and anions) by Inductively Coupled Plasma Atomic Emission Spectroscopy (ICP-AES). The filtrates were also analyzed for Total Inorganic Carbon (TIC) as all the alkali carbonates would have been soluble except for $CaCO_3$ and only traces of $CaCO_3$ are present in the IWTU samples. The soluble ICP-AES and IC analyses are given in Table A1.

For the TIC analyses a diluted aliquot of each soluble sample was analyzed in triplicate using an OI Analytical 1030W Total Organic Carbon Analyzer. Organic carbon was measured using wet chemical oxidation (sodium persulfate addition). Inorganic carbon (carbonate) was measured by acidification of the sample with 20% phosphoric acid followed by infrared measurement of the evolved CO_2. Opening and closing standards, blanks, and spike were used. %RSD values for triplicate measurements were all less than 4%. The dilution factor was 4 (10 mL sample up to 40 mL total volume). The reporting limit at this dilution is 0.4 ug/mL carbon. Carbon then mathematically converted to CO_3 for mass balance (multiply by 4.99985). The TIC analyses are given in Table A2.

The solids were dissolved by the methods given in ASTM C1463, which is for glass dissolution but is similar to ASTM D2795 for ash dissolution. However, the ASTM C1463 dissolution allows for the sulfur to be determined from the dissolution residue by ICP-AES instead of by precipitation (the withdrawn ASTM C1757). The solids were analyzed for Al, Ca, Fe, K, Mg, Mn, Na, Ni, P, S, Si, and Ti by ICP-AES at the SRNL Process Science Analytical Laboratory (PSAL).

The ICP-AES analyses of the soluble portions of the samples were reported in ppm. Since the grams of soluble sample were known the following equation was used to get the ppm converted into elemental weight percent

$$Element\,or\,anion\,wt\,percent = \left(\frac{ppm\,of\,element\,or\,anion}{10^6\,g\,so\ln}\right)\left(\frac{300}{1}mL\right)\left(\frac{1}{ML}g\,so\ln\right)\left(\frac{1}{x\,g\,solids\,dissolved}\right)*100$$

Once the element or anion wt% was known, a molar mass balance was performed against the phases that were identified as soluble phases during XRD analysis in each of the tables given in the body of this document. Sums within ±100% were considered excellent on a soluble phase basis.

The ICP-AES analyses from the ASTM C1463 dissolutions were reported in element wt% and a molar mass balance was performed against the phases that were identified as insoluble phases during XRD analysis in each of the tables given in the body of this document. Sums within ±100% were considered excellent on a soluble phase basis.

Lastly, the soluble phase concentrations were weighted by the amount of the soluble component determined during the filtration of the water dissolved species. Likewise, the insoluble species were weighted by the amount of the insoluble component determined during the filtration of the water dissolved species. The soluble and insoluble species were summed to a whole element chemistry for each sample. Summed soluble insoluble species within ±100% were considered excellent.

The ashed samples were also dissolved by ASTM 1463 followed by ICP-AES analyses. The analyses were reported on both an elemental and an oxide wt% basis. Since all of the carbonate species and coal

are decomposed during the ashing, these results are reported on an oxide basis in the tables given in the body of this document.

Table A1. ICP-AES and IC analysis of Soluble Species

Report of Analysis
SRNL Process Science Analytical Laboratory
Customer: Charles Crawford
Date: 1/20/16
Sample ID: DMR Bed Media leachate, DMR Bark leachate, DMR Bed Media moreprod leachate, AugGrind leachate
Lab ID: S-5017-5020
Units: mg/L

Sample ID	Lab ID	Al	Ca	Cr	Fe	K	Mg	Mn	Na	Ni	P	S	Si	Ti
DMR Bed Media leachate	S-5017	0.633	0.951	<0.100	<1.00	<1.00	<0.100	<0.100	4.68	<0.100	<5.00	1.58	<1.00	<0.100
DMR Bed Media leachate	S-5017	0.606	1.02	<0.100	<1.00	<1.00	<0.100	<0.100	4.61	<0.100	<5.00	1.60	<1.00	<0.100
DMR Bark leachate	S-5018	682	3.63	<0.100	<1.00	16.1	<0.100	<0.100	3329	<0.100	6.28	9.28	15.0	<0.100
DMR Bark leachate	S-5018	697	3.79	<0.100	<1.00	16.0	<0.100	<0.100	3272	<0.100	6.20	9.35	15.0	<0.100
DMR Bed Media moreprod leachate	S-5019	216	1.76	<0.100	<1.00	112	<0.100	<0.100	675	<0.100	<5.00	80.9	15.1	<0.100
DMR Bed Media moreprod leachate	S-5019	208	1.95	<0.100	<1.00	113	<0.100	<0.100	669	<0.100	<5.00	95.9	16.5	<0.100
AugGrind leachate	S-5020	749	4.40	<0.100	<1.00	20.5	<0.100	<0.100	3256	<0.100	6.02	53.4	15.0	<0.100
AugGrind leachate	S-5020	757	4.56	<0.100	<1.00	20.3	<0.100	<0.100	3263	<0.100	6.00	54.1	15.1	<0.100

Sample ID	Lab ID	F	Cl	NO2	NO3	SO4	PO4	pH
DMR Bed Media leachate	S-5017	<100	<100	<100	<100	<100	<100	9.55
DMR Bed Media leachate	S-5017	<100	<100	<100	<100	<100	<100	
DMR Bark leachate	S-5018	<100	<100	<100	<100	<100	<100	11.8
DMR Bark leachate	S-5018	<100	<100	<100	<100	<100	<100	
DMR Bed Media moreprod leachate	S-5019	<100	<100	<100	<100	<100	<100	11.0
DMR Bed Media moreprod leachate	S-5019	<100	<100	<100	<100	<100	<100	
AugGrind leachate	S-5020	<100	<100	<100	<100	124	<100	11.8
AugGrind leachate	S-5020	<100	<100	<100	<100	119	<100	

Table A2. Total Inorganic Carbon/Total Organic Carbon (TIC/TOC)

Sample	TIC (ug/mL)	TOC (ug/mL)	TC (ug/mL)
AG bark	646	<2	646
DMR bark	692	<2	692
DRM Bed	<2	<2	<4
DMR Bed (other product)	144	<2	144

Table A3. ICP-AES and IC analysis of Inoluble Species

Report of Analysis
SRNL Process Science Analytical Laboratory
Customer: Charles Crawford
Date: 1/25/16
Sample ID: DMR Bed Media leachsolid, DMR Bark leachsolid, DMR Bed Media moreprod leachsolid, AugGrind leachsolid
Lab ID: S-5023-5026
Units: wt%

Sample ID	Lab ID	Al	Ca	Cr	Fe	K	Mg	Mn	Na	Ni	P	S	Si	Ti
DMR Bed Media leachsolid	S-5023	50.9	<0.100	<0.010	0.238	<0.100	<0.010	<0.010	0.111	<0.010	<0.010	<0.050	1.65	<0.050
DMR Bed Media leachsolid	S-5023	50.7	<0.100	<0.010	0.266	<0.100	<0.010	<0.010	0.103	<0.010	<0.010	<0.050	1.60	<0.050
DMR Bark leachsolid	S-5024	19.8	1.70	0.023	1.21	2.01	0.273	0.025	7.55	0.022	0.050	<0.050	12.6	0.157
DMR Bark leachsolid	S-5024	19.6	1.74	0.023	1.19	1.99	0.275	0.025	7.70	0.020	0.050	<0.050	12.6	0.158
MR Bed Media moreprod leachsol	S-5025	39.2	0.135	0.012	1.44	0.654	0.084	0.050	0.399	<0.010	0.015	<0.050	3.16	0.069
MR Bed Media moreprod leachsol	S-5025	38.3	0.132	0.008	1.54	0.642	0.088	0.055	0.383	<0.010	0.015	<0.050	3.12	0.064
AugGrind leachsolid	S-5026	20.0	1.56	0.024	1.44	1.54	0.269	0.032	7.63	0.017	0.057	0.082	11.2	0.134
AugGrind leachsolid	S-5026	19.9	1.59	0.026	1.44	1.56	0.270	0.032	7.72	0.018	0.059	0.080	11.3	0.134

	Lab ID	Al2O3 for bed and Al(OH)3 for bark	CaCO3	Cr2O3	Fe2O3	K2O	MgO	MnO	Na2O	NiO	P2O5	SO4	SiO2	TiO2	SUM	COAL	SUM with Coal
DMR Bed Media leachsolid	S-5023	96.2			0.34				0.15				3.5		100.190	0.78	100.970
DMR Bed Media leachsolid	S-5023	95.8			0.38				0.14				3.4		99.741	0.78	100.521
DMR Bark leachsolid	S-5024	57.2	4.24	0.033	1.73	2.42	0.452391	0.032301	10.18	0.027851	0.115057		27.0	0.261242	103.663	1.3	104.963
DMR Bark leachsolid	S-5024	56.7	4.34	0.033	1.71	2.39	0.456643	0.031975	10.38	0.025082	0.115451		27.1	0.263329	103.462	1.3	104.762
MR Bed Media moreprod leachsol	S-5025	74.1	0.34	0.017	2.06	0.79	0.138483	0.064676	0.54		0.034289		6.8	0.115534	84.943	14.37	99.313
MR Bed Media moreprod leachsol	S-5025	72.4	0.33	0.012	2.21	0.77	0.146317	0.071415	0.52		0.034954		6.7	0.107199	83.253	14.37	97.623
AugGrind leachsolid	S-5026	58.0	3.90	0.034	2.06	1.86	0.446806	0.041641	10.28	0.021078	0.130475	0.247	24.1	0.222706	101.265	1.46	102.725
AugGrind leachsolid	S-5026	57.6	3.97	0.039	2.05	1.87	0.447953	0.041085	10.41	0.023397	0.135764	0.241	24.2	0.224244	101.237	1.46	102.697

Sample ID	Lab ID	F	Cl	NO2	NO3	SO4	PO4
DMR Bed Media leachsolid	S-5023	<0.010	<0.010	<0.010	<0.010	0.017	0.011
DMR Bed Media leachsolid	S-5023	<0.010	<0.010	<0.010	<0.010	0.016	0.017
DMR Bark leachsolid	S-5024	<0.010	0.014	<0.010	<0.010	0.035	0.151
DMR Bark leachsolid	S-5024	<0.010	0.014	<0.010	<0.010	0.034	0.154
MR Bed Media moreprod leachsol	S-5025	<0.010	0.012	<0.010	<0.010	0.083	0.050
MR Bed Media moreprod leachsol	S-5025	<0.010	0.012	<0.010	<0.010	0.080	0.046
AugGrind leachsolid	S-5026	<0.010	0.014	<0.010	<0.010	0.238	0.175
AugGrind leachsolid	S-5026	<0.010	0.012	<0.010	<0.010	0.225	0.173

*Green shaded samples were balanced on Al(OH)$_3$ all the rest were balanced on Al$_2$O$_3$. The choice of which aluminate species to balance on were determined by the insoluble XRD analyses given in the tables in the text.

DISTRIBUTION

K. Picha, DOE-EM
J.R. Shultz, DOE-EM
S. VanCamp, DOE-EM
J.E. Marra, DOE-EM
C.P. Guenther, NETL
P.L. Rozelle, DOE-FE
D. E. Dooley, 773-A
C.C. Herman, 773-A
E.N. Hoffman, 999-W
C.L. Trivelpiece, 999-W
M.R. Porier, 773-42A
Leo Thompson, IWTU
S. Bates, IWTU
S. Agnew, Columbia Energy
B. Mason, Studsvik
N. Soelberg, INL-BEA
J. Zimerman, DOE-ID
K. Whitham, DOE-ID
J. Case, DOE-ID
C. Roth, DOE-ID
M.J. Cercy, 773-42A